ABSTRACT

Title of dissertation: INTERACTIONS BETWEEN CHEMICAL, PHYSICAL, AND BIOLOGICAL PROCESSES DURING DESERTIFICATION OF GROUNDWATER-DEPENDENT SEMI-ARID GRASSLANDS

Kimberly Rae Vest, Doctor of Philosophy, 2015

Dissertation directed by: Associate Professor, Andrew Elmore, University of Maryland Center for Environmental Science

Desertification is estimated to cost $26 billion per year through loss of agricultural production, water reserves, and air quality. Semi-arid grasslands are prone to desertification through many factors including groundwater pumping. Groundwater pumping below the root-zone of groundwater-dependent vegetation leads to a decrease in vegetation cover exposing bare soil to wind erosion. Desertification of semi-arid grasslands can lead to a permanent change in vegetation state. Identifying when and where ecological changes are irreversible is problematic, requiring observations of a new ecological state that favors the continued process of wind erosion and depletion of soil resources. To determine biological, physical, and chemical processes affecting desertification in semi-arid groundwater-dependent grasslands, I examined hydrological and ecological factors across groundwater-dependent meadows in Owens Valley, California. First, I developed and compared

empirical, process-based, and mechanistic models that predict mass transport. I found that scaled gap size explains 56% of the variation in total horizontal flux (Q), and the process-based model predicts Q better than the mechanistic model indicating the importance of scaled gap size in wind erosion modeling of heterogeneous vegetation. Second, I explored the role of landscape connectivity of bare soil in enhancing Q and quantifying the magnitude of desertification across the landscape using circuit theory and Qrule. I found that landscapes that were more connected than neutral landscapes with the same bare soil cover were associated with groundwater decline during the California drought and greater Q. This is consistent with the idea that the enhanced formation of connected pathways (representing functional connectivity) is evident at plots that arrived at a particular bare-soil cover via groundwater decline and wind erosion, rather than another process. Third, I analyzed vegetation structure and monitored Q, air quality data, and PM_{10} emissions to evaluate the relationship between meadow degradation and air quality. I found that management practices have generated a new mid-valley meadow source of PM_{10} pollution. These results provide information and tools for resource managers of groundwater-dependent semi-arid grasslands to identify areas degraded by wind erosion, producing Q and PM_{10}, and prone to desertification. Managers can use the information and tools to better gauge a well field's health and adjust the groundwater amount pumped from wells.

INTERACTIONS BETWEEN CHEMICAL, PHYSICAL, AND BIOLOGICAL PROCESSES DURING DESERTIFICATION OF GROUNDWATER-DEPENDENT SEMI-ARID GRASSLANDS

By

Kimberly Rae Vest

Dissertation submitted to the Faculty of the Graduate School of the
University of Maryland, College Park, in partial fulfillment
of the requirements for the degree of
Doctor of Philosophy
2015

Advisory Committee:
Professor Andrew Elmore, Chair
Dr. Kaye Brubaker
Dr. Mark Castro
Dr. Keith Eshelman
Dr. Matthew Fitzpatrick

Preface

This dissertation contains an overall abstract and five chapters. Chapter II, III, and IV are presented in manuscript form; therefore, the study area may be repeated, pronouns reflect manuscript authorship, and tables and figures appear at the end. A single reference section occurs at the end for literature cited throughout the dissertation.

Dedication

I dedicate my dissertation work to my family and friends. A special feeling of gratitude to my loving husband, Nathaniel Gardner, for his words of encouragement and sacrifice of sleep to take care of the kids. I also dedicate this dissertation to my friends and church family that supported me throughout the process by providing childcare and meals when I needed to work.

Acknowledgements

I would like to express my deepest gratitude to my advisor, Dr. Andrew Elmore, for his guidance, caring, support, patience especially in correcting my writing, and finding financial support for my research. I would also like to than my committee members: Drs. Kaye Brubaker, Mark Castro, Keith Eshleman, and Matthew Fitzpatrick for their insight and guidance. I would like to thank Dr. James Kaste for his help in the field and guidance on the chemical aspects of this study. Thanks to Dr. Gregory Okin for his fruitful discussion and comments on wind erosion modeling, the Okin model, scaled gap size, and functional connectivity. Thanks to Dr. Junrun Li for his calculations of the threshold sheer velocity for Chapter II and his advice on replicating his methods for the chemistry appendix.

Thanks to Helen Aubult, Keith Gigliello, and Jacob King for helping with field work. Thanks to Dr. Sally Manning for her expertise in Owens Valley vegetation, groundwater, and policy issues. I would also like to thank everyone at White Mountain Research Station that supported my research by housing, feeding, and storing my equipment. I would like to thank LADWP and ICWD for providing groundwater depth measurements, and LADWP for permitting me to perform experiments on their land. I would also like to thank Greg McCurdy for installing additional anemometers on two of his MET towers in the valley and allowing me to access all his tower data.

Many thanks to Steven Guinn for his assistance with ENVI and GIS for Chapter IV and python code for the Okin model; Katie Kline and Robin Shanholtzer Paulman for their help with chemical analyses; Dr. Robert Hildebrand for answering

questions regarding statistical analysis; and Dr. Robert Gardner for help in developing neutral landscape models in Qrule. Thanks to WMRS, University of California for a mini-grant to assist with the cost of fieldwork. Thanks to the National Science Foundation (Award #EAR0719793) for funding the research and the AL for providing financial support through teaching assistantships. Additional thanks to the administration at AL for assisting with my questions, and the Appalachian Lab travel awards committee for supporting my attendance at national conferences.

Table of Contents

List of Tables

List of Figures

Chapter 1: Introduction

Desertification impacts approximately 15% of the Earth's surface affecting over 100 countries by reducing ecosystem productivity (Schlesinger et al. 1990; Helldén 1991; Hulme and Kelly 1993; Belnap 1995; Rubio and Bochet 1998; Reynolds et al. 2007a) and impacting social and economic factors (Helldén 1991; Hulme and Kelly 1993; Reynolds et al. 2007a). Desertification is, "land degradation in arid, semi-arid, and dry sub-humid areas resulting from climatic variations and human activities" (Helldén 1991; Hulme and Kelly 1993; Le Houffrou 1996; Nicholson et al. 1998; Rubio and Bochet 1998; Huenneke et al. 2002). Areas undergoing desertification can be characterized by increased aeolian sediment (dust) transport, changes in soil biological, chemical, and physical characteristics, and changes in vegetation structure (Rubio and Bochet 1998). Research suggests that once desertification has been initiated, it is hard to reverse. This is supported by research that once increasing heterogeneity of soil resources has begun, positive feedback processes are likely to develop that reinforces the new functional system properties. (Schlesinger et al. 1990; Peters et al. 2006; Turnbull et al. 2008).

Water mismanagement, particularly of groundwater resources, is of special concern because of the increasing demand on water in semi-arid and arid regions to supply growing urban populations (Ragab and Prudhomme 2002). In arid and semi-arid regions, plant communities are inherently water limited and changes in hydrology can have devastating effects on ecosystem functioning, including a tendency to initiate desertification (Sharma 1998). Of particular concern are hydrologically closed (endorheic) basins where sediment and evaporite minerals

collect in valleys creating saline lakes of temporally varying size and fluctuating shallow groundwater tables (Elmore et al. 2008). Examples of these conditions include Lake Chad in sahelian Africa and the Aral Sea in central Asia where water diversions combined with recent climate change, produce large, globally-relevant dust emissions (Wiggs et al. 2003; Elmore et al. 2008). For example, groundwater supports vegetation cover that reduces wind erosion, influences surface chemistry (e.g., salt crust anions), and is integral to the formation of soil crusts, which physically inhibit wind erosion. Small changes in vegetation and soil structure due to groundwater withdrawal might initiate a feedback process leading to greater structural and functional connectivity eventually causing a threshold change from grassland to shrubland permanently leading to desertification.

As vegetation structure changes, soil degradation occurs (e.g., includes wind erosion, water erosion and chemical degradation) (Schlesinger et al. 1990) exposing fertile soils in shrub interspaces to wind and water erosion removing them and producing dust (Schlesinger et al. 1996b; Lal 2003). The dust changes the landscape by redistributing soil to form islands of fertility (i.e., fertile soil is only located under shrubs) that further promote shrub growth to the detriment of grasses (Schlesinger et al. 1996b; Schlesinger and Pilmanis 1998). Increasing non-fertile shrub interspaces cause crustal hardening, decreasing infiltration, decreasing the likelihood of vegetation reestablishment, increasing soil temperature, and increasing the susceptibility of islands of fertility to erosion (Schlesinger et al. 1990; Belnap 1995; Schlesinger and Pilmanis 1998; Okin et al. 2001; Lal 2003). These changes are generally more conducive to the maintenance of shrubland, thus constituting a

positive feedback exacerbating desertification (Schlesinger et al. 1990; Kieft et al. 1998; Schlesinger and Pilmanis 1998). Dust also affects human health by increasing respiratory disorders (Zhang et al. 2013), lung disease (Fubini and Fenogolio 2007), and bacterial dispersion (Hervàs et al. 2009).

The Great Basin is the largest endorheic basin in the United States and contains many playas, the dustiest of which exhibit shallow groundwater (Reynolds et al. 2007b). Historically, one of the largest remaining saline Pleistocene lakes of the Great Basin was the Owens Lake, which received recharge from the extensive snowpack of eastern Sierra Nevada. Through the late 19^{th} and early 20^{th} century, water diversions caused Owens Lake to begin to desiccate, leaving behind an alkali playa with shallow groundwater. In 1913, the city of Los Angeles (LA) built the LA Aqueduct and diverted the Owens River, ensuring the complete desiccation of Owens Lake thereafter referred to as Owens Dry Lake. In 1973, LA built a second aqueduct and increased groundwater pumping in the northern sections of the valley. The increasing pressure on groundwater resources led to changes in regional vegetation (Elmore et al. 2003), especially during the California drought from 1987 to 1992 (Elmore et al. 2006b; Elmore et al. 2008). Owens Dry Lake is currently the largest source of PM_{10} emission (i.e., particulate matter < 10 μm) in North America (GBUAPCD 2008).

Owens Valley, CA was chosen for this work because it has been an outdoor experimental laboratory for dust research for several decades. Work on the Owens dry lake playa has been central to our understanding of aeolian processes in a groundwater-dominated system; however, this work has been largely constrained to

the non-vegetated portions of the playa. Owens Valley groundwater is pumped from extensive regions of alkali meadow vegetation to the north of the dry lake, a system that has not been previously studied in the context of wind erosion and desertification. The information garnered from this study will inform the management of these groundwater resources, with the goal of avoiding desertification.

1.1 Dissertation Overview: Objectives and Questions

The dissertation is organized around four general goals addressing the magnitude of wind erosion, methodologies for modeling wind erosion, and understanding the physical, biological, and chemical changes that occur in the study system during desertification. The main goals were to (1) measure the magnitude of wind erosion between groundwater-dependent alkali meadow with depth to water dependent vegetation changes and groundwater-dependent alkali meadow with static vegetation conditions and compare these values with wind erosion rates in other parts of the world and with projected consequences for air quality, (2) develop and compare empirical, process-based and mechanistic models that predict mass transport from field measurements of vegetation and soil structure within groundwater-dependent plant communities, (3) determine the composition and spatial distribution of soil crust properties that influence surface strength, and (4) explore the role of landscape connectivity of bare soil gaps in enhancing aeolian transport and quantifying the magnitude of desertification across the landscape. Chapter I (this chapter) is an overview and introduction to the later original research chapters.

Chapter II develops and compares empirical and mechanistic models that predict mass transport from field measurements of vegetation and soil structure

within groundwater-dependent plant communities. The question addressed is ***can measurements of vegetation structure be used to model areas at risk of wind erosion?*** Wind erosion is a significant environmental problem that removes soil resources from sensitive ecosystems and contributes to air pollution. When a reduction in vegetation cover occurs through any disturbance process there is potential for aeolian transport and dust emission. I found that as the mean gap size between vegetation elements scaled by vegetation height increases, aeolian sediment transport increases. I also tested a probabilistic model of wind erosion based on gap size between vegetation elements scaled by vegetation height (the Okin model) (Okin 2008), which predicts measured total horizontal aeolian sediment flux more closely than another commonly used model based on the average plant area observed in profile (the Raupach model) (Raupach et al. 1993). The threshold shear velocity of bare soil appears to increase as gap size between vegetation elements scaled by vegetation height increases, reflecting either surface armoring or reduced interaction between the groundwater capillary zone and surface sediments. Natural resource managers can use both the Okin model and simple empirical models to target management actions in alkali meadow vegetation.

Chapter III explores the role of landscape connectivity of bare soil gaps in enhancing aeolian transport and quantifying the magnitude of desertification across the landscape. The primary question ***is vegetation structure change coupled with wind erosion associated with thresholds that lead to permanent vegetation structure change?*** Okin et al. (2009) and Turnbull et al. (2008) hypothesized that an indicator of irreversibility in desertification might be "connected pathways" (i.e., structural -

vegetation structure is changing and functional - wind erosion begins to increase bare soil area). Connectivity of a landscape is related to the length and size of pathways through vegetation created by wind erosion (Okin et al. 2009). I analyzed differing connectivity across certain areas of the landscape using graph theory, so that the degree of desertification across the landscape might be determined. Most studies have focused on population movement between habitats (Bunn et al. 2000; Fuller et al. 2006; Minor and Urban 2007; Urban et al. 2009), but I focused on wind movement within the landscape. I used circuit theory based on Ohm's law (McRae 2006; McRae et al. 2008), which assumes set of similarities between wind and electrical currents, possibly representing an appropriate functional connectivity model for desertification. I analyzed the connectivity between grassland locations representing a gradient in degradation and theoretical neutral landscape models (NLM) with bare soil cover identical to the degradation gradient. Results show that Q increased as connectivity at our plots increased supporting the theory that connected pathways form in the landscape promoting dust emission. Further, long connected pathways form in our plots producing higher amounts of Q from wind erosion, and our plots that were more connected than NLM had higher groundwater declines during the California drought in the 1980s than plots above the NLM. Using Circuitscape coupled with Qrule to understand the degradedness of an area may help managers to mitigate the effects of desertification in an area.

Chapter IV focuses on determining the magnitude of wind erosion between depth to water dependent changes and static vegetation conditions in groundwater-dependent alkali meadow and compare these values with wind erosion rates in other

parts of the world and with projected consequences for air quality. The main question was ***are Owens Valley alkali meadows eroding in areas of groundwater decline and does this erosion contribute to regional air pollution?*** I used plot-based observations of total horizontal flux across a gradient of meadow degradation; plot based measurements of vegetation cover and structure; and PM_{10} observations at locations along a north to south transect in Owens Valley, CA. I analyzed vegetation structure and monitored aeolian sediment transport to evaluate the relationship between meadow degradation and air quality. Results show that (1) management practices have generated a new mid-valley alkali meadow source of PM_{10} pollution that was previously unrecognized in Owens Valley; (2) there is a need for more comprehensive ecosystem and groundwater management to mitigate the air quality issues within Owens Valley; and (3) Los Angeles must reduce their current demand for water from Owens Valley through mandatory water restrictions in both drought and non-drought periods.

Chapter V stands as a concluding statement for the entire dissertation. It summarizes the observations and application of the modeling; identifies vegetation degradation and wind erosion in the field; integrates field and modeling results; determines thresholds for state changes from grassland to shrubland; shows the implications of continued pumping of groundwater; and implications of future drought and climate change on vegetation and groundwater.

Chapter 2: Estimating total horizontal aeolian flux within shrub-invaded groundwater-dependent meadows using empirical and mechanistic models

Published in the *Journal of Geophysical Research*

2.1 Abstract

Wind erosion is a significant environmental problem that removes soil resources from sensitive ecosystems and contributes to air pollution. In regions of shallow groundwater, friable (puffy) soils are maintained through capillary action, surface evaporation of solute rich soil moisture, and protection from mobilization by groundwater dependent grasses and shrubs. When a reduction in vegetation cover occurs through any disturbance process there is potential for aeolian transport and dust emission. We find that as mean gap size between vegetation elements scaled by vegetation height increases, total horizontal aeolian sediment flux increases and explains 58% of the variation in total horizontal aeolian sediment flux. We also test a probabilistic model of wind erosion based on gap size between vegetation elements scaled by vegetation height (the Okin model) (Okin 2008), which predicts measured total horizontal aeolian sediment flux more closely than another commonly used model based on the average plant area observed in profile (Raupach model) (Raupach et al. 1993). The threshold shear velocity of bare soil appears to increase as gap size between vegetation elements scaled by vegetation height increases, reflecting either surface armoring or reduced interaction between the groundwater capillary zone and surface sediments. This work advances understanding of the importance of measuring gap size between vegetation elements scaled by vegetation height for empirically

estimating Q and for structuring process-based models of desert wind erosion in groundwater dependent vegetation.

2.2 Introduction

A leading challenge in aeolian geomorphology is understanding the influence of vegetation structure on total horizontal aeolian sediment flux, Q (kg m^{-1} s^{-1}) (Musick and Gillette 1990; Musick et al. 1996; Wolfe and Nickling 1996; Lancaster and Baas 1998; Belnap and Gillette 1998; Okin and Gillette 2001; King et al. 2005; Peters et al. 2006; Li et al. 2007; Li et al. 2009; Okin et al. 2009). Because vegetation structure influences flow regimes, shear stress, and surface erodibility (Shao 2000), the absence of vegetation raises the potential for increased Q (King et al. 2006; Elmore et al. 2008). Likewise, dust emissions to the atmosphere are proportional to the horizontal flux of saltating grains, aerodynamic entrainment, and aggregate disintegration at the surface, with proportionality related to the structure and texture of the underlying soil (Gillette et al. 1997; Shao et al. 2011). Therefore, land-use activities that alter the cover or 3-dimensional structure of desert vegetation pose a challenge to resource managers seeking to maintain soil stability and limit air pollution. Of particular concern are land-use practices that contribute to woody encroachment of grasslands (Schlesinger et al. 1990), destroy biological soil crusts (Belnap 1995), or otherwise lead to conditions of increasing shear velocity at the soil surface.

In desert systems prone to high winds and friable soils, vegetation structure must be actively managed, either through direct (e.g., seeding of grass, fire

treatments, etc.) or indirect methods (e.g., modification of grazing intensity, management of groundwater depth, etc.). For management to be successful, methods are needed for predicting Q from a limited number of observations. In empirical models, these observations are used to develop statistical relationships between vegetation structure and Q, both measured in natural settings. Once constructed, empirical models might be used for quick assessment of site conditions and for estimating the potential for future erosion. Careful use of process-based models, on the other hand, requires observations of both soil and vegetation properties but has the potential to reveal how these properties influence Q. Here, the choice of how to represent vegetation structure and distribution can be informed by empirical models as the choice appears in part to determine model success.

Parameters that quantify the average profile area of vegetation (per unit ground area) encountered by the wind (e.g., "lateral cover" (Marticorena and Bergametti 1995; Musick et al. 1996; Wolfe and Nickling 1996; Marticorena et al. 1997; Dong et al. 2001)), have long been considered useful for estimating the shear velocity at the soil surface. Although there is evidence that the configuration of vegetation and other roughness elements have a limited impact on wind erosion (Brown et al. 2008), recent work suggests otherwise. The spatial distribution of vegetation elements (e.g., vegetation clumping and connectivity of bare soil patches) is expected to have a strong effect on wind erosion reflecting the fact that shear velocity is spatially variable across a vegetated surface (Okin 2008; Okin et al. 2009). Okin (2008) compared the theoretical underpinnings of the Raupach model (1993) (based on lateral cover) to a new model that uses scaled gap size ($\overline{L}/h$, average gap

size divided by average vegetation height) to represent vegetation structure. By representing bare soil surfaces as a probabilistic distribution of gaps of a certain size, Okin (2008) suggested that Q is more sensitive to vegetation structure and distribution than to vegetation (lateral) cover (see also (Okin et al. 2006)). However, the Okin model has yet to be tested in a variety of settings using field observations collected for this purpose.

In this paper, we evaluated a suite of vegetation parameters identified from the literature (Marshall 1971; Okin 2008; Breshears et al. 2009) including those described above, for their capability to explain variability in Q across a shrubland to grassland gradient within groundwater dependent vegetation in the Owens Valley, California. Although extensive work has explored dust emission from Owens dry lake (Goudie and Middleton 1992; Cahill et al. 1996; Gill 1996; Reheis 1997; Gillette et al. 2001; Reheis 2006), to the best of our knowledge this study is the first to measure and analyze Q in vegetated portions of the valley to the north of the exposed lake bed (Fig. 3.1). Vegetation cover and structure in Owens Valley has been adversely affected by groundwater pumping over the past several decades (Elmore et al. 2003; Elmore et al. 2006b; Elmore et al. 2008). Mata-Gonzalez et al (2012) looked at microtopograpic effects, which can be created by wind or water erosion. The finding that shrubs are more often located on relatively high locations is consistent with the idea that shrubs trap sediment carried by wind from bare soil areas. Today, groundwater pumping is actively managed using, to some extent, observations of change in vegetation structure, making this a useful study system for developing tools that model Q across vegetation gradients that correlate with groundwater depth and

history. Further, the importance of groundwater dependent systems as sources of atmospheric dust emission has recently been highlighted (Reynolds et al. 2007b) adding additional motivation for understanding these systems. We intend the results of this work to lend insight into future model development and testing as well as into the development of sustainable management plans.

2.3 Methods

2.3.1 Study site

Owens Valley is a semiarid endorheic basin in California situated between the Sierra Nevada and the White-Inyo mountain ranges, receiving a median precipitation of 0.13 m annually. Snowmelt from the Sierra Nevada results in 5.8×10^8 m^3 – 6.3×10^8 m^3 annual runoff that recharges groundwater and surface water in the Owens River drainage basin (Danskin 1998). Originally these waters flowed to the Owens Lake located at the southern terminus of the Owens River Basin (Hollett et al. 1991; Danskin 1998). Due to annual recharge, the groundwater table is close to the surface across much of the Owens Valley floor supporting the shallow-rooted alkali meadow vegetation community (Sorenson et al. 1991; Elmore et al. 2003; Elmore et al. 2006b). Saltgrass (*Distichlis spicata* (L.) Greene) and alkali sacaton (*Sporobulus airoides* Torr.) are characteristic grass species of alkali meadow and form dense grasslands in areas where the water table is within 1.5 m of the soil surface (Sorenson et al. 1991). Alkali meadow also contains shrub species, such as greasewood (*Sarcobatus vermiculatus),* Nevada saltbush (*Atriplex lentiformis* ssp. *torreyi)*, and rubber rabbitbush *(Ericameria nauseosa),* which occur in areas with greater than 2.5 m, but still accessible, groundwater (Sorenson et al. 1991).

In 1913, the city of Los Angeles (LA) built the LA Aqueduct and diverted the Owens River contributing to the complete desiccation of Owens Lake around 1920. Subsequent dust storms in Owens Valley lead to non-compliance with National Ambient Air Quality Standards (NAAQS) for airborne particulate matter (PM_{10}) (US EPA 2008; Reheis et al. 2009). Although restoration work on Owens Lake has begun to mitigate dust emissions, (document available from the (US EPA 2008) (http://epa.gov/region09/air/owens/pmplan.html#52507)), increasing pressure on groundwater resources in the northern portions of the valley has led to the drying of springs and seeps (Danskin 1998) and changes in regional vegetation (Elmore et al. 2003). In particular, during the California drought from 1987 to 1992, LA increased groundwater pumping, lowering the water table below the root zone of alkali meadows in much of the valley, causing the decline of grass cover, shrub encroachment, and exposing bare soil areas (Elmore et al. 2006b; Elmore et al. 2008). Due to fluctuations in groundwater depth in some areas (but not all), the cover and spatial structure of vegetation within alkali meadow are highly variable. Although the largest source of dust emission is from Owens dry lake, the similarities between the soils (e.g., puffy salt crusts that are highly susceptible to wind erosion (Reynolds et al. 2007b)), shallow groundwater tables and geologic history of the Owens dry lake and alkali meadow (Orme and Orme 2008) suggest that alkali meadow soils would be susceptible to wind erosion wherever bare soil is exposed (Saint-Amand et al. 1987).

2.3.2 Plot Selection

Our analysis focused on thirteen plots (10,000 m^2 each) that were monitored for three years from May to September: 2008, 2009, and 2010. Plot selection focused

on covering a range in vegetation structure, from shrubs separated by bare soil, through shrubs separated by meadow, to continuous meadow. Based on research linking vegetation structure and groundwater (Elmore et al. 2003; Elmore et al. 2006b), we found it possible to use spatial and recent temporal variation in groundwater depth to capture the needed variability in vegetation structure. However, we also required that groundwater be sufficiently close to the surface to justify a characterization of "groundwater dependent" and the soil characteristics associated with shallow groundwater dominated systems (generally thought of as requiring groundwater within 5 m of the surface (Reynolds et al. 2007b)). Although cattle grazing occurs across the entire study area, data on spatial variability in grazing intensity is unavailable, and we were forced to work under the assumption that grazing had a similar impact on vegetation structure across all plots. To enable the establishment of plots along the required gradient in vegetation structure, plots were identified that were (1) within 100 m of a long-term monitoring well with recorded groundwater depths since 1986 (measured in April of each year); (2) located within alkali meadow, as identified by a 1986 vegetation survey (City of Los Angeles and County of Inyo 1990); and (3) within soil identified as mollisol or aridisol in Soil Survey Geographic Database (SSURGO) (Soil Survey Staff). Sixteen plots were initially selected in these areas. However, in 2008, destruction of three plots by cattle that had not been removed at the time of sediment trap installation reduced the number of study plots to thirteen (Fig. 3.1). We did not re-deploy at these three sites in 2009 or 2010. At eight of the thirteen plots, (Aubault 2009) performed soil texture analyses.

2.3.3 Field Measurements

At each plot, Q was measured using four Big Spring Number Eight (BSNE) sediment traps (Custom Products and Consulting, Big Spring, TX) placed on a 1-m pole at heights of 0.1, 0.2, 0.5, and 1 m. This arrangement will henceforth be called a BSNE stem. BSNE stems were installed for three seasons (May to September 2008, 2009, and 2010) within each plot. Although dust emission during the winter might be significant (Saint-Amand et al. 1987), we avoided this season due to the pervasive presence of cattle over-wintering across most of the Owens Valley floor. During the summer, cattle are typically moved to higher elevation grazing lands. Although cattle likely influence vegetation structure, we know from previous research that groundwater decline is the main source of vegetation structure change (Elmore et al. 2003). Also, we do not believe that cattle changed the vegetation structure considerably during the study period because the mean vegetation structure at each plot was not significantly different across years, and we saw no evidence that there was between-plot variation in grazing intensity to the degree that it influenced vegetation structure at one plot more than another. In 2008, we placed a BSNE stem at each plot in a location characterized by either grass or a bare soil. In 2008 and 2009, we did not find differences in the amount of sediment collected between grass and bare soil locations (suggesting low within plot variability in Q and sediment sources from outside the immediate vicinity of the BSNE stem). Therefore, in 2010, we placed all BSNE stems in bare soil locations. The reason the location did not effect the sediment collected was because the sediment in each of the traps was from a wider area than where the BSNE stem was placed. The average diameter of bare

soil around the BSNE stems was approximately 3.16 m in 2008, 4.41 m in 2009, and 5.23 m in 2010. In 2009 and 2010, two BSNE stems were placed at two of the plots to explore spatial variation in Q, and tiles were placed around the BSNE stem at each plot to prevent vegetation growth around the lowest trap that might prevent trap movement and obstruct the inlet (something that occurred at plots 1, 4, 7, 10, 20, and 25 in 2008). BSNE stems were not placed within one meter of shrubs. The height of each trap was measured from the ground surface to the bottom of the inlet. The mass of the sample collected in each trap was divided by sampler inlet area and the duration of collection time, q(z) (kg m^{-2} s^{-1}). The results from each trap were fit to an exponential equation that was integrated from the ground surface to 1 m to estimate Q (kg m^{-1} s^{-1}) (Shao and Raupach 1992; Gillette et al. 1997). The Q was adjusted to account for the known efficiency of the BSNE stem, 90% ± 5% (Shao et al. 1993).

Vegetation cover, gap distribution and vegetation height for each plot was determined using four 50 m line intercept transects run in cardinal directions from the BSNE stem (USDA and NRCS 2004). For each transect, along-transect width (greater than 0.03 m), species, height of vegetation (greater than 0.08 m), and along-transect width of bare soil patches (greater than 0.03 m) were measured. Despite the imposed detection limit in vegetation height, we found that even the shortest vegetation elements were taller than 0.08 m. The vegetation height was measured using a regulation Frisbee® with a hole carved into the center through which a wooden meter stick could be threaded. The meter stick was placed in each individual plant along the transect, and the Frisbee® was dropped vertically with the meter stick penetrating the hole in the disk. The top of the plastic disk at its stopping location was

recorded as the vegetation height. Vegetation transects were conducted only in May of 2008, 2009, and 2010 during BSNE stem deployment.

Meteorological data were measured at three locations across Owens Valley (Fig. 3.1). Wind velocities were measured in 2009 and 2010 using five tower-mounted anemometers positioned above the ground at 0.5, 1, 2, 5 and 10 m (wind velocity height used to estimate *U*). In 2008 at the two southern towers, wind velocity was only measured at 10m. Average wind velocities were recorded every 10 minutes on the two southern towers and every 5 minutes on the northern tower. Data from an air temperature and humidity sensor mounted at 2 m were collected every 3 seconds and averaged at 10 minute intervals at the two most southern towers. These measurements were collected over the duration of each sampling period in 2008, 2009, and 2010. Precipitation measurements were collected by Los Angeles Department of Water and Power and Inyo County Water Department at rain gauges across Owens Valley.

Threshold shear velocity (u_{*t}) is the minimum shear velocity that generates the force required to begin moving particles on bare soil generating Q (Table 2.1) (Belnap and Gillette 1998). When shear velocity is less than u_{*t}, there is no sediment movement. u_{*t} can be measured directly using a wind tunnel (this method is expensive and logistically difficult (Li et al. 2009)) or by using a particle sensor attached to a tower fitted with anemometers (Lancaster and Baas 1998). We were not able to use either of these methods at our plots; therefore, we estimated u_{*t} using (1) a relationship between soil texture and u_{*t} identified from the literature (Gillette et al.

1980; Gillette et al. 1982; Gillette and Passi 1988; Cahill et al. 1996), and (2) a relationship between surface strength and u_{*t} (Li et al. 2010).

The threshold shear velocity of bare soil ($u_{*t\ \text{field}}$) was estimated by firing a spherical copper pellet (0.0045 m diameter BB) into the bare soil surface at 45º using a 760 Pumpmaster air gun with a muzzle height of 0.15 m (following methods described by Li et al (2010)). For each plot, a 50 m tape was run in a cardinal direction from the BSNE stem, and a BB was shot every 5 m. The BB-holes were typically elliptical, and the area of the hole (m^2) was calculated using the maximum diameter and a line perpendicular to the maximum diameter. In addition, a pocket penetrometer (QA Supplies, FT011) applied at 45 º to the soil surface was used to measure the resistance of the soil surface (Li et al. 2010). Working with desert soils at lands near Moab in SE Utah, Li et al (2010) calculated $u_{*t\ \text{field}}$ using a linear relationship with the area of the hole produced by the BB (*BB,* Li et al (2010) uses BB_{area}) and the force for the penetrometer to puncture the soil surface (*F,* Li et al (2010) uses *Penetrometer*), and $u_{*t\ \text{field}}$ (Table 3.1).

$$u_{*tfield} = e^{4.095-(0.078*BB)+(0.191*F)} + 10 \quad (1)$$

We used this method and applied equation (1) to soils at our plots in 2009. Although there might have been changes in u_{*t} annually, there were no detectable differences in depth to water, gap size, or vegetation structure. Therefore, we do not find it likely that u_{*t} changed across the three study years.

3.3.4 Remote sensing of vegetation cover

We acquired Landsat ETM+ images in September 2008, 2009, and 2010 to estimate the fraction of photosynthetic vegetation (%PV) at each site using linear spectral mixture analysis (Elmore et al. 2000). These data were previously validated against field measurements of leaf area along 33 permanent transects and found to be accurate to within ± 4.0% PV (absolute percent cover units) and are therefore useful for a variety of land-use and land-cover change investigations (Elmore et al. 2003; Elmore et al. 2006b). We sampled %PV cover at each plot from these raster data sets and calculated three different %PV statistics: single pixel, nine-pixel mean, and the standard deviation of the nine pixels, at and around each plot.

2.3.5 Field measured parameters

We evaluated the capability of six different vegetation parameters to explain variation in Q: lateral cover (λ) (1.3×10^{-5} to 0.18), concentration of roughness elements (C_r) (4.7×10^{-2} to 11), percent cover of woody vegetation ($\%W_c$) (6.1% to 79%), percent cover (%C) (23% to 96%), average gap size ($\overline{L}$) (0.20 m to 3.9 m), and scaled gap size ($\overline{L}/h$) (1.8 to 10) (Table 3.1). All vegetation parameters were chosen from literature and were calculated from the described field observations.

Lateral cover (λ) was chosen as a parameter because it has been used to define vegetation structure in wind erosion research since Marshall (1971). λ is the plant area observed in profile encountered by the wind as it flows over the surface. Due to the difficulty of calculating a true lateral cover parameter from transect data, we used an equation from Okin (2008) that relates lateral cover to average gap size ($\overline{L}$) with the following formula:

$$\lambda = \frac{A_P \overline{W}}{A_B\left(\overline{L} + \overline{W}\right)}, \quad (2)$$

where A_P is profile area of the plant, A_B is the basal area, $\overline{W}$ is the average plant width and $\overline{L}$ is the average gap size. We calculated A_P assuming plant profiles resemble an ellipse defined by plant height and plant diameter along the transect, which we measured in the field. The basal area was estimated by assuming plants resemble a circle (as viewed from above) with a radius equal to half the shrub diameter.

Percent woody cover (%W_c) was chosen for two reasons: (1) variation in woody vegetation amount and density was immediately apparent across our plots and (2) shrublands generally exhibit elevated Q over grasslands (Breshears et al. 2009). %W_c was calculated as the fraction of ground covered by the characteristic shrub species, live and dead.

Fryrear (1985) found that any type of roughness element (e.g., soil clods, plant litter, etc.) decreased wind erosion on bare soil. Therefore, we chose to use the vegetation parameter percent cover (%C) to represent the total amount of roughness elements in an area. %C was estimated by calculating the percentage of vegetation and litter covering all transects compared to bare soil area.

The aforementioned vegetation parameters focused primarily on quantifying the vegetation amount (%W_c and %C) and arrangement in the landscape (λ and C_r). However, bare soil is the erodible substrate; therefore, the following parameters focus on estimating the area of susceptible bare soil to wind erosion: average gap size $\left(\overline{L}\right)$ and gap size scaled by vegetation height $\left(\overline{L}/h\right)$. $\overline{L}$ is calculated as the average distance between shrubs and grass plants along transects. $\overline{L}/h$, where h is the

average plant height in transects, accounts for the fact that the length of the wake downwind of a plant depends upon the plant height (Okin 2008).

2.3.6 Statistical Analysis

Using an ANOVA with Tukey Honestly Significant Difference (HSD), we examined whether there were differences between Q and vegetation parameters collected annually over the three-year period. We then used an ANOVA with Tukey HSD to examine the differences in the means of relative humidity (a higher relative humidity increases u_{*_t} which decreases dust emission (Nickling and Neuman 1997; Park and In 2003)), wind velocity, and temperature to try and explain any observed differences. Using linear and rank regression, we examined the relative capability of each parameter (derived from remote sensing, vegetation, or gap measurements) to explain the variability between plots and years in the measured Q. To determine the most explanatory model for Q using any combination of vegetation parameters, all the parameters were linearly regressed against Q using all possible regressions, step-wise regression, forward entry regression and backward regression using a *P* value cut off of 0.01.

2.3.7 Process-based Modeling: the Okin Model

The goal of wind erosion models is to calculate total horizontal sediment flux (Q) from a limited set of lab and field measured parameters. A principal challenge in modeling wind erosion on vegetated landscapes is the choice of a vegetation distribution parameter that does not describe shear stress on the surface as homogeneous (Okin 2005; Okin 2008). Since 1971, vegetation measurements for

wind erosion models have used lateral cover (λ) (Marshall 1971; Raupach et al. 1993; Okin 2008). Yet, λ (i.e., plant area observed in profile) is an imperfect representation of vegetation cover because a few tall plants are treated equally to a greater number of short plants, and field observations demonstrate that Q can be dependent on vegetation distribution (Okin and Gillette 2001; Gillette et al. 2006; Okin 2008). Furthermore, λ is difficult to calculate because both the frontal silhouette area of vegetation and average footprint per plant are required measurements (Marshall 1971; Okin 2008). The Okin model, on the other hand, uses the full probability distribution of gap sizes scaled by vegetation height as measured in the field (Okin 2008).

The model itself is described in detail by Okin (2008). Briefly, Q^U (total horizontal flux at a certain wind velocity *U*) is modeled using the distribution of gaps downwind of the nearest upwind plants as:

$$Q^U = F_g \int_0^\infty Q^U_{x/h} P_d\left(x/h\right) d\left(x/h\right) \tag{3}$$

where $P_d(x/h)$ is the probability that any point is a distance, *x*, downwind of vegetation of height, *h*; F_g is the fraction of bare ground; and $Q^U{}_{(x/h)}$ is the horizontal flux associated with bare soil at the *x/h* position.

The reduction in shear velocity associated with a plant spacing of *x/h* is described by an exponential curve:

$$\frac{u_{*_S}}{u_*} = \left(\frac{u_{*_S}}{u_*}\right)_{x=0} + \left[1 - \left(\frac{u_{*_S}}{u_*}\right)_{x=0}\right] * \left[1 - e^{-xc_1/h}\right] \tag{4}$$

where u_{*s}/u_* is the ratio of shear velocity in the presence of plants (u_{*s}) to the shear velocity in the absence of vegetation (u_*), $(u_{*s}/u_*)_{x=0}$ is the depressed shear velocity

in the immediate lee of a plant, and c_1 is the e-folding length expressed in units of height (4.8) (Okin 2008). We studied the literature (King et al. 2005) and compared the description of vegetation type and associated values for $(u_{*s}/u_{*})_{x=0}$ with vegetation at our plots. From this analysis we arrived at the value of 0.2 for $(u_{*s}/u_{*})_{x=0}$. We then calculated u_{*} (i.e., the law of the wall [see Priestley 1959]), as

$$u_{*} = \frac{U(z)\kappa}{\ln((z-D)/z_o)}, \quad (5)$$

where U(z) (m s^{-1}) is the wind velocity at height z (m) measured at each tower, κ =0.4, D is the displacement height (i.e., 0 so that wind erosion is allowed on vegetated surfaces), and z_0 is the roughness height of bare soil (m) (0.001). In many wind erosion models, z_0 is the roughness height that varies over heterogeneous surfaces related to both plant cover and canopy height. However, in the Okin model, z_0 is the roughness height of bare soil between plants and is considered to be independent of plant parameters. We assume that z_0 defined in this way, is the same for all plots. We chose the value because it was the average estimate between the roughness height of bare soil (0.0001 m to 0.0008 m) in arid and semi-arid regions using an ERS scatterometer (Prigent et al. 2005) and the roughness height of biological crusts ((0.0006 m to 0.0137 m) in Table 1 of Rodriquez-Caballero et al (2012)). We did not independently measure a roughness height ourselves, and we acknowledge that the roughness exhibited by soils will lead to differences in z_0. We also assume that the variance in roughness length due to soil roughness (z_0) is small compared to that imposed by vegetation structure and therefore, use the same z_0 for all plots.

Flux at any plant spacing, $Q^{U}_{(x/h)}$, was calculated by using the formulation by Shao et al (1993) later modified to include the distance (x/h) from the nearest upwind plant:

$$Q^{U}_{(x/h)} = \mathrm{A}\frac{\rho}{g}u_{*}\left(u_{*}^{2} - u_{*t}^{2}\right)\delta \tag{6}$$

where A is a constant equal to one that accounts for the relative availability of sand particles for transport (Gillette et al. 2001), ρ is air density at 23.3 °C and 1,400 m (average temperature over BSNE deployment for three years and average elevation of Owens Valley; 1.01 kg m^{-3}), g is acceleration due to gravity (9.8 m s^{-2}), u_{*} is the surface shear velocity, u_{*t} is the threshold shear velocity of bare soil, and δ is set to 0 when ($u_{*t} > u_{*}$) and 1 otherwise. The units of $Q^{U}_{(x/h)}$ are horizontal mass flux (kg m^{-1} s^{-1}). Finally Q for all wind velocities were calculated by:

$$Q = \int_{0}^{\infty} P_{d}^{U} Q^{U} d(U) \tag{7}$$

which integrates Q^{U} over the full probability distribution of measured wind velocities $P_{d}{}^{U}$.

2.3.8 Mechanistic Modeling: the Raupach model

The Raupach model calculates threshold shear velocity by using the parameter λ (i.e., plant area observed in profile) (Raupach et al. 1993).

$$u_{*} = u_{*t}\sqrt{(1 - m\sigma\lambda)(1 + m\beta\lambda)} \tag{8}$$

where u_{*} is the threshold shear velocity in the presence of vegetation and μ_{*t} is the threshold shear velocity of the bare soil surface. β is the ratio of the drag coefficient

of a single element divided by the drag coefficient of the bare ground. β=100 and *m*=1 because these are the values recommended by Raupach et al (1993) for flat erodible surfaces. σ is the ratio of the basal area to the frontal area of the vegetation, $\sigma = \frac{A_B}{A_P}$, (Table 1) (Okin 2008).

To incorporate the relationship between λ and percent vegetation cover, C, the Raupach model can be re-expressed as

$$u_{*_t} = u_* \sqrt{(1-C)\left(1+\beta C \frac{A_p}{A_B}\right)} \tag{9}$$

The terms $(1-m\sigma\lambda)$ in equation (8) and $(1-C)$ in equation (9) each account for vegetation covering part of the surface, thus resulting in greater shear stress on the remaining bare ground (Okin 2005). The terms $(1+m\beta\lambda)$ in equation (8) and $(1+\beta C \frac{A_p}{A_B})$ in equation (9) account for the partition of some of the shear stress onto the vegetation and away from the soil surface.

By combining equations (6) and (9) and using the u_{*_t} field, we solved for $Q_{Raupach}$:

$$Q_{Raupach} = A\frac{\rho}{g}u_*\left(u_*^2 - \left(u_{*_t}\sqrt{(1-C)\left(1+\beta C\frac{A_p}{A_B}\right)}\right)^2\right) \tag{10}$$

2.3.9 Model Comparison

We used the Okin model to calculate the total horizontal aeolian sediment flux at each plot using a uniform u_{*_t} (0.56 m s^{-1}) ($Q_{Uniform}$) and a u_{*_t} estimated using data collected separately at each plot (Q_{Okin}) (Table 2.2). The uniform u_{*_t} value was

chosen based on published values (Table 2.3), suggesting that a u_{*t} of 0.56 m s^{-1} was an appropriate average value for alkali meadow in Owens Valley. We compared modeling results to measured Q (Q_{field}) (Table 2.5) from, the deployed BSNE stems by using a nonparametric ANOVA. We measured u_{*t} at each plot separately using equation (1) and recalculated Q using the Okin model (Q_{Okin}). We also calculated Q using the Raupach model ($Q_{Raupach}$) for each plot, using $u_{*t\ field}$. To determine whether the Okin model predicts Q better than the Raupach model at our plots, a nonparametric ANOVA was performed in R between the Q_{Okin}, $Q_{Raupach}$, and Q_{field}. In all statistical analyses, we used a critical *P*-value of 0.01 to determine significance.

2.4 Results

3.4.1 Comparing 2008, 2009, and 2010 data

The seven different vegetation parameters (Table 2.4) were similar in 2008, 2009, and 2010 (ANOVA with Tukey HSD) except for $\%W_c$, which was significantly different between the years 2008 and 2010 (P=0.003) and 2009 and 2010 (P=0.002). The Q_{field} was also significantly different between the years 2008 and 2010 (P<0.001) and 2009 and 2010 (P<0.001) (ANOVA with Tukey HSD), but the Q_{field} in 2008 and 2009 was not significantly different (P=0.99). This led us to run ANOVAs with Tukey HSD between wind velocities, depth to water (DTW), relative humidity, and temperature for these three different years. We also compared precipitation during BSNE deployment for the three-year period. The mean wind velocities in 2009 and 2008 were not significantly different (P=0.74); however, the mean wind velocities in 2008 and 2010 (P<0.001) and 2009 and 2010 (P<0.001) were significantly different,

with a higher average wind velocity in 2010. During the duration of BSNE stem deployment in 2010, 4.6 % of days exhibited wind velocities greater than 10 m s^{-1} (at 10 m height) compared to 3.50 % and 1.40 % in 2008 and 2009, respectively, indicating that the wind velocity distribution was more skewed toward higher values in 2010. The means of DTW between 2008, 2009, and 2010 were not significantly different (P=0.81). The means between relative humidity were different between 2008 and 2009 (P<0.001) and 2009 and 2010 (P<0.001) but indistinguishable between 2008 and 2010 (P=0.54); however, the number of days with relative humidity greater than 60% during BSNE stem deployment in 2010 was <1 % compared to 3.5 % and 1.40 % for 2008 and 2009, respectively. Mean temperature between 2010 and 2009, and 2010 and 2008 were significantly different with temperatures being colder in 2010 (P<0.001 for both). Reynolds et al (2007) notes that dust emission suppression only occurs during heavy rainfall, but the largest average event in Owens Valley was only 0.003 m during BSNE deployment in 2008. Although 2010 had the lowest amount of precipitation during BSNE deployment of the three years, we do not believe that rainfall influenced changes in Q greatly. Therefore, compared with 2008 and 2009, the summer of 2010 exhibited a higher average wind velocity, greater number of days with high winds, low humidity, and on average colder temperatures.

2.4.2 Empirical relationship between Q_{field} and vegetation

We combined the field measurements (Q_{field} and each vegetation parameter) for all years (i.e., 2008, 2009, and 2010) and analyzed the vegetation parameters against $Q_{field,}$ but this did not result in any vegetation parameter explaining greater

than 50 % of the variation in Q_{field} using a critical *P*-value of 0.01. Therefore, we analyzed vegetation parameters from 2008 and 2009 separately from vegetation parameters from 2010 against Q_{field} (Table 2.4). We felt this was justified by the differences in Q_{field} in 2010 apparently driven by drier, colder, gustier conditions. The vegetation parameters from 2008 and 2009 analyzed independently against Q_{field} only resulted in one parameter (scaled gap size, $\overline{L}/h$) explaining greater than 50 % of the variation in Q_{field} (adjusted R^2=0.56; *P*<0.001) (Table 2.4 and Fig. 2.2d). The vegetation parameters from 2010 analyzed independently against Q_{field} did not result in any parameters explaining greater than 50 % of the variation in Q_{field} (Table 2.4). The most commonly used vegetation parameter in aeolian research, λ, did not explain any variation in Q (2008 and 2009: adjusted R^2<0.001; *P*=0.76 and 2010: adjusted R^2<0.001; *P*=0.44) (Table 2.4). The combined 2008 and 2009 empirical model that explained the most variation in Q_{field} (58 %) contained the vegetation parameters, average gap size ($\overline{L}$) (*P*<0.001) and scaled gap size ($\overline{L}/h$) (*P*<0.001) (adjusted R^2=0.58; *P*<0.0001), and took the form:

$$Log(1+Q) = -2.1x10^{-10} + 3.6x10^{-9}(\overline{L}/h) + 2.7x10^{-11}(\overline{L}) \qquad (11)$$

The strongest relationship between q(z) (i.e., the sediment amount in the BSNE stem trap at each height divided by deployment time) and $\overline{L}/h$ was found at traps set at 0.2 m and 0.1 m (the lowest traps), with an adjusted R^2=0.54 (*P*<0.0001) and 0.50 (*P*<0.0001), respectively (Fig. 2.3). As the heights of the traps increase, the relationship between q(z) and $\overline{L}/h$ decreased to an adjusted R^2=0.36 (*P*<0.001) at

0.5 m and an adjusted R^2=0.19 (*P*=0.01) at 1 m (Fig. 2.2). For 2010 data, $\overline{L}/h$ at 0.1 m and 0.2 m explained less variation in q(z) than in 2008 and 2009 with an adjusted R^2=0.23 (*P*=0.04) and an adjusted R^2=0.14 (*P*=0.01). For 0.5 m and 1 m heights in 2010, $\overline{L}/h$ was an insignificant explanatory variable at a height 0.5 m (adjusted R^2=0.02; *P*=0.29) but became significant again at a height of 1 m (adjusted R^2=0.38; *P*=0.01).

2.4.3 Model Results

The means of $Q_{Uniform}$ and Q_{field} were significantly different (*P*<0.001). $Q_{Uniform}$ resulted in an overestimate at a majority of plots, but one plot (plot 12 in 2010) exhibited an underestimate (Table 2.5). Eighteen plots had $Q_{Uniform}$ (Table 2.5) values that were greatly overestimated (Table 2.5). These plots had a larger average $\overline{L}/h$ value than other plots (Table 2.2 and Table 2.5).

Mean Q_{Okin} and mean Q_{field} were not significantly different (*P*=0.02) (Table 2.5). However, the Okin model seemed to overestimate Q for plots located in the mid-valley (plots 7, 9, and 11). The overestimate of Q in the mid-valley might be mechanistically related to strong cross-valley winds [*Raab and Mayr*, 2008], which could lead to soil armoring in larger gaps (i.e., an elevated u_{*t}). Mean $Q_{field,}$ and mean $Q_{Raupach,}$ differed (*P*=0.005), and the means were also different between Q_{Okin} and $Q_{Raupach}$ (*P*<0.001). Minimum values for $Q_{Raupach}$ and Q_{Okin} were 0 g m^{-1} s^{-1}; these values were less than the minimum Q_{field} value of 2.59×10^{-9} g m^{-1} s^{-1}. Maximum values for $Q_{Raupach}$ and Q_{Okin} were 1.03×10^{-8} g m^{-1} s^{-1} and 1.69×10^{-5} g m^{-1} s^{-1}, respectively. The maximum value for Q_{field} was 1.94×10^{-6} g m^{-1} s^{-1}, thus closer to the

Q_{Okin} maximum value. Plot by plot, $Q_{Raupach,}$ values were generally less than Q_{field} values.

To explore the behavior of Q_{Okin} with increasing $\overline{L}/h$, we ran the Okin model using some hypothetical parameter sets. We held % bare soil constant at an average value of 64 % and varied u_{*_t} from 0.2 m s^{-1} to 0.6 m s^{-1} while also varying $\overline{L}/h$ across the range measured at our plots (1.9 to 10). Results of this exercise demonstrated the non-linear behavior of Q with increasing $\overline{L}/h$ (Fig. 2.4). A linear relationship between Q and $\overline{L}/h$ (such as seen in Fig. 2.2d and Fig. 2.4) crosses successive lines of constant u_{*_t}. Across a larger range in $\overline{L}/h$ than measured at our plots, we observed that if u_{*_t} is held constant at 0.56 m s^{-1}, Q increases exponentially until $\overline{L}/h$ equals 20 at which point, Q increases at a decreasing rate.

2.5 Discussion

Many of our plots have experienced periods of groundwater pumping, contributing to the decline of alkali meadow grasses and replacement by shrubs (Elmore et al. 2006b). Given previous work that describes the impacts of groundwater pumping on vegetation cover and the cover of perennial grasses in particular (Elmore et al. 2003; Elmore et al. 2006b), we interpret the relationships that we observe between field measured total horizontal aeolian sediment flux (Q_{field}) of the BSNE stems for 2008 and 2009 and vegetation structure (known to be caused in part by land use change) (Fig. 2.2). The Q_{field} is comparable to other values of Q in similar environments (Minqin, China (Dong et al. 2010) and Chihuahaun Desert Playas (Bergametti and Gillette 2010)). Although horizontal transport and dust

emission are not always correlated, Gillette et al (1997) showed a relationship between horizontal flux and vertical flux at the Owens Lake, which exhibits similar soils to those found at our plots. This combination of evidence supports the idea that dust emission is occurring at our plots. Plots with intact, continuous grass cover or taller shrubs with small inter-shrub spaces each exhibited small scaled gaps sizes and generally reported the lowest Q (Fig. 2.2d). Groundwater depth is known to influence both the cover of alkali meadow grasses (Elmore et al. 2006b) and the formation of puffy ground, through evaporation of solute-rich soil moisture (Gillette et al. 2001; Elmore et al. 2006b). Most research has focused on Owens Lake as the source of dust emission to the valley (Goudie and Middleton 1992; Cahill et al. 1996; Gill 1996; Reheis 1997; Okin et al. 2001; Reheis 2006); however, as indicated by Figure 2.2, the wind erosion from the vegetated portion of the valley floor can be considerable.

The λ parameter has been used in wind erosion research since *(Marshall 1971)* and has been included in shear stress partitioning models and models of wind erosion with roughness elements (Raupach et al. 1993; Marticorena and Bergametti 1995; Musick et al. 1996; Wolfe and Nickling 1996; Marticorena et al. 1997; Dong et al. 2001). However, λ parameter was not correlated with Q at our plots (Table 2.4). We attribute this to the inability of λ to quantify differences between plots with many small roughness elements from plots with few large roughness elements (e.g., compare plots 1 and 10). Several of the other vegetation parameters were likewise not correlated with Q (Table 2.2) because like the λ parameter, they explained the quantity but not the distribution of roughness elements on the landscape. Scaled gap size, $\overline{L}/h$, on the other hand, was correlated with Q_{field} (Table 2.4 and Fig. 2.2). The

success of $\overline{L}/h$ as a vegetation parameter is due to its ability to describe the heterogeneous distribution of vegetation (e.g., mixture of shrubs, grass and bare soil gaps) and the amount of sheltered bare soil (i.e., reduced shear wake zone) behind the vegetation (Okin 2008). The relationship between $\overline{L}/h$ and Q in empirical and process-based models is important in understanding wind erosion in groundwater-dependent meadows.

The most explanatory empirical model predicting Q (equation (11)) utilized two vegetation parameters to model Q ($\overline{L}/h$ and $\overline{L}$) in 2008 and 2009 (but not 2010). Although, $\overline{L}$ was slightly correlated with Q, combining $\overline{L}$ and $\overline{L}/h$ in the regression explained a slightly greater variability in Q, which led to a slight increase in prediction of the model (Parameter $\overline{L}/h$; R^2=0.56 and Parameters: $\overline{L}/h$ and $\overline{L}$; R^2=0.58). This might occur because together $\overline{L}$ and $\overline{L}/h$ help draw out the differences between grass dominated and shrub dominated plots. Extending measurements of $\overline{L}/h$ and the relationship in Figure 2.2 and equation (11) to estimate Q of other sites in the Owens Valley or elsewhere should be done with extreme caution as variation in soil and vegetation characteristics are more likely to influence this relationship. Where appropriate, Q derived from the described empirical relationships could be used to help managers target areas susceptible to wind erosion. This approach would be valid under the assumption that u_{*t} and wind fields are the same for all plots.

The Raupach model estimated lower Q values than measured in the field due to the inability of lateral cover to appropriately characterize the vegetation structure at our plots. To obtain Q values from the Raupach model that match Q values obtained

from the field, the u_{*_t} of bare soil would have to be lower than both values found in the literature (Table 2.3) as well as those estimated in the field. However, field measures of u_{*_t} show values similar to literature cited values at comparable plots (Table 2.2 and Table 2.3). The Okin model does a better job at predicting Q in vegetated landscapes because it represents the distribution of vegetation cover, recognizing that large soil gaps can produce Q despite significant vegetation cover. The mean Q_{Okin} and mean Q_{field} were not significantly different (P of 0.02; Table 2.5). However, the mean $Q_{Unifrom}$ and Q_{field} were significantly different (Table 2.5) indicating that a single value of u_{*_t} estimated from literature across this study site is insufficient to characterize the inherent spatial variability. Further, where individual plots reported different Q_{Okin} and Q_{field}, we generally observed a diversity of soil surfaces (salt crusts, packed clay, etc.) and gap sizes (e.g., a few large gaps) suggesting that a single u_{*_t} value for the entire plot might not be appropriate.

The Okin model predicts that as $\overline{L}/h$ increases, the Q response resembles a sigmoid growth pattern. Over the range in $\overline{L}/h$ observed at our plots, a linear relationship between $\overline{L}/h$ and Q can only be achieved if the u_{*_t} increases with increasing $\overline{L}/h$ (Fig. 2.4). In other words, our data supports the idea that, in this study area, as gaps increase in size they become increasingly resistant to wind erosion and form streets (Okin et al. 2001). As vegetation cover is diminished in and around gaps, the longer wind fetch enables the erosion of an increasing area leading to increased dust emissions. However, as gaps increase in size, the edges of the gaps maintain loose, easily erodible soil. These observations support our understanding of

groundwater influences on Q (Elmore et al. 2008); plots with larger gaps usually have deeper groundwater (Elmore et al. 2006b) and groundwater depth has been found to be inversely related to dust emissions, at least for playas (Reynolds et al. 2007b). Although u_{*_t} is higher in streets, these areas have the ability to produce large amounts of horizontal flux due to a large fetch (Okin et al. 2001) causing saltation and dust emission along the length of the street and burying and damaging vegetation on the periphery of the street (Okin et al. 2009) leading to increased bare soil area. This study has shown the utility of the Okin model and the measurement of $\overline{L}/h$ to be important in modeling aeolian transport in complex vegetation.

The results from this study are applicable to any environment with sparse vegetation and high wind velocities, but vegetated coastal dunes might be one of the more interesting comparisons. Unvegetated surfaces are seldom found in coastal aeolian environments, but vegetation cover can be spatially variable and dependent on disturbance history (Alcantara-Carrio and Alonso 2002). Therefore coastal dune stabilization depends on vegetation cover change (Levin et al. 2006), and the degree to which vegetation moderates wind erosion (Fulbright et al. 2006). Wind erosion models that include vegetation parameters such as percent cover and mean vegetation height to characterize vegetation have been effective in modeling these processes (Buckley 1987; Alcantara-Carrio and Alonso 2002; Levin et al. 2006), suggesting $\overline{L}/h$ and the Okin model might provide beneficial information in vegetated coastal dune environments.

There are many interesting uncertainties remaining to be investigated, including quantifying the impacts of grazing and other disturbances and understanding the source and consequences of spatial and temporal variability in model parameters influencing Q. Grazing is known to increase the bare soil area and decrease grass height (Nash et al. 2004). Grazing animals also disturb soil crusts enabling wind erosion, particularly along frequently used paths (Belnap 1995). We saw little evidence that inter-plot variation in grazing intensity influenced vegetation structural differences between our plots and therefore did not attempt to quantify the effect of cattle. This being said, the interpretation of our results does not depend on an understanding of the causes of vegetation structural differences between plots, only on their magnitude and on the relationship between vegetation structure and estimates of Q. Therefore, the most difficult disturbance to incorporate are those that increase the transport of sediment to our plots from locations outside the range of our transects, which extended 50 m from each BSNE stem. For example, it cannot be ruled out that activity on local roads (many of which are unpaved) or off-road all terrain vehicle (ATV) activities had an impact on our measurements and model success [e.g., Belnap 1995]. In Owens Valley, ATVs are permitted on dirt roads located within 500 m of our plots and roadwork (grading, paving, etc.) is ongoing in many areas. Although it would be hard to measure the impact of these dust sources on measurements of Q at our plots, it is possible they lead to temporal or spatial variability in the success of empirical and mechanistic models to predict Q.

Further refinements to the models used here will likely require a more detailed representation of spatial and temporal variability in model parameters (e.g., u_{*t}, in

particular) and Q. Although we found that measurements of Q were not sensitive to the placement of BSNE stems in 2008 and 2009, the placement in 2010 might have contributed to the increase in Q observed at some plots. This possibility brings into question several assumptions we made regarding the spatial and temporal variability in model parameters. For example, a single value of u_{*t} was used at each plot, yet we commonly observed loose soil at the edges of gaps in the vicinity of vegetation indicating a range in values exists. Likewise, vegetation structure was measured only at BSNE stem deployment, which does not account for vegetation structural changes throughout the growing season. Finally, we only measured u_{*t} and Q in the summer, potentially missing significant changes in soil condition and Q during winter (31% of Q events as measured from MET stations). During BSNE stem deployment, wind velocity at 0.5 m exceeded u_{*t} an average of 60 % of the time in 2009 at the two southern MET stations. During 2010, wind velocity exceeded u_{*t} at our plots an average of 75 % of the time at the two southern MET stations, which might explain the greater Q observed in 2010 at some plots. However, this comparison of wind velocity at 0.5 m and u_{*t} does not take into account the sheltering effect of vegetation. In combination, these unmeasured factors call for work that incorporates spatial and temporal variability in model parameters into models of Q. The strongest empirical model found here explained 58 % of the variation in Q, leaving considerable variability for measurements and approaches for estimating Q.

2.6 Conclusions

Determining which vegetation parameter best relates to Q is important, both for understanding the mechanics of wind erosion models and for using these models to manage for soil stability. In this study, scaled gap size better explained Q than other vegetation parameters including lateral cover, the vegetation parameter most widely used in wind erosion modeling (Table 2.4). Adding an additional vegetation parameter, gap size, slightly increased the prediction of Q (from 56 % to 58 % variance explained; equation (11)). These two vegetation parameters are easily measured in the field; therefore, offering land and resource managers a useful option when assessing the potential wind erosion at any site. The scaled gap size in particular appears to be a useful metric in systems impacted by disturbance processes that decrease inter-shrub grass cover.

Wind erosion models that use scaled gap size instead of lateral cover are more successful in predicting Q in areas of heterogeneous vegetation. The Okin model, using scaled gap size, better predicted Q_{field} than the commonly used Raupach model, using λ (Table 2.5) suggesting the Okin model should be used where vegetation cover is spatially heterogeneous. However, predictive capability of the Okin model using a single average u_{*t} for all plots (0.56 m s^{-1}; Table 2.5) overestimated Q (Table 2.5), demonstrating the importance of knowing u_{*t} at each plot. Further, across our study plots u_{*t} correlated with bare soil area, which is consistent with the idea that soil surfaces in large gaps become more resistant to erosion over time. Practical applications of the Okin model might use a range of u_{*t} values to produce a range of potential Q values, or attempt to parameterize u_{*t} as a function of bare soil area.

Further, modeling work might benefit by taking into account within-plot variability in u_{*t} . For example, u_{*t} could be varied based upon gap size and position within a gap.

Natural resource managers can use both the Okin model and simple empirical models to target management actions in alkali meadow vegetation. Wind erosion causes reduced soil fertility that is unfavorable to vegetation reestablishment (Belnap and Gillette 1998; Li et al. 2007; Elmore et al. 2008) eventually forming streets and areas of reduced fertility (Okin et al. 2001). Continued disturbance of vegetation in Owens valley, for example, has the potential to cause the formation of streets, elevating u_{*t} as bare soils become more common and allowing for a longer fetch for saltation and dust emission, thus burying and damaging plants and creating more bare soil area (Okin et al. 2001; Okin et al. 2009). Understanding the interaction of soil resources, groundwater depth, and vegetation structure may illuminate whether wind erosion promotes these positive feedbacks eventually leading to desertification, increased dust emissions, reduce air quality and associated human health problems.

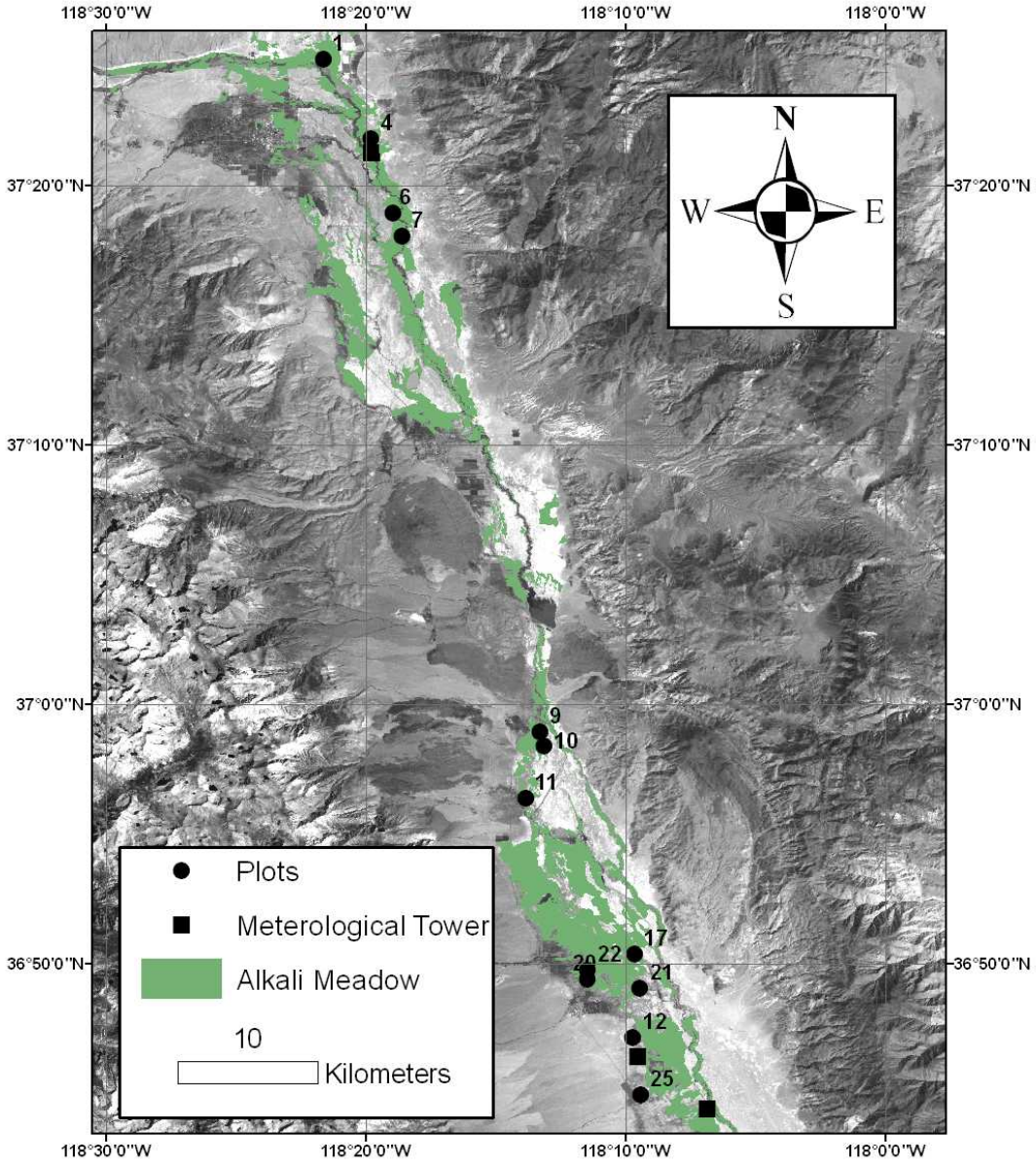

Figure 2.1 The plots where BSNEs stems were installed across the Owens Valley in alkali meadow identified using the vegetation survey of 1986 (City of Los Angeles and County of Inyo 1990). There are two meterological towers located in the southern half of the valley and one located in the north (squares). The background is a Landsat TM image from September 8, 1992.

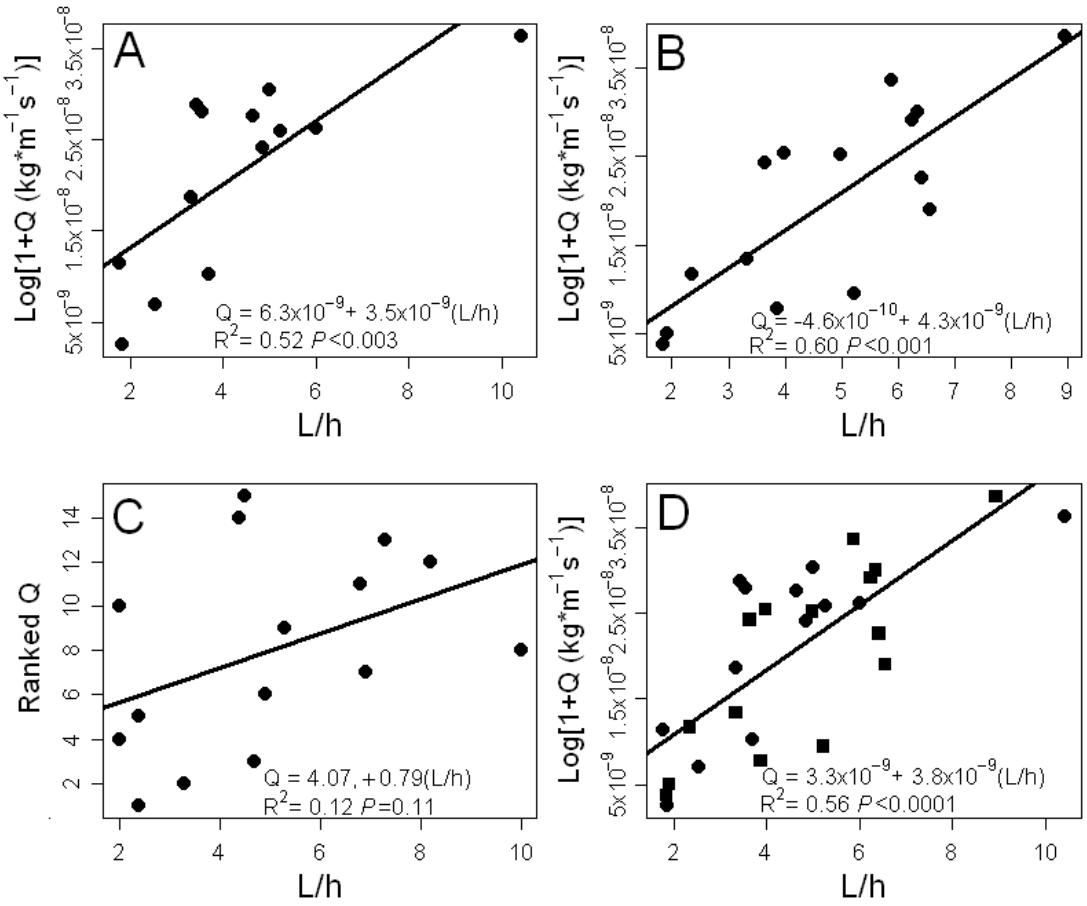

Figure 2.2 Scaled gap size ($\overline{L}/h$) vs. log normalized horizontal flux (Q) for 2008 (A), 2009 (B), 2010 (C), and 2008 (circles) and 2009 (blocks) combined (D). $\overline{L}/h$ in 2008 and 2009 explained 52% and 60% of the variability in Q, respectively; however, in 2010, $\overline{L}/h$ did not explain the variability in Q. Therefore, we combined the 2008 and 2009 data for our analysis and analyzed the 2010 data separately (e.g., Table 3.4). Together, the 2008 and 2009 data explained 56% of the variability in Q. In 2008 and 2009, lower scaled gap size results in lower Q.

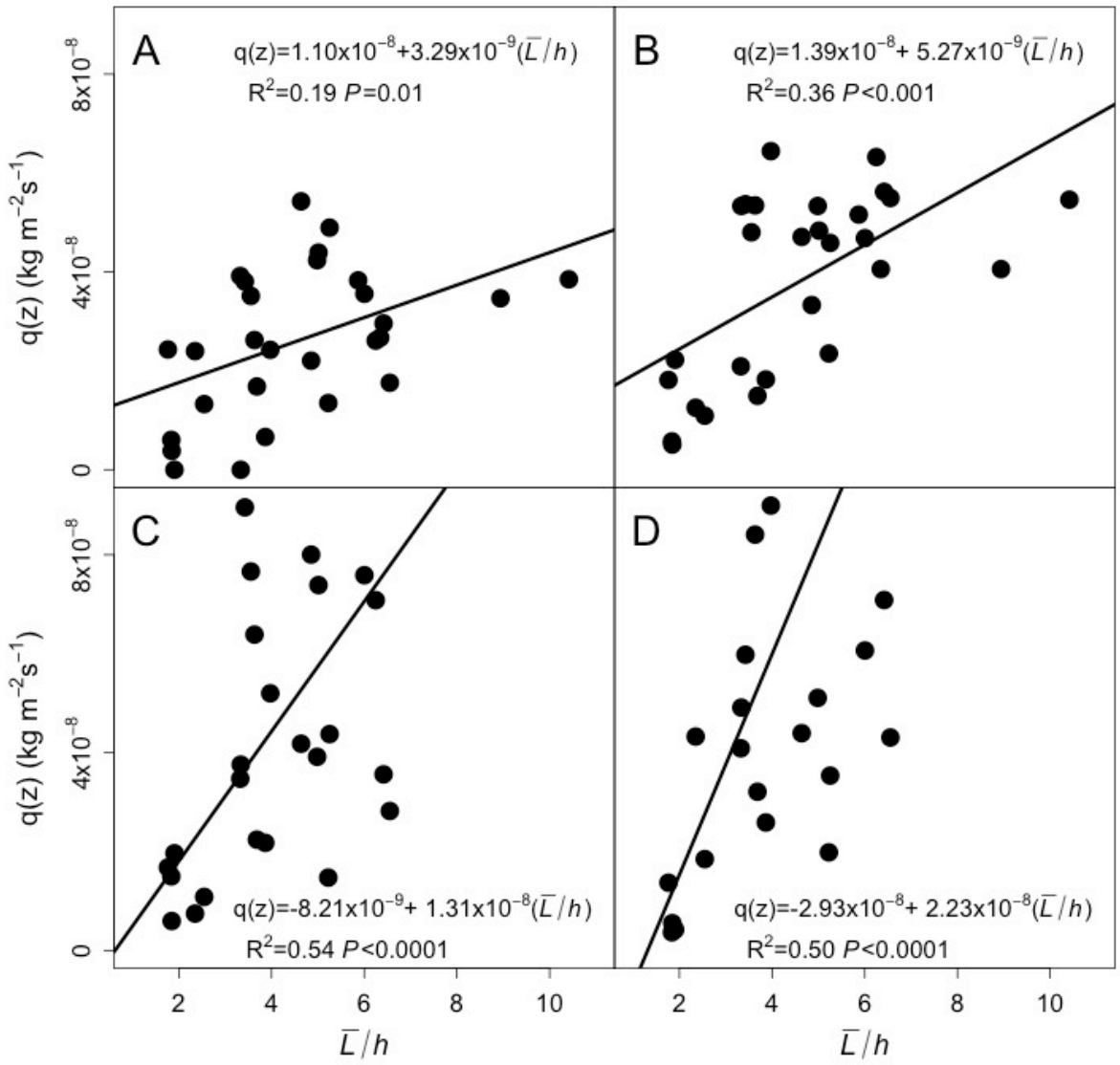

Figure 2.3 The effect of scaled gap size ($\bar{L}/h$) on the amount of sediment collected by BSNE stems across plots in 2008 and 2009 increased with decreasing BSNE height (A-D). The scaled gap size ($\bar{L}/h$) explains more variability in q(z) at 0.2 m (C) and 0.1 m (D) than at 0.5 m (B) and 1 m (A). All results are normalized by duration of sampling time.

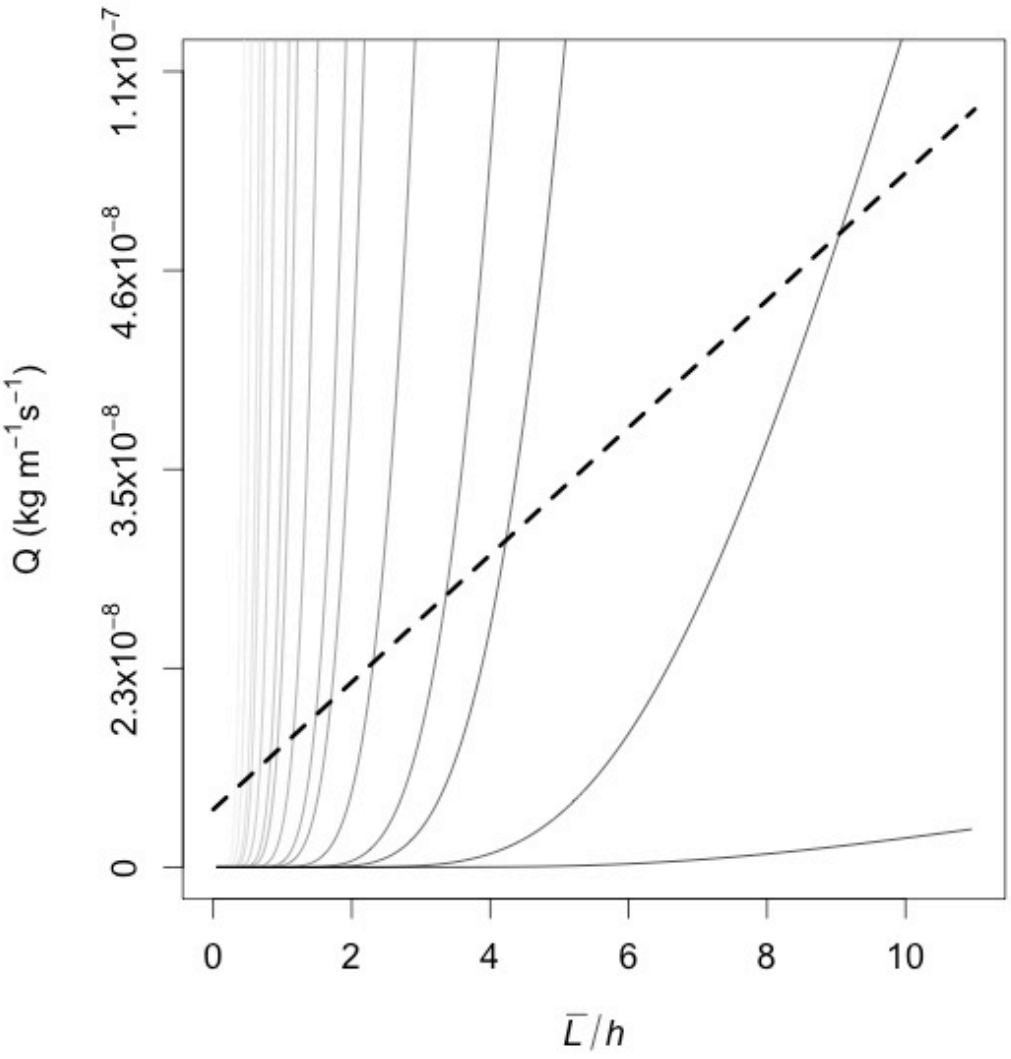

Figure 2.4 Q increases exponentially with increasing $\overline{L}/h$ across a range of $u*_t$ (light gray (0.2 m s-1) to black (0.6 m s-1)). However, $\overline{L}/h$ and Q increase linearly for our plots as in Fig. 2d (dashed line). One explanation is that $u*_t$ increases with increasing $\overline{L}/h$, perhaps through wind erosion and surface armoring.

Table 2.1: Description of Parameters used in Paper

Table 2.1. Description of Parameters used in Paper

Parameter	Equations	Description	Units
A	6 and 10	This is a constant equal to 1 that accounts for relative availability of sand particles for transport.	unitless
A_B	2 and 9	This is the average basal area of the plants from transect data.	m^2
A_P	2 and 9	This is the average profile area of plants from transect data.	m^2
β	8, 9 and 10	This is the ratio of element to surface drag coefficients (~100).	unitless
C	9 and 10	This is the percent vegetation cover of an area.	%
$\%C$	Not applicable	The percentage of the total amount of roughness elements in an area.	%
C_r	Not applicable	This is the concentration of roughness elements	unitless
D	5	This is the displacement height from the ground to the anemometer.	m
F_g	3	This is the fraction of bare ground.	unitless
g	6 and 10	This is the acceleration due to gravity	$m\ s^{-2}$
κ	5	The Kármán constant is used to describe the logarithmic velocity profile of wind velocity near a boundary.	unitless
$\overline{L}$	2 and 11	This is the average gap size length from transect data.	m
$\overline{L}/h$	11	This is the scaled gap size	unitless
λ	2 and 8	This is the canopy cover as viewed from the side (most commonly used parameter to define vegetation structure in wind erosion models).	unitless
m	8	This has the value of 1 for surfaces that are topographically stable.	unitless
$P_d(x/h)$	3	This is the probability that any point is a distance, x, from the nearest upwind plant of height, h.	unitless
$P_d{}^U(x/h)$	7	This is the probability that any point is a certain distance, x/h, at wind speed U.	unitless

Table 2.1. Description of Parameters used in Paper

Parameter	Equations	Description	Units
$q(z)$	Not applicable	The mass of the sample collected in each trap divided by sampler inlet area and the duration of collection time	kg m^{-2} s^{-1}
Q	7, 10, and 11	This is the total horizontal flux.	kg m^{-1} s^{-1}
Q^U	3 and 7	This is the total horizontal flux at a certain wind speed U.	kg m^{-1} s^{-1}
$Q^U_{(x/h)}$	3 and 6	This is the horizontal flux for any points a distance x/h from the nearest upwind plant.	kg m^{-1} s^{-1}
ρ	6 and 10	This is the air density at STP.	kg m^{-3}
σ	8	This is the ratio of the basal area to the frontal area of the vegetation. $\sigma = \frac{A_B}{A_P}$	unitless
$U(z)$	5	This is the wind speed at height (z).	m s^{-1}
u_*	4, 5, 6, 8 and 10	This is the surface shear velocity.	m s^{-1}
u_{*s}	6	This is the surface shear velocity in presence of vegetation	m s^{-1}
$\left(\frac{u_{*s}}{u_*}\right)$	4	Ratio of shear velocity in the presence of plants to shear velocity in the absence of plants	unitless
u_{*t}	6, 8, 9, and 10	Threshold shear velocity of bare soil is the shear speed at which particles on bare soil begin to move generating particle movement.	m s^{-1}
u_{*t} field	1	Threshold shear velocity (u_{*t}) estimated from penetrometer and BB-hole measurements.	m s^{-1}
$\overline{W}$	2	The average plant width from transect data.	m
$\%W_C$	Not applicable	The percent of the fraction of ground covered by woody perennial plants, live and dead.	%
z_o	5	Roughness height	m

Table 2.2: Results of field data

Table 2.2 Results of field data

Year	Plot	$u_{*t\ \text{field}}$, m s^{-1}	L/h	%Bare Soil	Q kg $m^{-1}s^{-1}$	Soil Type
2008	1	0.83	1.9	5.6	$2.6x10^{-9}$	NM
2008	4	0.68	10	77	$3.6x10^{-8}$	sandy/silty loams
2008	6	0.58	3.6	58	$2.8x10^{-8}$	NM
2008	7	0.36	6.0	68	$2.6x10^{-8}$	loamy sands
2008	9	0.40	3.4	36	$2.9x10^{-8}$	loamy sands
2008	10	0.91	5.3	54	$2.6x10^{-8}$	loamy sands
2008	11	0.40	4.7	54	$2.8\ x10^{-8}$	NM
2008	12	0.51	5.0	49	$3.0\ x10^{-8}$	NM
2008	17	0.51	3.7	40	$1.0\ x10^{-8}$	sandy/silty loams
2008	20	0.58	1.8	31	$1.1\ x10^{-8}$	loamy sands
2008	21	0.51	3.3	48	$1.9\ x10^{-8}$	sandy/silty loams
2008	22	0.43	2.6	11	$7.0x10^{-9}$	NM
2008	25	0.56	4.9	24	$2.4\ x10^{-8}$	sandy/silty loams
2009	1	0.83	1.8	2.0	$3.7\ x10^{-9}$	NM
2009	4	0.68	6.2	58	$2.9\ x10^{-8}$	sandy/silty loams
2009	6	0.58	3.6	59	$2.4\ x10^{-8}$	NM
2009	7	0.36	6.4	71	$2.3\ x10^{-8}$	loamy sands
2009	9	0.40	4.0	47	$2.5\ x10^{-8}$	loamy sands
2009	10	0.91	6.6	53	$1.9\ x10^{-8}$	loamy sands
2009	11	0.40	5.9	58	$3.4\ x10^{-8}$	NM
2009	12*	0.51	4.1	35	$1.9\ x10^{-8}$	NM
2009	17	0.51	3.9	58	$7.8\ x10^{-9}$	sandy/silty loams
2009	20	0.58	1.9	30	$5.0\ x10^{-9}$	loamy sands
2009	21	0.51	5.2	76	$9.5\ x10^{-9}$	sandy/silty loams

Table 2.2 Results of field data

Year	Plot	$u_{*t\ \text{field}}$, m s^{-1}	L/h	%Bare Soil	Q kg $m^{-1}s^{-1}$	Soil Type
2009	22	0.43	2.4	22	$1.2x10^{-8}$	NM
2009	25*	0.56	7.6	57	$3.4\ x10^{-8}$	sandy/silty loams
2010	1	0.83	2.4	4.0	$2.8x10^{-8}$	NM
2010	4	0.68	8.2	66	$4.0x10^{-7}$	sandy/silty loams
2010	6	0.58	4.7	32	$5.0x10^{-8}$	NM
2010	7	0.36	4.9	50	$1.2x10^{-7}$	loamy sands
2010	9	0.40	6.9	67	$1.9x10^{-7}$	loamy sands
2010	10	0.91	7.3	72	$4.2x10^{-7}$	loamy sands
2010	11	0.40	6.8	63	$3.8x10^{-7}$	NM
2010	12*	0.51	4.5	25	$1.9x10^{-6}$	NM
2010	17	0.51	5.3	46	$2.3x10^{-7}$	sandy/silty loams
2010	20	0.58	3.3	35	$4.7x10^{-8}$	loamy sands
2010	21	0.51	2.4	34	$1.2x10^{-7}$	sandy/silty loams
2010	22	0.43	2.0	22	$5.0x10^{-8}$	NM
2010	25*	0.56	6.0	71	$2.5x10^{-7}$	sandy/silty loams

'The $u_{*t\ \text{field}}$ was only measured in 2009 *Plot 12 and 25 had two BSNE stems each. The u_{*t}, L/h, % Bare Soil, and Q are an average of these two BSNE stems. Not measured (NM) means that texture analysis was not completed for the plot.

Table 2.3: $u*_t$ from literature

Table 2.3. Threshold Shear Velocity (Average =0.56 m s^{-1})

u_{*t} **Ranges**	**Soil Type**	**Study Site**	**Citation**
0.4 - >1.54[b] m s^{-1}	Silt Loam	Lake Danby, CA	(Gillette et al. 1980)
0.4 – 0.75[b] m s^{-1}	Loamy Sand	Shadow Mnt, CA	(Gillette et al. 1980)
0.59 – 2.78[b] m s^{-1}	Sandy Loam	Lake Danby, CA	(Gillette et al. 1980)
~0.3 – 1.8[b] m s^{-1}	Dry Lake	Owens Lake, CA	(Gillette et al. 1982)
0.4 – 1.14[b] m s^{-1}	Sandy Crust	Owens Lake, CA	(Gillette et al. 1982)
0.49 – 0.67[b] m s^{-1}	Coarse Sand	Owens Lake, CA	(Gillette et al. 1982)
Smooth – 0.35[b] m s^{-1} Rough – 1.5[b] m s^{-1} Crusted – 0.8[b] m s^{-1}	Sandy Loam	Panhandle TX and OK	(Gillette and Passi 1988)
Smooth – 0.75[b] m s^{-1} Rough – 1.5[b] m s^{-1} Crusted – 2.0[b] m s^{-1}	Silt Loam	Panhandle TX and OK	(Gillette and Passi 1988)
Smooth – 0.3[b] m s^{-1} Rough – 1.0[b] m s^{-1} Crusted – 0.35[b] m s^{-1}	Loamy Sand	Panhandle TX and OK	(Gillette and Passi 1988)
0.3 -1.1[a] m s^{-1}	Unknown	Jornada, NM	(Cahill et al 1996)
0.28 – 0.9[a] m s^{-1}	Unknown	Yuma, AZ	(Cahill et al 1996)
0.37 – 0.56 m s^{-1}	Sandy/silty loams and Loamy sands	Owens Valley, CA	Current study

Vegetated plots are indicated by [a] and undisturbed plots are indicated by [b]

Table 2.4: Regression Results

Table 2.4. Regression Results

Vegetation	R^2: 2008 and 2009[3]	P value: 2008 and 2009	R^2: 2010[4]	P Value: 2010
λ	<0.001[1]	0.76	<0.001	0.44
C_r	0.26[1]	<0.01	0.33	0.02
$\%W_c$	<0.001	0.85	<0.001[1]	0.68
%C	0.41	<0.001	0.03	0.26
$\overline{L}$	0.38	<0.001	0.48	<0.01
$\overline{L}/h$	0.56	<0.001	0.15	0.09
Percent Live Cover	0.25[1]	<0.01	0.11	0.12
Percent Live Cover	0.28[1,2]	<0.01	0.40[2]	0.01
Standard Deviation from Percent Live Cover	0.058	0.11	<0.001	0.83

[1]Log-transformed data; [2]Average of nine pixels; [3]Q is Log-transformed; [4]Q is ranked in the regressions

Table 2.5: Comparison between $Q_{Uniform}$, Q_{Okin}, Q_{field}, and $Q_{Raupach}$, including ANOVA results

Table 2.5 Comparison between $Q_{Uniform}$, Q_{Okin}, Q_{field}, and $Q_{Raupach}$, and ANOVA results

Year	Plot	$Q_{Uniform}$ (kg $m^{-1}s^{-1}$)	Q_{Field} (kg $m^{-1}s^{-1}$)	Q_{Diff} (kg $m^{-1}s^{-1}$)	Q_{Okin}[b] (kg $m^{-1}s^{-1}$)	$Q_{Raupach}$[b] (kg $m^{-1}s^{-1}$)
2008	1	$2.2x10^{-7}$	$2.6x10^{-9}$	$2.1x10^{-7}$	0.00	0.00
2008	4	$5.8x10^{-7}$	$3.6x10^{-8}$	$5.4x10^{-7}$	$1.5x10^{-8}$	$3.1x10^{-10}$
2008	6	$1.4x10^{-6}$	$2.8x10^{-8}$	$1.4x10^{-6}$	$9.0x10^{-7}$	$1.6x10^{-9}$
2008	7	$7.9x10^{-7}$	$2.6x10^{-8}$	$7.6x10^{-7}$	$1.7x10^{-5}$	$9.2x10^{-9}$
2008	9	$1.0x10^{-6}$	$2.9x10^{-8}$	$1.0x10^{-6}$	$1.3x10^{-5}$	$7.3x10^{-9}$
2008	10	$6.5x10^{-7}$	$2.6x10^{-8}$	$6.5x10^{-7}$	0.00	0.00
2008	11	$1.2x10^{-6}$	$2.8x10^{-8}$	$1.2x10^{-6}$	$1.5x10^{-5}$	$7.2x10^{-9}$
2008	12	$1.0x10^{-6}$	$3.0x10^{-8}$	$1.0x10^{-6}$	$2.6x10^{-6}$	$3.6x10^{-9}$
2008	17	$9.6x10^{-7}$	$1.0x10^{-8}$	$9.6x10^{-7}$	$2.4x10^{-6}$	$3.6x10^{-9}$
2008	20	$1.6x10^{-6}$	$1.1x10^{-8}$	$1.6x10^{-6}$	$1.1x10^{-6}$	$2.6x10^{-9}$
2008	21	$1.2x10^{-6}$	$1.9x10^{-8}$	$1.2x10^{-6}$	$3.0x10^{-6}$	$3.6x10^{-9}$
2008	22	$3.6x10^{-7}$	$7.0x10^{-9}$	$3.6x10^{-7}$	$3.0x10^{-6}$	$6.0x10^{-9}$
2008	25	$8.5x10^{-7}$	$2.4x10^{-8}$	$8.5x10^{-7}$	$8.5x10^{-7}$	$2.1x10^{-9}$
2009	1	$1.0x10^{-7}$	$3.7\ x10^{-9}$	$9.9x10^{-8}$	0.00	0.00
2009	4	$6.1x10^{-7}$	$2.9\ x10^{-8}$	$5.8x10^{-7}$	$2.4x10^{-10}$	$9.8x10^{-12}$
2009	6	$1.0x10^{-6}$	$2.4\ x10^{-8}$	$1.0x10^{-6}$	$3.0x10^{-8}$	$1.2x10^{-10}$
2009	7	$5.6x10^{-7}$	$2.3\ x10^{-8}$	$5.4x10^{-7}$	$3.0x10^{-6}$	$3.8x10^{-9}$
2009	9	$1.2x10^{-6}$	$2.5\ x10^{-8}$	$1.2x10^{-6}$	$3.0x10^{-6}$	$2.6x10^{-9}$
2009	10	$6.7x10^{-7}$	$1.9\ x10^{-8}$	$6.5x10^{-7}$	0.00	0.00
2009	11	$6.7x10^{-7}$	$3.4\ x10^{-8}$	$6.4x10^{-7}$	$1.7x10^{-6}$	$2.5x10^{-9}$
2009	12[a]	$7.6x10^{-7}$	$1.9\ x10^{-8}$	$7.4x10^{-7}$	$1.5x10^{-7}$	$5.3x10^{-10}$
2009	17	$1.8x10^{-6}$	$7.8\ x10^{-9}$	$1.8x10^{-6}$	$3.7x10^{-7}$	$5.0x10^{-10}$
2009	20	$1.3x10^{-6}$	$5.0\ x10^{-9}$	$1.3x10^{-6}$	$3.8x10^{-8}$	$1.2x10^{-10}$
2009	21	$1.8x10^{-6}$	$9.5\ x10^{-9}$	$1.8x10^{-6}$	$3.6x10^{-7}$	$5.6x10^{-10}$
2009	22	$6.7x10^{-7}$	$1.2x10^{-8}$	$6.6x10^{-7}$	$8.8x10^{-7}$	$1.9x10^{-9}$
2009	25[a]	$1.2x10^{-6}$	$3.4\ x10^{-8}$	$1.2x10^{-6}$	$6.3x10^{-8}$	$1.9x10^{-10}$
2010	1	$1.1x10^{-7}$	$2.8x10^{-8}$	$8.2x10^{-8}$	0.00	0.00

Table 2.5 Comparison between $Q_{Uniform}$, Q_{Okin}, Q_{field}, and $Q_{Raupach}$, and ANOVA results

Year	Plot	$Q_{Uniform}$ (kg $m^{-1}s^{-1}$)	Q_{Field} (kg $m^{-1}s^{-1}$)	Q_{Diff} (kg $m^{-1}s^{-1}$)	Q_{Okin}[b] (kg $m^{-1}s^{-1}$)	$Q_{Raupach}$[b] (kg $m^{-1}s^{-1}$)
2010	4	$4.4x10^{-7}$	$4.0x10^{-7}$	$4.7x10^{-8}$	$6.0x10^{-9}$	$1.6x10^{-10}$
2010	6	$3.9x10^{-7}$	$5.0x10^{-8}$	$3.4x10^{-7}$	$2.4x10^{-7}$	$1.4x10^{-9}$
2010	7	$5.0x10^{-7}$	$1.2x10^{-7}$	$3.7x10^{-7}$	$1.5x10^{-5}$	$1.0x10^{-8}$
2010	9	$4.0x10^{-7}$	$1.9x10^{-7}$	$2.2x10^{-7}$	$7.5x10^{-6}$	$7.6x10^{-9}$
2010	10	$7.7x10^{-7}$	$4.2x10^{-7}$	$3.6x10^{-7}$	0.00	0.00
2010	11	$6.7x10^{-7}$	$3.8x10^{-7}$	$2.9x10^{-7}$	$1.2x10^{-5}$	$8.0x10^{-9}$
2010	12[a]	$3.3x10^{-7}$	$1.9x10^{-6}$	$-1.6x10^{-6}$	$9.9x10^{-7}$	$3.8x10^{-9}$
2010	17	$5.5x10^{-7}$	$2.3x10^{-7}$	$3.1x10^{-7}$	$1.6x10^{-6}$	$3.5x10^{-9}$
2010	20	$6.8x10^{-7}$	$4.7x10^{-8}$	$6.4x10^{-7}$	$4.2x10^{-7}$	$1.3x10^{-9}$
2010	21	$1.0x10^{-6}$	$1.2x10^{-7}$	$9.3x10^{-7}$	$3.1x10^{-6}$	$3.4x10^{-9}$
2010	22	$5.0x10^{-7}$	$5.0x10^{-8}$	$4.5x10^{-7}$	$5.6x10^{-6}$	$1.9x10^{-9}$
2010	25[a]	$7.4x10^{-7}$	$2.5x10^{-7}$	$4.9x10^{-7}$	$7.4x10^{-7}$	$1.8x10^{-9}$

ANOVA

u_{*t}	u_{*t}	Adjusted P value	Different
Uniform	field	<0.001	YES
Okin	field	0.02	[c]NO
Okin	Raupach	<0.001	YES
field	Raupach	0.005	[c]YES

[a]Average of two BSNE stems;[b] numbers are not normalized or adjusted for homoscedasticity; [c]Nonparametric ANOVA.

Chapter 3: Functional connectivity as a possible indicator of desertification in degraded grasslands

Prepared for submission to *Landscape Ecology*

3.1 Abstract

Changes in vegetation structure within semi-arid grasslands towards increased bare soil and shrub cover and decreased grass cover can be driven by a variety of abiotic and biotic conditions and are associated with impacts to primary productivity, air quality, and biodiversity. In mountain valleys, flood plains, or wherever shallow groundwater supports groundwater-dependent vegetation, vegetation change of this type can be driven by groundwater pumping and water table decline. Theoretical and empirical understanding suggests that as these processes progress, wind erosion increases leading to a reorganization of soil resources potentially supporting continued degradation. One hypothesis is that evidence of connected pathways between bare soil patches, which elevates wind erosion above levels expected from a simple analysis of bare soil area, is an indicator of desertification. To test this hypothesis, we used a combination of field measurements and landscape modeling to examine variation in functional connectivity among (A) grassland locations representing a gradient in degradation, and (B) theoretical neutral landscape models with bare soil cover identical to the degradation gradient. To estimate functional connectivity, we used circuit theory, which integrates all possible pathways to determine a "resistance distance" between any landscape locations. To estimate wind erosion, we deployed sediment traps for three growing seasons (2008-2010). We found that landscapes that were more connected than neutral landscapes with the

same bare soil cover were associated with groundwater decline during the California drought (1987-1992) and greater horizontal sediment flux. This result suggests the enhanced formation of connected pathways at sites that arrived at a particular bare-soil cover via degradation, rather than some other process. Our results support the idea that functional connectivity above that expected by a neutral landscape model is a possible indicator of desertification and that managing for reduced connectivity might limit the effects and extent of desertification.

3.2 Introduction

Grassland ecosystems are imperiled worldwide due to land conversion, desertification, and loss of native plant and animal populations (Kepner et al. 2000; Ceballos et al. 2010). Desertification (i.e., "land degradation in arid, semi-arid, and dry sub-humid areas resulting from climatic variations and human activities" (Helldén 1991; Hulme and Kelly 1993; Le Houffrou 1996; Nicholson et al. 1998; Rubio and Bochet 1998; Huenneke et al. 2002)) of grasslands affects air quality (Schlesinger et al. 1990), climate change (Schlesinger et al. 1990), animal biodiversity (Bestelmeyer 2005), and a myriad of other processes. Aridity is predicted to increase in the next few decades in areas prone to desertification (Seager 2007). Desertification might be expected when and where aridity coincides with over-exploitation of groundwater, intensive grazing, or other forms of disturbance. However, the role of groundwater decline beneath vegetation dependent on saturated sediments within the root zone for all or part of the year has not been extensively evaluated as a driver of desertification. Groundwater decline has been shown to be associated with changes in vegetation structure, from high-cover grasslands to low-cover shrublands, in some cases

dominated by invasive annuals in the intershrub spaces (Elmore et al. 2003). However, there are multiple pathways through which this vegetation change might be observed (Archer et al. 1995; Throop et al. 2012), and since spatial variability in shrub spacing and bare soil cover is inherent to the system even in the absence of groundwater decline, evidence of bare soil by itself is not a convincing indication that desertification has occurred (Helldén 1991; Prince et al. 1998; Nicholson et al. 1998; Prince et al. 2009). For desertification to occur, there must be a process driving soil erosion, declining nutrient availability to plants (Schlesinger and Pilmanis 1998), declining soil moisture (Sharma 1998), and local climate change (i.e., energy and moisture balance within 2m of the surface) (Schlesinger et al. 1990) that leads to a permanent vegetation structure change. To date, research has mainly focused characteristics of desertification: vegetation structure change, soil redistribution, and local climate change (Schlesinger et al. 1990; Peters et al. 2006) yet identifying when and where vegetation change represents desertification, and possible irreversible change, has been problematic.

Okin et al (2009) and Turnbull et al (2008) hypothesized that an indicator of irreversibility in desertification might be the presence of "connected pathways". Connectivity of a landscape is related to the length and size of pathways through vegetation created by wind erosion (Okin et al. 2009). This can be described in terms of "structural connectivity", which is purely related to vegetation structure (i.e., the spacing of shrubs and grasses on the landscape), or functional connectivity (i.e., the length and size of pathways through vegetation linking bare soil patches through a process (e.g., wind erosion)) and how they respond to structural variation (Turnbull et

al. 2008)), which is an assessment of the ability of wind to move sediments between bare soil patches. The ability of wind to cause soil erosion, redistribute nutrients into islands of fertility, and create "streets" in the landscape through connected pathways, offers a mechanism inhibiting the reestablishment of grasslands (Okin et al. 2001; Okin et al. 2009). Due to the reinforcing effects of wind erosion, the establishment of highly connected bare soil patches represents a state change that is functionally different from the previous system (Turnbull et al. 2008). Although connectivity between habitats by biological species has been studied in-depth in landscape ecology (Turner et al. 2001), a framework for how functional connectivity might be implicated in the desertification processes is lacking.

Habitat connectivity models have been used to analyze the spatial distribution of plant and animal species (Turner et al. 2001) and compare connectivity between actual and theoretical neutral landscapes to test hypotheses regarding the controls on connectivity. One widely used approach is to apply graph theory (adopted from disciplines such as geography, information technology, and computer science) to model multiple aspects of landscape connectivity in a single conceptual framework (Bunn et al. 2000; Gardner and Urban 2007; Ferrari et al. 2007; Minor and Urban 2008). Most studies have focused on the movement of plant propagules or animals between habitats (Bunn et al. 2000; Fuller et al. 2006; Minor and Urban 2007; Urban et al. 2009), but we suggest that the applicability of these tools to model wind movement across a landscape should be explored. In one relevant example from Minquin County, China a measurement of cost-distance was used to represent landscape connectivity in a desert environment (Sun et al. 2007); however, cost-

distance only conceptualizes one pathway between bare soil nodes and it is unidirectional (McRae 2006; McRae et al. 2008; Urban et al. 2009; Spear et al. 2010), which might not be appropriate for representing wind movement through a landscape. There is also a recognized need for neutral models of landscapes that can be compared against actual landscapes. Neutral landscape models are produced from random processes that are designed to be free from external forces influencing landscape structure (Gardner and Urban 2007). A neutral landscape could be created, for example, that exhibits the same bare soil patchiness but no more connectivity between bare soil patches than would be expected by chance.

In this paper we use the functional connectivity theoretical framework to assess evidence of desertification across 13 plots in the Owens Valley, California. At each plot we measured total horizontal flux for three growing seasons using standard sediment traps. We then compare these measurements against modeled landscape connectivity using circuit theory, a novel graph based approach to model all possible pathways through a landscape. Circuit theory is based on Ohm's law (McRae 2006; McRae et al. 2008), and in this context, assumes a set of similarities between wind and electrical currents, possibly representing an appropriate functional connectivity model for desertification. Finally, we generate neutral landscape models across a gradient in vegetation cover and compare landscape connectivity of these with actual landscapes at each plot. If circuit theoretical estimates of landscape resistance are an appropriate indicator of desertification, degraded landscapes are expected to be more connected than neutral landscapes, even at the same level of vegetation cover.

3.3 Methods

3.3.1 Study Site

Owens Valley is a semiarid endorheic basin in eastern California situated between the Sierra Nevada and the White-Inyo mountain ranges, receiving a median precipitation of 0.13 m annually. Snowmelt from the Sierra Nevada results in 5.8×10^8 m^3 – 6.3×10^8 m^3 annual runoff that recharges groundwater and surface water in the Owens River drainage basin. Originally these waters flowed to the Owens Lake located at the southern terminus of the Owens River Basin (Hollett et al. 1991; Danskin 1998). Due to annual recharge, the groundwater table is close to the surface across much of the Owens Valley floor supporting alkali meadow vegetation (Sorenson et al. 1991; Elmore et al. 2003; Elmore et al. 2006b).

In 1913, the city of Los Angeles (LA) built the LA Aqueduct and diverted the Owens River leading to the complete desiccation of Owens Lake around 1920. During the California drought from 1987 to 1992, LA increased groundwater pumping, lowering the water table below the root zone of alkali meadows in much of the valley, causing the decline of grass cover, shrub encroachment, and exposing bare soil areas (Elmore et al. 2006b; Elmore et al. 2008). Due to fluctuations in groundwater depth in some areas (but not all), the percent cover and spatial structure of vegetation within alkali meadow are highly variable. Although the largest source of dust emission is from Owens Dry Lake, the similarities between the soils (e.g., puffy salt crusts that are highly susceptible to wind erosion (Reynolds et al. 2007b)), shallow groundwater tables and geologic history of the Owens dry lake and alkali meadow (Orme and Orme 2008) suggest that alkali meadow soils would be

susceptible to wind erosion wherever bare soil is exposed (Saint-Amand et al. 1987). Subsequent dust storms in Owens Valley via Owens Lake and alkali meadow areas (Chapter II) lead to non-compliance with National Ambient Air Quality Standards (NAAQS) for airborne particulate matter (PM_{10}) (US EPA 2008; Reheis et al. 2009).

3.3.2 Plot Selection

Our analysis focused on thirteen plots that were monitored for three growing seasons: 2008, 2009, and 2010. Plot selection focused on covering a range in vegetation structure, from shrubs separated by bare soil, through shrubs separated by meadow, to continuous meadow. Based on research linking vegetation structure and groundwater (Elmore et al. 2003; Elmore et al. 2006b), we found it possible to use spatial and recent temporal variation in groundwater depth to capture the needed variability in vegetation structure. However, we also required that groundwater be sufficiently close to the surface to justify a characterization of "groundwater-dependent" and the soil characteristics associated with shallow groundwater dominated systems (generally thought of as requiring groundwater within 5 m of the surface (Reynolds et al. 2007b)). Control plots were identified that experienced no groundwater decline in the historical record, yet also exhibited a range of vegetation structure, including bare soil area ranging from 32-50%. Plots were identified that were (1) within 100 m of a long-term monitoring well with recorded groundwater depths since 1986 (measured in April of each year); and located within alkali meadow, as identified by a 1986 vegetation survey (City of Los Angeles and County of Inyo 1990). Sixteen plots were initially selected in these areas. However, in 2008, destruction of three plots by cattle that had not been removed at the time of sediment

trap installation reduced the number of study plots to thirteen (Fig. 3.1). We did not re-deploy at these three sites in 2009 or 2010.

3.3.3 Field Measurements

At each plot, Q was measured using four Big Spring Number Eight (BSNE) sediment traps (Custom Products and Consulting, Big Spring, TX) placed on a 1-m pole at heights of 0.1, 0.2, 0.5, and 1 m. This arrangement will henceforth be called a BSNE stem. BSNE stems were installed for three seasons (May to September 2008, 2009, and 2010) within each plot. Although wind erosion during the winter might be significant (Saint-Amand et al. 1987), we avoided this season due to the pervasive presence of cattle over-wintering across most of the Owens Valley floor. During the summer, cattle are typically moved to higher elevation grazing lands. In 2008, we placed a BSNE stem at each plot in a location characterized by either grass or a bare soil. In 2008 and 2009, we did not find differences in the amount of sediment collected between grass and bare soil locations (suggesting low within plot variability in Q, and sensitivity of the BSNE collectors to vegetation and soil conditions in a wider area than the immediate vicinity of the BSNE stem (Vest et al, 2013). Therefore, in 2010, we placed all BSNE stems in bare soil locations. The average diameter of bare soil around the BSNE stems was approximately 3.16 m in 2008, 4.41 m in 2009, and 5.23 m in 2010. In 2009 and 2010, two BSNE stems were placed at two of the plots to explore spatial variation in Q, and tiles were placed around the BSNE stem at each plot to prevent vegetation growth around the lowest trap that might prevent trap movement and obstruct the inlet (something that occurred at plots 1, 4, 7, 10, 20, and 25 in 2008). BSNE stems were not placed within one meter of

shrubs. The height of each trap was measured from the ground surface to the bottom of the inlet. The mass of the sample collected in each trap was divided by sampler inlet area and the duration of collection time, q(z) (kg m^{-2} s^{-1}). The results from each trap were fit to an exponential equation that was integrated from the ground surface to 1 m to estimate Q (kg m^{-1} s^{-1}) (Shao and Raupach 1992; Gillette 1997). The Q was adjusted to account for the known efficiency of the BSNE stem, 90% ± 5% (Shao et al. 1993).

Vegetation cover, gap distribution and vegetation height for each plot was determined using four 50 m line intercept transects run in cardinal directions from the BSNE stem (USDA and NRCS 2004). For each transect, along-transect width (greater than 0.03 m), species, height of vegetation (greater than 0.08 m), and along-transect width of bare soil patches (greater than 0.03 m) were measured. Despite the imposed detection limit in vegetation height, we found that even the shortest vegetation elements were taller than 0.08 m. The vegetation height was measured using a regulation Frisbee® with a hole carved into the center through which a wooden meter stick could be threaded (Mannetje and Jones 2000). The meter stick was placed in each individual plant along the transect, and the Frisbee® was dropped vertically with the meter stick penetrating the hole in the disk. The top of the plastic disk at its stopping location was recorded as the vegetation height. Vegetation transects were conducted in May of 2008, 2009, and 2010 during BSNE stem deployment.

3.3.4 Remote Sensing of Vegetation Cover

National Agricultural Imagery Program (NAIP) 1m color aerial photos from United States Department of Agriculture (USDA) Natural Resource Conservation Service (NRCS) GeoSpatialDataGateway for 2008, 2009, and 2010 were downloaded for Owens Valley, California. In ENVI (Exelis Visual Information Solutions, Inc. 2014), the locations of the thirteen plots with dust collectors were located on these aerial photographs and a 200m x 200m area surrounding each was clipped (i.e., double the area of our vegetation transects at each plot to help with classification). This created 13 different image subsets around the dust collectors for each study year. The NAIP imagery in 2010 included the infrared band. The 2008 and 2009 NAIP imagery lacked the infrared band.

3.3.5 Classification

The decision tree tool in ENVI was used to classify pixels in each image into shrub, grass, and bare soil. The decision tree classification was based on field data collected (i.e., vegetation type and structure) at each plot, indicating where areas of bare soil, shrub, and grass were located. We developed a decision tree using the natural color band 2 (blue) and band 3 (green) from the NAIP imagery (Fig. 3.2). The first step of our decision tree was to identify soil pixels from vegetation pixels. We used band 2 for its ability to distinguish soil and shrub pixels from grass pixels (USGS 2013). For these pixels to be identified as bare soil, they had to have band 2 values greater than 121 (i.e., brighter pixels). The second and third steps of the decision tree distinguished grass from shrub pixels. In the second step, we looked at the contrast between unclassified pixels using band 3. Band 3 was useful for its

ability to access plant vigor (USGS 2013). If these band 3 pixels were greater than 100, we classified them as shrubs, if they were less than 100, they went through another step of classification. The third step used band 2 to identify shrub pixels from grass pixels. If the unclassified band 2 pixel values were less than 70, they were classified as shrubs, and if they were greater than 70, they were classified as grass. The classification image was then compared to the original image to see if the bare soil, shrub, and grass areas matched. If the classification image did not match, we adjusted the values on the tree, but we did not change its structure.

3.3.6 Circuitscape

The first step in running Circuitscape is developing a resistance grid (McRae and Shah 2009). Electrical resistance is the opposition that a resistor offers to the flow of electrical current in a circuit (McRae et al. 2008). In our application of Circuitscape, wind blowing (i.e., electrical current) through a vegetated landscape is diminished when it blows through shrubs or grass, and this effect persists for some distance downwind of the plant (Okin 2008). Therefore, we ranked land cover resistance values between 1 and 9 with 1 representing low resistance and 9 representing high resistance. The following rules were used:

- Resistance values for bare soil: We gave bare soil a resistance value of 1 to represent a high likelihood of sediment movement by wind (Okin et al. 2009). Although, different bare soil surfaces have different soil stability properties due to roughness, particle size, and/or soil crusts (Nickling and Ecclestone 1981; Nickling 1984; Saint-Amand et al. 1987; Gillette et al. 2001; Reynolds et al. 2007b), we could not distinguish these differences from NAIP imagery.

- Resistance values for grass: We gave grass a resistance value of 9 to represent a low likelihood of aeolian sediment movement by wind (Okin et al. 2009).
- Resistance values for shrub: Shrubs reduce shear stress less well than grass but better than bare soil (Okin 2008). Therefore, shrubs were given the value of 3 in our landscape.
- Resistance values in the vicinity of shrubs: Shrubs are taller, therefore influencing shear stress further from the vegetation (Okin 2008). To mimic this effect, we used the neighborhood statistics tool in the Spatial Analyst toolbox in ArcGIS that assigns values to unknown points based on their distance to known points. We applied a filter of a mean radius of 5 pixels to each pixel in the image.

The second step in running circuit theory is developing a focal region grid containing source and sink regions for current to flow, among which landscape resistance is modeled (McRae and Shah 2009). We created four different focal node regions representing the different cardinal directions (N, E, S, W), and connectivity was modeled between each opposite pair (i.e., N to S and E to W). A current map is generated in Circuitscape for each wind position that shows the current density at each raster cell (McRae and Shah 2009). From this current map, Circuitscape calculates a total resistance distance for the landscape based upon N-S and S-N and E-W and W-E wind directions. To develop the resistance distance for the landscape, these resistance distances (n = 2) were averaged for each plot.

3.3.7 Model comparison to field observations

The average resistance distance across each landscape was compared against the total horizontal flux (Q) measured from the deployed BSNEs. The BSNE stem collects soil particles from a lateral area 10 times the height of the dust collector (Okin 2010). As connected pathways increase in grasslands and shrublands, wind erosion removes an increasing amount of aeolian sediment from vegetation interfaces creating higher amounts of aeolian flux (Q) (Okin et al. 2009). Therefore, using linear regression, we examined the relative capability of average current from the wind directions (N, S, E, W) at the thirteen different plots to explain the variability in Q at each plot for 2008, 2009, and 2010.

3.3.8 Vegetation Configuration

To test the effect of vegetation configuration above and beyond that of total cover, we developed neutral landscapes across a wide range of land cover percentages (bare soil, shrub, and grass). Neutral landscape models (NLMs) generate an expected system performance in absence of human-processes in that system (Caswell 1976; Gardner et al. 1987). To develop NLMs, we used Qrule that was developed for scale-dependent analysis of landscape patterns and requires the specification of: (1) type of map (e.g., random map); (2) map characteristics (e.g., land cover percentages); and (3) output generated (Gardner 1986). For the map characteristics, we used different land cover percentages from 0% to 100% (e.g., bare soil, 10%; shrub, 60%; grass, 30%) based upon land cover at our actual landscapes. We took each plot developed by Qrule and created a resistance grid following the methods described for the actual landscapes, and these resistance grids were analyzed by Circuitscape to develop

resistance distance measurements for each plot. Next, we regressed the resistance distance against percent bare soil, percent grass, and percent shrub and the plotted the same for each of our actual landscapes. If our actual landscapes were below the NLMs regression line, we used this as evidence that our actual plots were more connected (lower resistance) than by chance. Okin et al (2009) hypothesizes that connected pathways (i.e., bare soil areas) are an important factor in movement of aeolian sediment and eventual desertification. Therefore, we focus on the percent bare soil regression line to analyze the degradation of our plots. Elmore et al (2003; 2006) indicates that groundwater pumping caused vegetation change in our plots. To evaluate if groundwater decline due to pumping during the California drought (i.e., 1987 to 1996) affected the vegetation structure of our plots resulting in more connectivity, we performed an ANOVA to see if depth to water (DTW) from 1987 to 1996 was different between plots above and below the neutral model regression line. Further, we know that as plots become more connected, bare soil corridors increase resulting in greater amounts of Q (Okin et al. 2009). To see if vegetation configuration below our NLMs regression line produces more Q indicating a more connected landscape with connected pathways, we performed an ANOVA to see if Q is different between plots above and below the neutral model regression line.

3.4 Results

3.4.1 Comparison of Q and landscape resistance

We analyzed Q for all years (i.e., 2008, 2009, and 2010) against resistance distance and found that the relationship depended on year of analysis, but this did not result in a significant relationship between Q and resistance distance using a critical

P-value of 0.05. The resistance distance from 2008 and 2009 explained greater than 50% of the variability in Q (adjusted R^2 = 59%; *P*<0.0001) (Fig. 3.3). There was one plot (22) (Fig. 3.4B) that contained a road that had a lower resistance distance than expected based on the Q. The resistance distance from 2010 explained greater than 50% of the variability in Q (adjusted R^2 = 61%; *P*<0.001) (Fig. 3.3).

3.4.2 Comparison of vegetation configuration

We correlated % shrub, % grass, and % bare soil against resistance distance modeled from the neutral landscapes resulting in the revelation that % shrub (slope = -32.15; offset =168.39), % bare soil (slope = -0.05; offset = 5.69, and % grass (slope = 0.07; offset = 1.96) of neutral landscapes are almost perfectly correlated with resistance distance (adjusted R^2 =98%; *P*<.001) (Fig. 3.5). When we plotted the resistance distance from our actual landscapes (Fig. 3.6), we found that while our landscapes generally followed the same pattern as the NLMs there was scatter, with some landscapes plotting above and some below that expected from a neutral landscape. The mean DTW during the drought of 1987-1992 of plots above and below the NLMs regression line was significantly different (*P*=0.04), with groundwater during the California drought being deeper in plots below the NLMS regression line than above (i.e., less resistance). The mean Q in landscapes plotting above and below the NLMs regression line was also significantly different (*P*=0.002). Therefore, at any given level of bare soil, landscapes plotting below the regression line were those that experienced deeper groundwater during the drought and exhibited greater total horizontal flux than landscapes plotting above the NLMs regression line.

3.5 Discussion

Many of our plots have declining alkali meadow grasses with shrub replacement and exposed bare soil (Elmore et al. 2006b). Given previous work that showed as grasslands degrade forming long connected pathways, fetch size increases for wind erosion to promote saltation and increase Q (Okin et al. 2009), we interpret the relationship between Q measured in the field and resistance distance modeled in Circuitscape. Q increased as resistance distance decreased (i.e., more connected) (Fig. 3.3) supporting the idea that connected pathways form in the landscape promoting dust emission. Plots with intact grass cover and low bare soil area reported the highest resistance distances and smallest Q (Fig. 3.3). Although vegetation cover is important, vegetation structure arrangement controls the development of connected pathways in the landscape (Peters et al. 2006; Turnbull et al. 2008; Okin et al. 2009).

Our plots with higher Q were more connected than plots with the same percent vegetation and bare soil cover indicating that functional connectivity is responsible for higher Q values (Fig. 3.6). Our plots below the NLMs regression line contain more connected pathways than NLM plots with similar percent cover (Fig. 3.4A and Fig. 3.4C). This indicates that long connected pathways form in our plots producing higher amounts of Q from wind erosion. This is supported by the work of Okin et al (2009), which argues that functional connectivity (e.g., the way wind moves through the vegetation structure) is the underlying and unifying concept for understanding desertification.

Our plots that were more connected than a corresponding NLM had higher groundwater declines during the California drought in the 1980s than plots above the

neutral model regression line (Fig. 3.6C). This indicates that increased groundwater decline does not just change the structure of vegetation (Elmore et al. 2003; Elmore et al. 2006b), but it also changes the functional connectivity by creating longer connected pathways allowing more wind erosion. Groundwater decline, even for only a few years, kills off grass giving shrub establishment (i.e., when soil moisture was high enough for shrub recruitment) a competitive advantage as long as soil is stable; however, within "streets" of bare soil (i.e., easily erodible soil), shrubs cannot establish. The vegetation structure following the drought reflects the formation of these "streets".

When analyzing groundwater decline above and below the NLMs regression line, two plots did not match the relationship. The first plot had increased groundwater decline due to pumping during the drought, but grass and shrubs recolonized bare soil areas after pumping was halted. Therefore, this vegetation structure would not be indicative of a heavily pumped meadow. However, when we examine this plot based on percent grass cover, we see that it is more connected than the same percent grass cover would indicate (Fig. 3.6A). This plot may still contain a remnant of degradedness indicating a permanent functional change (i.e., plot is below the NLM regression line for percent grass) although the structure recovered. This is supported by Turnbull et al (2008) that indicates once a structural and functional change have occurred the landscape contains hysteresis when trying to move back to the original state (i.e., alkali meadow). The second plot was not pumped heavily in the drought, but the vegetation structure is indicative of a heavily pumped meadow with increased groundwater decline. Based on field observations, this plot had a road

previously through it that was eventually abandoned, but we believe the legacy of the road's affect on vegetation structure lingers making it more degraded than groundwater pumping would indicate.

There are many remaining uncertainties to be investigated. Although, we used wind erosion theory to develop our resistance grids at each plot, we used only one value for each land cover class: shrubs, grasses, and bare soil. Yet, field observations of crustal differences in bare soil and differences in sheltering distances of different shrubs and grasses indicate that there is likely a range of values for different types of bare soil crusts, grasses, and shrubs. Unfortunately, air photos make these differences hard to quantify. In 2010, resistance distances explained more variability in Q (R^2=0.61) than in 2008 and 2009 (R^2=0.59). This could be due to air photos in 2010 containing an infrared band providing better classification than air photos without the infrared band in 2008 and 2009. This difference could also be explained by dryer and gustier conditions in 2010 in Owens Valley compared to 2008 and 2009 (Vest et al., 2013). Also, some of our plots showed more connectivity than expected by their Q value (Fig. 3.3), which may be due to our classification comprising an area of 200m x 200m while our Q measurements comprised an area of 100m x 100m. By expanding the classification area, we sometimes included dirt roads (e.g., plot 22) and other bare soil areas, which creates more connected areas (i.e., lower resistance distance) outside the Q measurements and predicted by NLMs (Fig. 3.4B & D).

For future research, a refinement of the resistance grid through fieldwork to determine average roughness values for bare soil at different locations and determine the differing sheer stresses of bare soil, shrubs and grass at certain distances

downwind could be used to reduce uncertainty in our model results. An expansion of the analysis to the entirety of Owens Valley using Circuitscape coupled with Qrule could also be useful, potentially highlighting currently unknown areas of desertification. We could also expand this analysis outside of Owens Valley into other groundwater-dependent systems such as in Minquin, China. Further research into the history of "memory" in vegetation structure change in groundwater-dependent meadows is needed.

3.6 Conclusions

We show here, that vegetation changes associated with increased groundwater decline are also associated with an increase in connectivity above and beyond that expected by a neutral model with the same bare soil area. In this study, plots that were below the NLM regression line (i.e., more connected than predicted by vegetation cover alone) (Fig. 3.6C) had significantly higher groundwater pumping during the 1980s California drought (P=0.04). Also, these same plots had higher Q values (P=0.002) indicating that the vegetation configuration for these plots formed a more connected landscape, and that this configuration is related to heavy groundwater pumping during the 1980s California drought. These plots spanned a large range in bare soil cover (from 11% to 50%), and therefore, based on casual inspection might not be categorized as degraded. This agrees with our working conceptual model and with previous research that as vegetation degrades in an alkali meadow, shrub invasion increases (Elmore et al. 2003; Elmore et al. 2006b) redistributing soil resources, opening up bare soil areas, and increasing wind erosion resulting in high

spatial variation in resources (Okin and Gillette 2001; Peters et al. 2006) generating feedbacks fueling sustained connectivity (Peters et al. 2006). We show that using NLMs in desertification research is useful because they provide a way to tests hypothesis concerning connectivity in different landscape structures, thus accounting for wide variability in structure due to external forces other than wind.

California is currently experiencing another drought that is persistent (Brewer 2014) with an estimated 50% less annual precipitation with 30% less snowpack derived runoff (LADWP 2014a); however, LA is demanding an increase in groundwater pumping for water year 2014-2015 (LADWP 2014a). Under these conditions of reduced climatic inputs but sustained or increased demand, it is important for natural resource managers to identify areas that may experience or are experiencing desertification. In these areas, sustainable management would dictate that groundwater tables be maintained within vegetation root zone. Use of the methods described here might be used to identify such areas and help natural resource managers target areas susceptible to desertification.

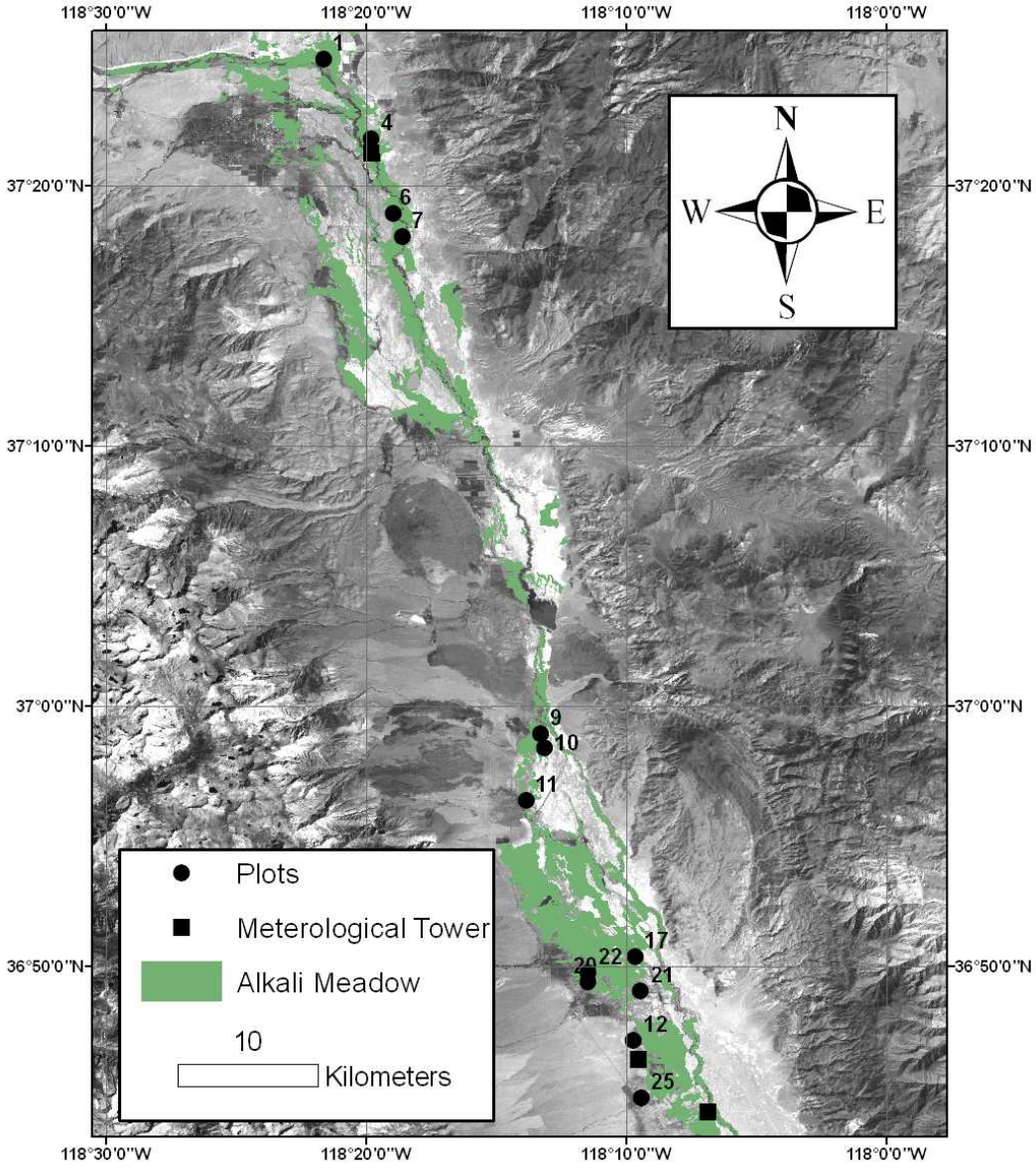

Figure 3.1 The plots where BSNEs stems were installed across the Owens Valley in alkali meadow identified using the vegetation survey of 1986 [James et al., 1990]. There are two meterologial towers located in the southern half of the valley and one located in the north (squares). The background is a Landsat TM image from September 8, 1992.

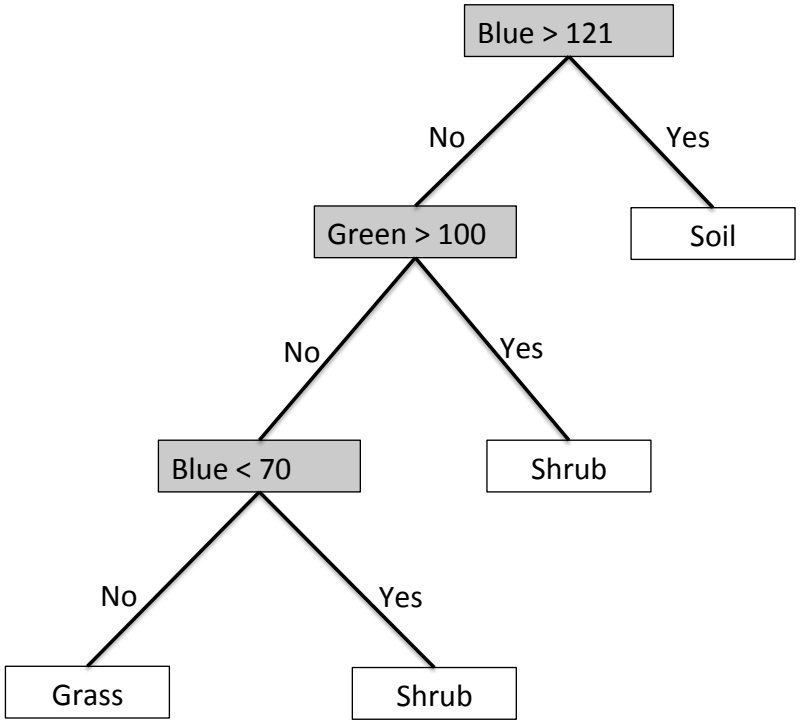

Figure 3.2 The decision tree classification was developed using the natural color band 2 (blue) and band 3 (green) from the NAIP imagery and field data at each plot to indicate where areas of bare soil, shrub, and grass were located.

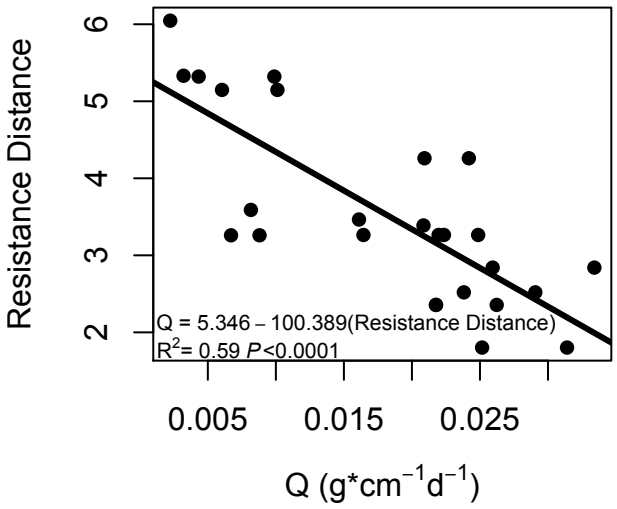

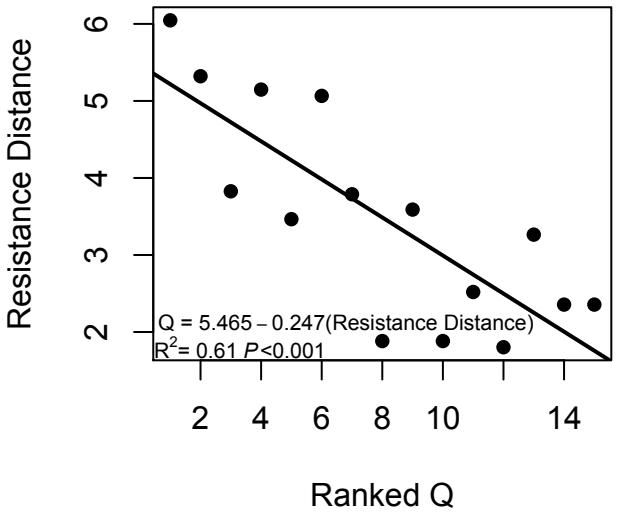

Figure 3.3 Resistance distance vs. total horizontal flux (Q) for 2008 and 2009. Resistance distance in 2008 and 2009 explained 59% of the variability in Q (P<0.0001). The resistance distance in 2010 explained 61% of the variability in Q.

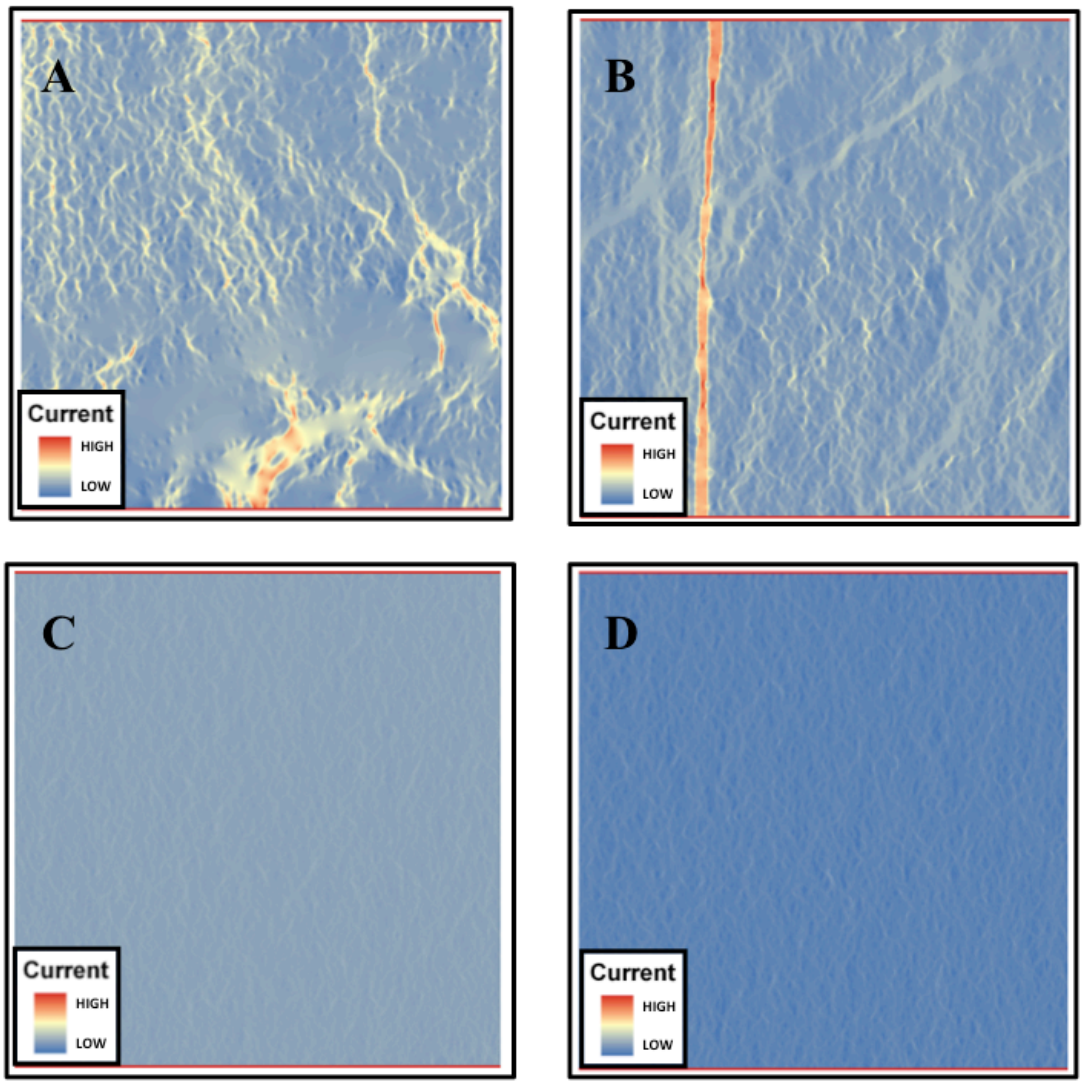
A
Current
HIGH
LOW
B
Current
HIGH
LOW
C
Current
HIGH
LOW
D
Current
HIGH
LOW

Figure 3.4 Images are the current maps at the same scale produced from running Circuitscape. The more connected an area is, the redder the area. Image A shows the current map for degraded plot 12. Image B shows the current map for intact plot 22. Plot 12 has more connected pathways than plot 22. In plot 22, the long straight connected pathway is a road. Image C shows the neutral landscape model for plot 12 at the same scale and percent vegetation cover. Image D shows the neutral landscape model for plot 22 with the same scale and vegetation cover. The neutral landscape models for both plots do not contain the long connected pathways that are in Images A and B, but NLM C has more connection than NLM D.

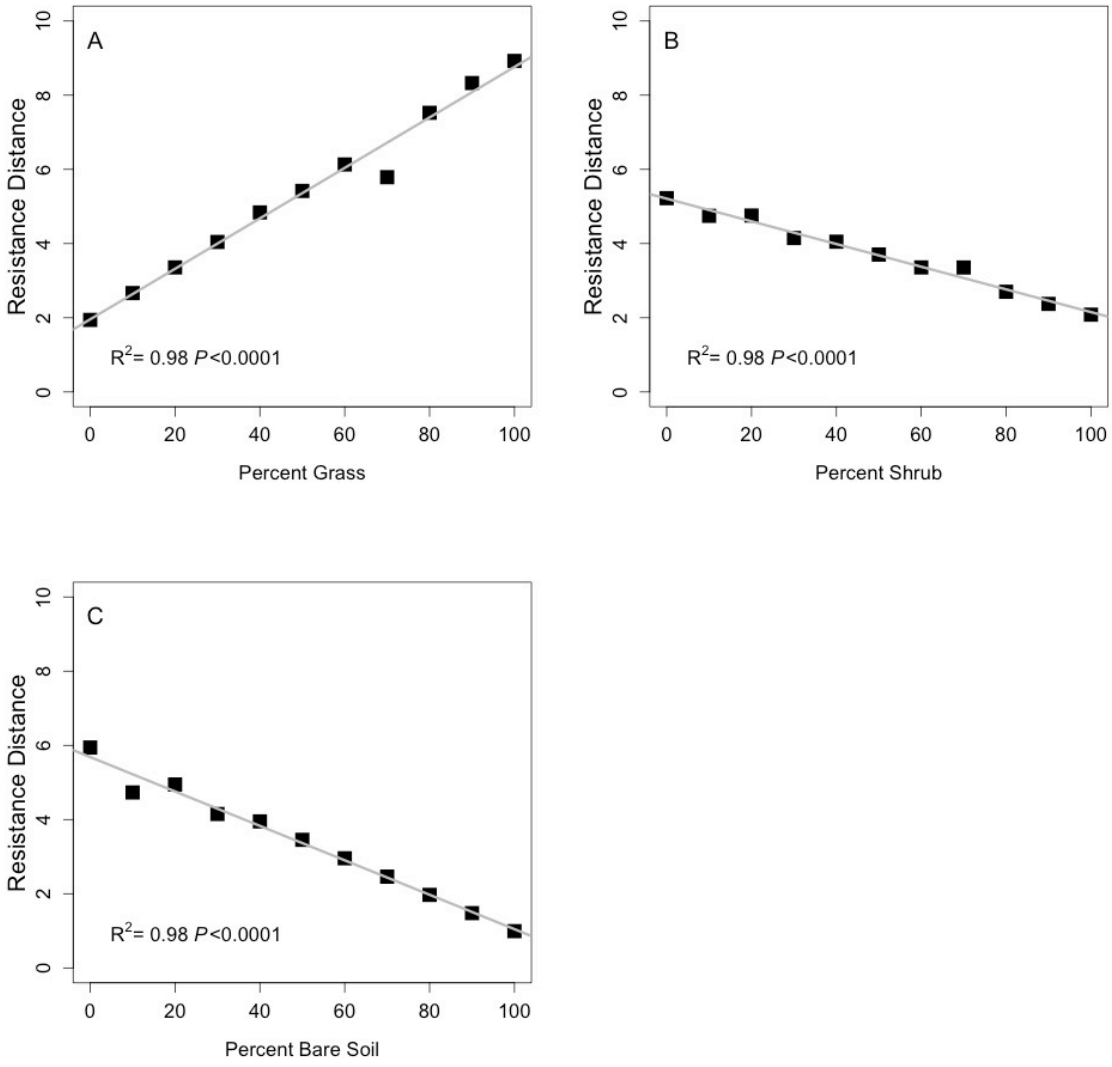

Figure 3.5 Percent grass vs. resistance distance for our neutral landscapes (adjusted R^2 = .98; P<0.0001)(A). Percent shrub vs. resistance distance for our neutral landscapes (adjusted R^2 = .98; P<0.0001) (B). Percent bare soil vs. resistance distance for our neutral landscapes (adjusted R^2 = .98; P<0.0001) (C).

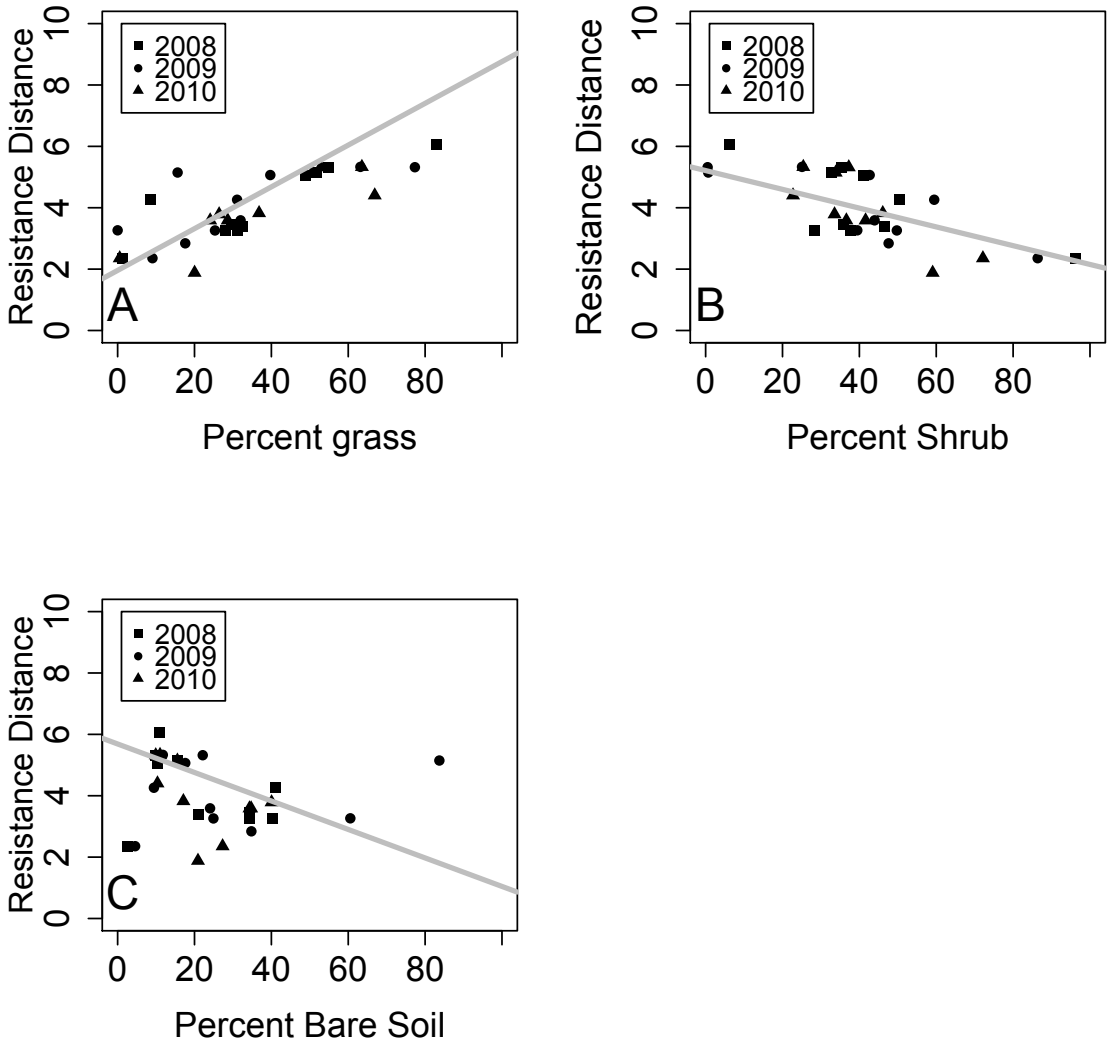

Figure 3.6 Percent grass vs. resistance distance for 2008, 2009, and 2010 plotted on the regression line for our neutral landscapes (adjusted R^2 = .98; P<0.0001)(A). Percent shrub vs. resistance distance for 2008, 2009, and 2010 plotted on the regression line for our neutral landscapes (adjusted R^2 = .98; P<0.0001) (B). Percent bare soil vs. resistance distance for 2008, 2009, and 2010 plotted on the regression line for our neutral landscapes (adjusted R^2 = .98; P<0.0001) (C).

Chapter 4: Dust suppression as an ecosystem service of groundwater-dependent meadow: a case study from Owens Valley, California

Prepared for submission to the *Journal of Arid Environments*

4.1 Abstract

Water transfers for agricultural and urban uses may alter the source regions' ecology leading to ecosystem service degradation. This is evident in Owens Valley, California where water withdrawals from groundwater pumping and surface water diversion to Los Angeles has led to the drying of Owens Lake and increases in particulate matter < 10 μm (PM_{10}) to levels that exceed National Ambient Air Quality Standards (NAAQS). Attempts to mitigate increased PM_{10} emissions in Owens Lake has been partially successful through the planting of alkali meadow, but this, in turn, has required groundwater pumping and water transfers within the Owens Valley. Vegetation structure and monitored aeolian sediment transport was analyzed to evaluate the relationship between meadow degradation and air quality. Also, air quality data was analyzed to evaluate the evidence that alkali meadows contribute to PM_{10} emissions in Owens Valley. Results show that (1) management practices have generated a new mid-valley alkali meadow source of PM_{10} pollution that was previously unrecognized in Owens Valley; (2) there is a need for more comprehensive ecosystem and groundwater management to mitigate the air quality issues within Owens Valley; and (3) Los Angeles must reduce their current demand for water from Owens Valley through mandatory water restrictions in both drought and non-drought periods.

4.2 Introduction

Human activities strongly influence dust generation and its subsequent transport and deposition (Schlesinger et al. 1990; Schlesinger et al. 1996a; Lal 2003). Grazing, off-road vehicle use, and water extraction have contributed to dust generation, leading to serious human health issues and negatively impacted land use sustainability (Prospero 1999; Wiggs et al. 2003; Fubini and Fenogolio 2007; Hervàs et al. 2009; Zhang et al. 2013). Of particular concern are hydrologically closed (endorheic) basins where sediment and evaporite minerals collect in valleys creating saline lakes of temporally varying size and variable, shallow groundwater tables (Elmore et al. 2008; Dorsaz et al. 2013; Seeboonruang 2014). Examples of these conditions include Lake Chad in sahelian Africa and the Aral Sea in central Asia where water diversions combined with recent climate change, produce large, globally-relevant dust emissions (Wiggs et al. 2003; Elmore et al. 2008).

The Great Basin is the largest endorheic basin in the United States and contains many playas, the dustiest of which exhibit shallow groundwater (Reynolds et al. 2007b). Historically, one of the largest remaining saline lakes of the Great Basin was the Owens Lake (Fig. 4.1), which received recharge from the extensive snowpack of the eastern Sierra Nevada Range. Through the late 19th and early 20th century, water diversions caused the Owens Lake to begin to desiccate, leaving behind an alkali playa with shallow groundwater. In 1913, the city of Los Angeles built the Los Angeles Aqueduct and diverted the Owens River, causing the complete desiccation of Owens Lake hereafter referred to as Owens Dry Lake. In 1973, Los

Angeles built a second aqueduct and increased groundwater pumping in the northern sections of the valley. The subsequent increasing pressure on groundwater resources led to changes in regional vegetation, including increases in shrub and exotic annual plant cover, especially during the California drought from 1987 to 1992 (Elmore et al. 2006b; Elmore et al. 2008).

During August 1987, the USEPA designated the southern Owens Valley as an area in violation of the National Ambient Air Quality Standards (NAAQS) for the generation of particulate matter < 10 μm (PM_{10}). In January 1993, southern Owens Valley was classified as "serious non-attainment" by the USEPA. The Los Angeles Department of Water and Power (LADWP) was required to meet the 24-hour NAAQS for PM_{10} by December 21, 2006, as mandated by the Clean Air Act Amendments (1990), by successive 5% reduction in PM_{10} emissions per year. The goal was to meet NAAQS by March 23, 2012, which was not met (GBUAPCD 2012) and was extended to March 23, 2017(USEPA 2007). Owens Dry Lake is now the largest source of PM_{10} emission in North America (GBUAPCD 2008). To achieve the ultimate attainment goal, Los Angeles is implementing gravel distribution and "within valley" uses of water such as shallow flooding and managed vegetation areas (i.e., alkali meadows). In addition, moat and row enhancements along with other control measures are used on the playa surface (GBUAPCD 2013). This dust mitigation project on the Owens Dry Lake bed will be the largest dust mitigation project worldwide. Nearly all of the water for shallow flooding and alkali meadow planting comes from surface and groundwater extracted from alkali meadow in the northern valley that is extensive and supported by a shallow groundwater aquifer.

Groundwater fluctuation (decline and recovery) is a common feature of northern Owens Valley due to groundwater pumping regulations. During the California drought from 1987 to 1996, groundwater was pumped below the alkali meadow vegetation root zones causing vegetation desiccation and opening up bare soil areas (Elmore et al. 2003; Elmore et al. 2006b). Groundwater pumping affects the spatial distribution of vegetation types and cover with overall cover declines and vegetation community changes from grass to shrubs and exotics (Muñoz-Reinoso 2001; Elmore et al. 2003; Barron et al. 2014). Alkali meadows are likely susceptible to degradation in the form of vegetation and soil structure changes that are connected with increases in dust emission resulting from groundwater withdrawals (Vest et al. 2013).

Implicit to the assumptions of the Owens Dry Lake mitigation effort, is the notion that transferring water from one area of the valley to another will reduce the overall magnitude of dust emissions. Vest et al. (2013) found that total horizontal flux (Q), which is related to vertical flux that produces PM_{10} (Gillette et al. 1997) was occurring in alkali meadows in the northern valley. Therefore, PM_{10} production may be occurring in the northern valley that was previously unknown. To test this assumption, we evaluated the effect of groundwater pumping on Q, PM_{10} generation, and air quality in Owens Valley. Atmospheric PM_{10} concentrations at 10-m elevation were measured throughout the valley to quantify spatial patterns in PM_{10} concentrations (i.e., northern valley, middle valley, and Owens Dry Lake). Further, we estimated PM_{10} emissions from mass transport measurements from alkali meadow plots and discuss the consequences for air quality.

4.3 Study sites

During the drought of the late 1980s and early 1990s in California, groundwater resources represented a large portion of water exported (Elmore et al. 2003) with water table depths between 2 and 10.9m (Fig 4.2). Before the drought in the mid-1980s, average water table depths beneath alkali meadows were between 2 to 2.4 m. Elmore et al. (2003) explored vegetation changes resulting from climate and hydrology by classifying vegetation response patterns using spectral mixture analysis and isodata clustering analysis that resulted in 13 distinct vegetation change classes. The effect of precipitation and/or declining water tables on these vegetation change classes were compared to precipitation for years 1990-1996 and water table data for the difference in years 1986 and 1992 (Elmore et al. 2003). These distinct vegetation change classes were grouped under three broad categories: depth to water (DTW) dependent changes, precipitation dependent changes, and static vegetation conditions (NoChg) (Elmore et al. 2003). Plots from Vest et al. (2013) were categorized based on these vegetation change classes to better understand the relationship between groundwater, vegetation, and Q. The plots were located within five change classes: static vegetation conditions (NoChg2) and DTW dependent vegetation changes (DTW3, DTW4, DTW5, and DTW6). NoChg2 contains 4 study plots and comprises the largest area (27,464 ha) in the valley (Elmore et al. 2003). This change class has both phreatophytic and nonphreatophytic species that were not correlated with precipitation (Elmore et al. 2003). It contains the most stable low cover vegetation parcels in the valley between 1986 and 1998 (Fig. 4.3) and has salt encrusted friable soil within large bare soil areas that are easily eroded. The next four DTW dependent

change classes (DTW3, DTW4, DTW5, and DTW6) occur in areas of groundwater extraction that have experienced a linear decrease in % live cover from 1986 to 1990 during the drought (Fig. 4.3). DTW3 contains 1 plot that is dominated by meadow communities that experienced increased cover following the drought due lower DTW allowing for reestablishment of native species (Fig. 4.2 & 4.3). The DTW4 change class contains 1 plot and is common in areas where water spreading occurred before the drought to augment the water table (Elmore et al. 2003). These areas, located in the mid-valley (Fig. 4.2), were pumped during the drought with subsequent declines in % live cover from meadow to alkali scrub (Fig. 4.3). This area's DTW is still higher than before the drought and continues to have high % live cover change (Fig. 4.2 & 4.3). DTW5 contains 5 plots that occur adjacent to DTW4 and is associated with changing pasture irrigation practices dominated by tamrisk, scrub parcels, and exotic species (Elmore et al. 2003). Alkali meadow vegetation was reestablished in some plots due to water table recovery, while other plots contain alkali scrub and exotics with higher DTW than pre-drought levels (Fig 4.2). The DTW6 change class contains 2 plots and is the largest DTW change class (7764 ha) (Elmore et al. 2003). It is characterized by meadow and phraetophytic scrub communities that had low cover prior to the drought and even lower cover since the drought (Elmore et al. 2003). The declining vegetation effects due to groundwater decline through pumping are similar to other areas around the world (Stromberg et al. 1996; Shafroth et al. 2000; O'Grady et al. 2006; Overton et al. 2006). This declining vegetation cover response is largest at the initiation of groundwater pumping (Elmore et al. 2006b).

4.4 Methods

We made measurements at several spatial scales over a three year period: plot-based observations of total horizontal flux (Q) (i.e., the horizontal movement of sediments within 1-m of the soil surface (Cahill et al. 1996)) across a gradient of meadow degradation; plot-based measurements of vegetation cover and structure; and PM_{10} observations at locations along a north-south transect in Owens Valley, CA. We identified thirteen plots across a gradient in meadow degradation based on Elmore et al. (2003) (Fig. 4.1). Q was measured using four Big Spring Number Eight (BSNE) aeolian sediment traps mounted on a 1m pole; henceforth, referred to as a BSNE stem. We placed a BSNE stem in each plot in 2008, 2009, and 2010 between May and September and an additional BSNE stem in two of the plots in 2009 and 2010. The mass of the sample collected in each trap was divided by sampler inlet area and the duration of the collection interval. The results from each trap were fit to an exponential equation then integrated from ground level to 1m to estimate Q (Gillette et al. 1997). The Q was adjusted based upon the efficiency of the BSNE stem, 90% ± 5% (Shao et al. 1993).

Vegetation structure was measured annually at each plot using four 50m line intercept transects run in cardinal directions from the BSNE stem. For each transect, along-transect plant width (greater than 3cm) species, height (greater than 8cm), and along-transect width of bare soil patches (greater than 3cm) were recorded. Next, we divided our thirteen sites into five change classes (DTW3, DTW4, DTW5, DTW6 and No Change 2) as determined by Elmore et al. (2003). We compared Q from each

of these change classes and Q from Owens Dry Lake using ANOVA of log-normalized data with a *post hoc* Tukey Honest Significant Difference (HSD).

Elmore et al. (2003 and 2006) found that, depth to water (DTW) causes desiccation of groundwater-dependent vegetation and an increase in bare soil area, which might lead to greater wind erosion and larger dust emission. Therefore, to determine whether DTW is related to Q, we acquired DTW measurements in April of each year when snowmelt causes low DTW values (Danskin 1998). The number of times DTW was higher than 2.5m (the average maximum affecting rooting depth of alkali meadow vegetation (Elmore et al. 2006b)) between 1986 and 2010 was regressed on Q to determine if the number of times water was below the root zone could influence the amount of Q. Next, we regressed the difference in DTW and average DTW between 1986 and 1997 (years affected by high groundwater pumping) on Q to determine if water levels during the drought affected current Q. Finally, DTW levels in 2008, 2009, and 2010 were regressed on Q to determine whether current DTW levels affected Q.

PM_{10} concentrations, wind velocity, and wind direction were acquired from five Great Basin Unified Air Pollution Control District (GBUAPCD) monitors that spanned the length of the Owens Valley (Fig. 4.1). We compared the average PM_{10} concentrations, peak PM_{10} concentrations, and 24-hour PM_{10} concentrations greater than 50 $\mu g\ m^{-3}$ (i.e., out of compliance with California Ambient Air Quality Standards) at the five locations in 2008, 2009, and 2010 during our sampling period (Fig. 4.1). We received data from GBUAPCD for the number of National Ambient Air Quality Standards (NAAQS) exceedances at the two locations near Owens Dry

Lake (0 and 9 km). For the other three locations in the valley, we compared 24-hour PM_{10} concentrations greater than 150 μg m^{-3} (i.e., out of compliance with NAAQS). To examine whether the PM_{10} concentrations at these sites were influenced by meadow or dry lake sources, we divided our PM_{10} concentrations into two groups (1) northerly winds (270° to 90°; winds originating north of Bishop, CA and presumed not to be influenced by the lake) and (2) southerly (90° to 270°; winds originating from the lake) based upon wind velocity data acquired concurrently and performed an ANOVA. Because variation in wind velocities may affect PM_{10} concentrations, we compared wind velocities at the five PM_{10} stations using ANOVA. A segmented regression of wind velocity on measured PM_{10} concentrations was used to test whether an increase in wind velocity increased PM_{10} concentration. Because we sampled during a limited time frame each year (May to September), an ANOVA on PM_{10} concentrations in each season (Fall, Winter, Spring, and Summer) was used to test whether the PM_{10} concentrations during the study period were higher than usual.

Gillette et al. (1997) determined the ratio of F_a (vertical flux of particles, PM_{10}) to Q to be 2.75×10^{-4} m^{-1} at Owens Dry Lake using a network of BSNE stems, anemometers and PM_{10} samplers directly aligned with the wind direction. We applied this relationship to Q measurements at our plots to estimate PM_{10} production from horizontal sediment transport. This calculation assumes a similarity between the playa soils and wind regime and conditions within alkali meadows, which is supported by the prevalence of groundwater effects on surface soil texture and composition throughout the Owens Valley and the relative proximity and geological setting of the two areas.

4.4.1 Case Study

Two sample plots were compared to assess the effect of DTW on levels of vegetation and Q (Fig. 4.4). One plot (plot 6) was not pumped and had a stable groundwater supply while the second plot (plot 12) was pumped during and after the drought with resulting variability in groundwater depth (Fig. 4.5). Measurements of DTW at each plot (i.e., highest DTW and lowest DTW) during the years of heavy groundwater pumping (1987-1996) were compared to understand how groundwater pumping affects both % live cover change during the drought and current Q measurements. Current measurements of DTW levels were compared to understand how DTW levels affect vegetation cover and Q. Vegetation measurements at the plots of scaled gap size (average bare soil area divided by average plant height) and average gap size (average bare soil area) during the sampling period were used to explore the role of vegetation on Q in each plot.

4.5 Results

The Q between cover change classes were not significantly different (P=0.131) (Fig. 4.6; Table 4.1). The Q between the plots in the change classes compared to Q in Owens Dry Lake were significantly different (P<0.001) (Fig. 4.6; Table 4.1). Owens Dry Lake had the largest Q followed by cover change class categories, DTW4, NoChg2, DTW5, DTW6, DTW3 (Fig. 4.6). The mean vertical flux followed the same trend in both the cover change classes and Owens Dry Lake (Table 4.1).

Regression analysis shows that DTW currently and during the drought did not explain the variance in Q. The difference between the highest and lowest DTW

during 1987 and 1996 did not explain the variance in Q (R^2=0.03; *P*=0.15) nor did the average DTW during the drought (R^2=-0.03; *P*=0.75). Also, the number of times DTW was higher than 2.5 m did not explain the variance in Q (R^2=0.08; *P*=0.16) nor did DTW during 2008, 2009, and 2010 sampling seasons (R^2=0.01; *P*=0.24).

The PM_{10} concentrations for northerly and southerly wind events, initially assumed to differ by direction due to the southerly position of Owens Dry Lake, were averaged because no significant effects of wind direction were found (*P*=0.456). Wind velocities did not differ between PM_{10} stations (*P*=0.171). Higher wind velocities did not explain the spatial variance in PM_{10} concentrations (R^2 = 0.18,). However, further examination of this relationship shows that above 12.17 m s^{-1} where the variability of PM_{10} concentration is minimal, concentrations rise with increasing wind velocities (R^2 = 0.18; *P* <0.001). Springtime exhibited significantly higher PM_{10} concentrations (*P*<0.001) than winter, fall, and summer (sampling season). Comparisons between PM_{10} concentrations in the winter, fall, and summer were not significantly different (summer and fall: *P*=0.10; winter and fall: *P*=0.99; winter and summer: *P*=0.06).

Peak concentrations for PM_{10} were the highest at Owens Dry Lake for all years and sample sites and decreased at farther distances from the lake (Fig. 4.7). The highest average annual PM_{10} exceedance also occurred at Owens Dry Lake during the 2010 sampling period (Fig. 4.7). Air quality exceeded PM_{10} CAAQS concentrations at all PM_{10} monitoring locations (Fig. 4.8). Air quality exceeded PM_{10} NAAQS concentrations at two PM_{10} monitoring locations for 2008 and three PM_{10} monitoring locations for 2009 and 2010 (Fig. 4.8).

4.5.1 Case Study

Plot 6 is within the NoChg2 cover class and is located in the northern valley above the aqueduct intake (Table 4.1). DTW has remained stable near the surface (Fig. 4.2; Table 4.1) and supports characteristic grass species of alkali meadow (i.e., saltgrass (*Distichlis spicata* (L.) Greene) and alkali sacaton (*Sporobulus airoides* Torr.) that form dense grasslands in areas where the water table is shallow (Sorenson et al., 1991) (Fig. 4.4). This vegetation cover did not change during the drought (1987 to 1992) and heavy groundwater pumping (1987 to 1996) (Fig 4.2). Plot 12 is within the DTW4 cover class (Table 4.2) and is located in the mid-valley below the aqueduct intake and near a pumping well. Plot 12 was heavily pumped during the drought between 1987 and 1996 (Fig. 4.2; Table 4.2) and again in 2005, and it still has not recovered to previous levels before the drought (Fig. 4.2). Plot 12 is dominated by alkali meadow shrub species (i.e., Nevada saltbush (*Atriplex lentiformis* ssp. *torreyi*) and rubber rabbitbrush (*Ericameria nauseosa*) that occur in areas with deeper groundwater (Sorenson et al. 1991) (Fig. 4.5). Plot 12 has Q similar to plot 6 for years 2008 and 2009; however, plot 12 in 2010 had significantly higher average Q that plot 6 (Table 4.2). Plot 12 also had higher scaled gap size and higher % live cover change than plot 6 but lower average gap size and resistance distance (i.e., bare soil areas are more connected in Plot 12) (Table 4.2). Plot 6 and 12 produce vertical flux that contributes to PM_{10} concentration, but plot 12's vertical and horizontal flux in 2010 are one to two orders of magnitude higher (Table 4.2). Not all plots within the study site behaved the same way as plot 6 and 12.

4.6 Discussion

Alkali meadows in Owens Valley are a source of PM_{10} air pollution (Fig. 4.6 and 4.7). Surface water diversions and groundwater pumping during the past several decades have caused declining grass cover and increasing cover of perennial shrubs and annual weeds (Elmore et al. 2003; Elmore et al. 2006b), increasing the susceptibility of puffy (sensu Reynolds et al., 2007) salt-affected soils to wind erosion. In alkali meadows affected by DTW changes in vegetation cover during the drought (DTW3, DTW4, DTW5, and DTW6) hereafter referred to as degraded alkali meadows, Q is similar to Q measured in degraded environments elsewhere, including Minquin, China (Dong et al. 2010) and Chichuahuan Desert mesquite dunelands (Bergametti and Gillette 2010). The Q from Owens Dry Lake is 3 orders of magnitude larger than Q from degraded alkali meadows (Fig. 4.6). Higher Q from Owens Dry Lake are most likely due to unhindered wind gusts across the lake (Gill 1996) that are able to remove more PM_{10} than in the more protected northern valley. The within plot variability of Q is large in every change class (Fig 4.6; Table 4.1) and can be explained by these plots having sufficient vegetation cover to stabilize the soil suggesting that remobilization of the soil can occur episodically instead of regularly possibly due to high winds, low humidity, and colder temperatures (e.g., 2010 measurements of Q). All the DTW trajectories demonstrate a partial recovery of groundwater and total vegetation cover (Fig 4.2), which have not resulted in a statistically significant increase in Q measured today (Fig 4.6). This is possibly due to densely growing shrubs in our DTW plots not allowing for a large enough scaled gap size conducive to regular wind erosion even though threshold shear velocity is

exceeded 60% - 75% of the time during the sampling period (Vest et al. 2013). Also, there could be other factors that may make this comparison complicated such as grain size (i.e., soil with a high clay fraction can stabilize soil (Singer and Shainberg 2004; Su et al. 2007), while soil with a high sand fraction can easily be destabilized by wind erosion (Singer and Shainberg 2004)), organic matter (i.e., stable soils have higher organic matter than disturbed soils (Day et al. 2015)), and only three years of measurements that may have missed a large wind erosion event. However, the northern valley contains a large area (606 km^2) of groundwater-dependent vegetation bigger than Owens Dry Lake (280 km^2) that is sensitive to groundwater decline potentially threatening future air quality in Owens Valley.

High PM_{10} concentration levels occur mostly in the spring and are episodic and not directly related to wind velocity. Wind dynamics in Owens Valley are complex due to the steep mountain ridgelines surrounding the valley and the high albedo of the valley floor. Most surface winds are thermally driven (i.e., blowing from the southeast during the day and northwest at night) (Cahill et al. 1996; Zhong et al. 2008). These winds usually do not displace high levels of surface soil, but high wind speeds due to trough location and surface low pressure systems displace high levels of surface soil (Zhong et al. 2008). This leads to large fluxes of PM_{10} emitted into the Sierra Nevada and White Mountain ranges and southeast and northwest of Owens Dry Lake following topography (Reid et al. 1994). This is supported by large PM_{10} concentrations occurring at wind velocities over 12.17 m s^{-1}, which is higher than the average wind velocity of 4.7 m s^{-1}. Most large PM_{10} and high wind events occur in the spring due to shallow groundwater from snowmelt that causes elevated

salt concentrations in surface sediments and lead to puffier soils that are easily eroded (Li et al. 2007; Reynolds et al. 2007b). Because most data collection occurred from the last weeks of spring to late summer, some large aeolian sediment and PM_{10} displacement events occurring in early spring were likely missed.

Evidence shows that before over-pumping of groundwater caused alkali meadow degradation, the particulate concentration, which is proportional to sulfur concentration, decreases from south to north from the Owens Dry Lake (Barone et al. 1981; Gill and Cahill 1992). Also, most moderate dust storms generated PM_{10} plumes that dissipated within 30 km north of the playa (i.e., before the mid-valley PM_{10} location) (Cahill et al. 1996), while the peak PM_{10} concentrations associated with high intensity dust storms dissipated before the PM_{10} samples were obtained at the monitoring station within the mid-valley (Figure 4.7). Further, PM_{10} concentrations that exceeded CAAQS did not always occur on the same day at Owens Dry Lake (0 km) and mid-valley (42 km) monitoring stations. Therefore, the source of higher average concentrations in the mid-valley region (Fig. 4.7) are likely from additional PM_{10} emissions from the degraded alkali meadow areas – patterns confirmed by data measurements of elevated Q in the mid-valley region with degraded alkali meadows. Also, CAAQS were exceeded more frequently in the mid-valley (42 km from Owens Dry Lake) than at PM_{10} stations near Owens Dry Lake (0 km and 9 km), providing further supporting evidence that new sources of PM_{10} are coming from mid-valley degraded alkali meadows. In 2010, CAAQS were exceeded more frequently at the lake monitoring station (0 km, Fig. 4.8) due to drier, colder, and gustier conditions conducive to greater PM_{10} emission. Between 2008 and 2010,

NAAQS was exceeded 63 times. These exceedances occurred mostly at Owens Dry Lake; however in 2009 and 2010, there were exceedances in the mid-valley possibly indicating a mid-valley contribution to degraded air quality (2009: 2 exceedances; 2010: 1 exceedance, Fig. 4.8). While we argue that the data supports a new source of PM_{10} from alkali meadows, we cannot discount a possibility that Owens Dry Lake PM_{10} is being remobilized at various distances down the valley exacerbating PM_{10} in the mid-valley. The degradation of alkali meadow to the north of the Owens Dry Lake has changed the regional pattern of PM_{10} concentrations, expanding the area of concern to include vegetated areas and human population centers located along the Owens Valley north of the lake. These areas include portions of the Native American Piute Tribal lands, and the towns of Bishop, Big Pine, Independence, and Lone Pine, and are not part of the current air quality litigation against LA (GBUAPCD 2012).

Ecosystem restoration will be expensive with estimates of $500 million to $1 billion dollars for Owens Dry Lake dust mitigation (LADWP 2010; LADWP 2011). Thresholds of change and significant feedback processes can dominate the dynamics of desert ecosystems leading to changes in ecosystem state that are difficult to reverse (Schlesinger et al. 1990; D'Odorico et al. 2012). In the case of Owens Dry Lake, mitigation was intended to form an irrigated alkali meadow (GBUAPCD 2008). The total annual water usage of this engineered system (69,597 acre feet (LADWP 2014b) along with other restoration activities (GBUAPCD 2008) is similar to the volume of water pumped from the northern alkali meadow to the Owens Valley aqueduct (62,380 acre feet; Year 2014-2015) (LADWP 2014b; LADWP 2014a) that has contributed to degradation of alkali meadow area. The actual degraded alkali meadow

area (155 km^2) in the northern valley due to groundwater pumping during the drought is greater than the managed vegetation (9 km^2) (GBUAPCD 2011) established for dust mitigation. Although Owens Dry Lake is still out of compliance with the NAAQS and CAAQS (Fig. 4.8) (Nichols 2011), the managed vegetation area has remained in compliance since implementation (GBUAPCD 2008). Therefore, alkali meadow is an excellent dust suppressor; however, alkali meadow requires a shallow water table, which in the northern meadows is being depleted through groundwater extraction to mitigate PM_{10} on Owens Dry Lake with serious long-term consequences for air pollution. The degradation of alkali meadow to the north of Owens Dry Lake has already added to PM_{10} pollution in the valley (Fig. 4.6, 4.7 & 4.8). If alkali meadow degradation increases, a "back of the envelope" estimate of vertical flux (i.e., flux that contributes to PM_{10}) from groundwater-dependent alkali meadows (i.e., NoChg2, DTW3, DTW4, DTW5, and DTW6) (410.9 km^2) is 3.04×10^3 g m^{-2} d^{-1}, which is two orders of magnitude smaller than the vertical flux estimate from Owens Dry Lake (8.14×10^5 g m^{-2} d^{-1} (estimated from Gillette et al. 1997)) at its dustiest (i.e., before mitigation on 125.9 km^2 (GBUAPCD 2015)). Dust mitigation is decreasing the vertical flux from Owens Dry Lake; however, the vertical flux from the alkali meadow areas may continue to increase due to groundwater pumping below the root-zone causing vegetation structure to change to a more conducive vegetation arrangement for wind erosion of sediment. This would exacerbate the PM_{10} concentration possibly beyond the ability to mitigate the PM_{10} levels to attainment standards.

4.6.1 Case Study

When analyzing the effect of groundwater decline on Q and vegetation, the Q produced from the plots were more affected by vegetation spatial patterns caused by depth to water (DTW) levels during the drought and heavy groundwater pumping (1987-1996) than by current DTW levels. Plot 12 was pumped heavily during the drought (Fig. 4.5) with vegetation structure changing from an alkali meadow to groundwater-dependent alkali scrub with increasing bare soil areas (Fig. 4.4). Although current DTW has recovered to almost pre-drought levels, plot 12 still produces high Q and vertical flux (Table 4.2). This is most likely due to spatial patterns of vegetation in plot 12 being more open and conducive to wind erosion of aeolian sediment (Table 4.2). This is supported by current DTW being unrelated to the variability in Q with scaled gap size of vegetation explaining higher variability in Q than other vegetation parameters (Vest et al. 2013). Plot 6 had stable groundwater with alkali meadow vegetation that mitigates wind erosion (Fig. 4.5). Although Plot 6's vegetation structure has not changed since pre-drought (Fig. 4.3), it has naturally low vegetation cover (Elmore et al. 2003) with large salt encrusted gaps providing a long fetch for removal of sediment (Table 4.2). Although current DTW levels do not seem to directly explain Q, they may play an indirect role. Plot 6 and plot 12 during 2008 and 2009 have similar Q most likely due to similar scaled gap sizes, average gap sizes (Table 4.2), and plot 6's highly erodible salt encrusted surface due to a low DTW (Reynolds et al. 2007b). However, during the high Q event in 2010, the Q in plot 6 did not increase as significantly compared to plot 12 (2 orders of magnitude), which might be due to the alkali meadow vegetation arrangement mitigating wind

erosion (i.e., the higher the resistance distance, the lower the connectivity of bare soil conducive to wind erosion (Table 4.2)). Therefore, low DTW may support a vegetation arrangement that mitigates large episodic wind erosion events.

4.7 Conclusions

Our analysis shows three preliminary outcomes of the restoration and mitigation effort: (1) alkali meadow is a novel source of PM_{10} pollution in Owens Valley possibly contributing to violation of CAAQS and NAAQS; (2) there is a need for ecosystem and groundwater management to mitigate the degraded air quality of Owens Valley; and (3) Los Angeles needs to find ways to decrease their water demand from the Owens Valley.

Alkali meadow is a novel source of PM_{10} pollution in Owens Valley; therefore, the transfer of pumped water from northern alkali meadow areas of Owens Valley for use in Owens Dry Lake PM_{10} mitigation has contributed to the detrimental effects on air quality in mid-valley alkali meadow. Horizontal and vertical flux is highest at mid-valley areas with high groundwater decline that are dominated by widely spaced shrubs. This vertical flux contributes to increasing PM_{10} concentrations in the mid-valley. Previous research shows that PM_{10} emissions dissipated before reaching mid-valley (Barone et al. 1981; Gill and Cahill 1992; Cahill et al. 1996); therefore, alkali meadow is a novel source of PM_{10} as indicated by an increase in average PM_{10} concentration in mid-valley (Fig 4.7), more frequent exceedances of CAAQS, and exceedances of NAAQS in the mid-valley (Fig 4.8). Although most violations of NAAQS and CAAQS occur near Owens Dry Lake, these violations are also occurring in the mid-valley indicating a need to manage water withdrawals from

alkali meadow. However, LADWP does not consider PM_{10} emissions from degraded northern meadows as part of the dust mitigation area (GBUAPCD 2008).

Using ecosystem management to mitigate the degraded air quality of Owens Valley is complex due to the link between shallow groundwater, groundwater pumping, and air pollution. Remote sensing measurements of vegetation cover do not correlate well with dust generation; instead, dust generation correlates with field measured vegetation structure (Vest et al., 2013) and soil properties (Reynolds et al., 2007). Therefore, ecosystem management solutions should place a priority on managing surface conditions such as alkali meadow vegetation by sustaining groundwater levels within their root-zone because we lack the ability to manage wind directly to reduce dust emission. Alkali meadow supported by shallow groundwater in the northern valley and irrigated on the Owens Dry Lake provides 95-100% control of PM_{10} emission when wind speeds are less than 48mph (GBUAPCD 2008). This ecosystem service of dust suppression provided by native vegetation has significant value to society by maintaining clean air and human health. Attempts to restore this lost ecosystem service (i.e., dust suppression by alkali meadow vegetation) have proven very costly as evidenced by the over $500 million investment LADWP has made towards restoring alkali meadow on the dry lake playa (LADWP 2011). PM_{10} mitigation activities at the Owens Dry Lake that result in a tradeoff between ecosystem services from elsewhere in the valley are unlikely to reduce the overall threat of fugitive dust throughout the region.

Los Angeles' export of water from Owens Valley has been reduced over the last several years (Fig. 4.9) mainly due to decreased snowpack in the Sierra Nevada

(LADWP 2014a) and mitigation/restoration projects in Owens Valley (Fig 4.9). In 2015, LA is extracting the same amount of water from Owens Valley that is being used on Owens Dry Lake dust mitigation (Fig 4.9). On April 1, 2015, Governor Brown announced that snowpack levels in the Sierra Nevada are 5% of average (Megerian et al. 2015) impacting all water in California but especially the amount of water Los Angeles exports from Owens Valley. Currently, Los Angeles is in a drought emergency with water use restrictions (LACWD 2015). On April 1, Governor Brown restricted Los Angeles' water usage further by requesting residents to reduce their water usage by 25% compared to 2013 water use (State of California 2015). These current restrictions call for replacement of 50 million square feet of lawns and ornamental turf with xeriscaping, a reduction in commercial, industrial, and institutional property water use by 25%, the prohibition of irrigation for ornamental turf and public street medians, and the prohibition of irrigation outside of new homes and buildings unless it is delivered by microspray or drip systems (State of California 2015). Further, the Governor offered monetary incentives such as an appliance rebate program to replace inefficient household appliances, and the Californian water board is tasked with directing water suppliers to develop rate structures and pricing mechanisms to conserve water (State of California 2015). Mandatory use restrictions are affective in reducing water usage (Megerian et al. 2015); however, once mandatory restrictions are lifted, residents may go back to using a similar level of water as before the drought. Unfortunately, water will remain scarce due to climate change decreasing snowpack and precipitation (Seager et al. 2013; Goulden and Bales 2014), which may continue to decrease Los Angeles' share

of Owens Valley water. Therefore, even during non-drought periods, the public needs to voluntarily conserve water. Unfortunately, voluntary restrictions are less effective in reducing water use than mandatory use restrictions implemented by LADWP (Mini et al. 2015). Los Angeles not only needs to implement water saving strategies by using reclamation, rebate programs, and cash for grass (LACWD 2015), but they also need to set mandatory use restrictions and/or implement water use education programs (especially in elementary to high schools). These water saving strategies may help to reduce their dependence on this scarce commodity even in non-drought periods.

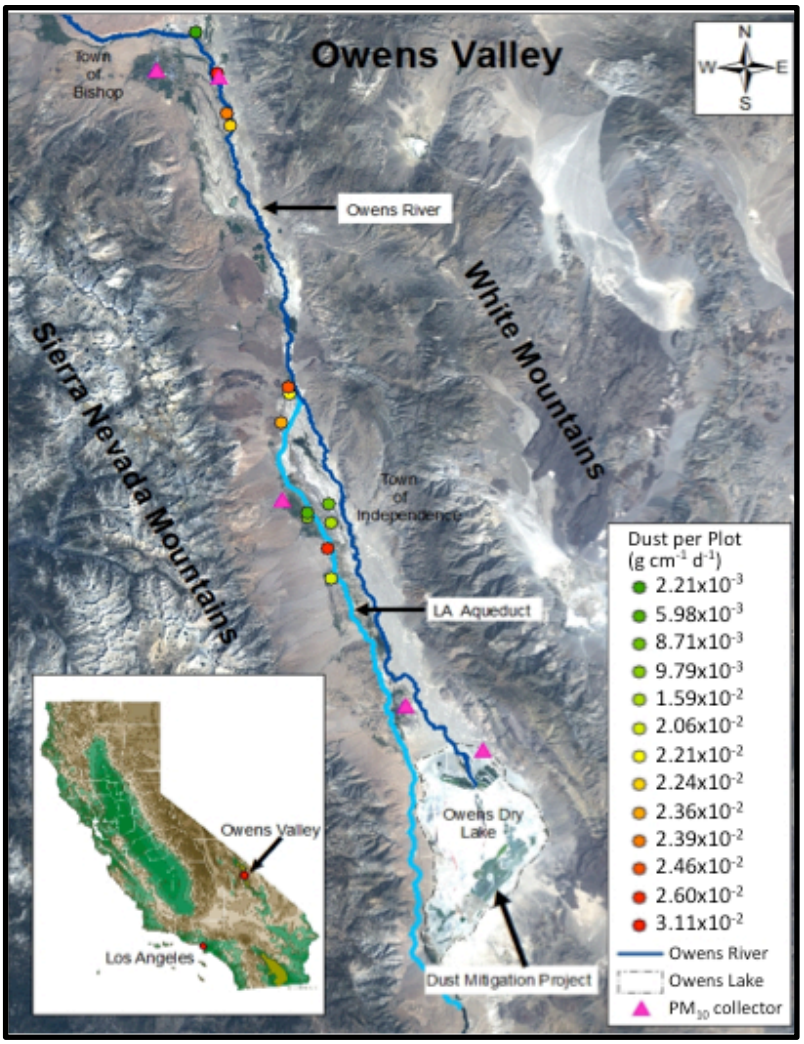

Figure 4.1. The Owens Valley, showing the location of instrumentation used, including the 13 BSNE-equipped sites and 5 PM_{10} monitor equipped meteorological stations. The background is a 2010 Landsat image.

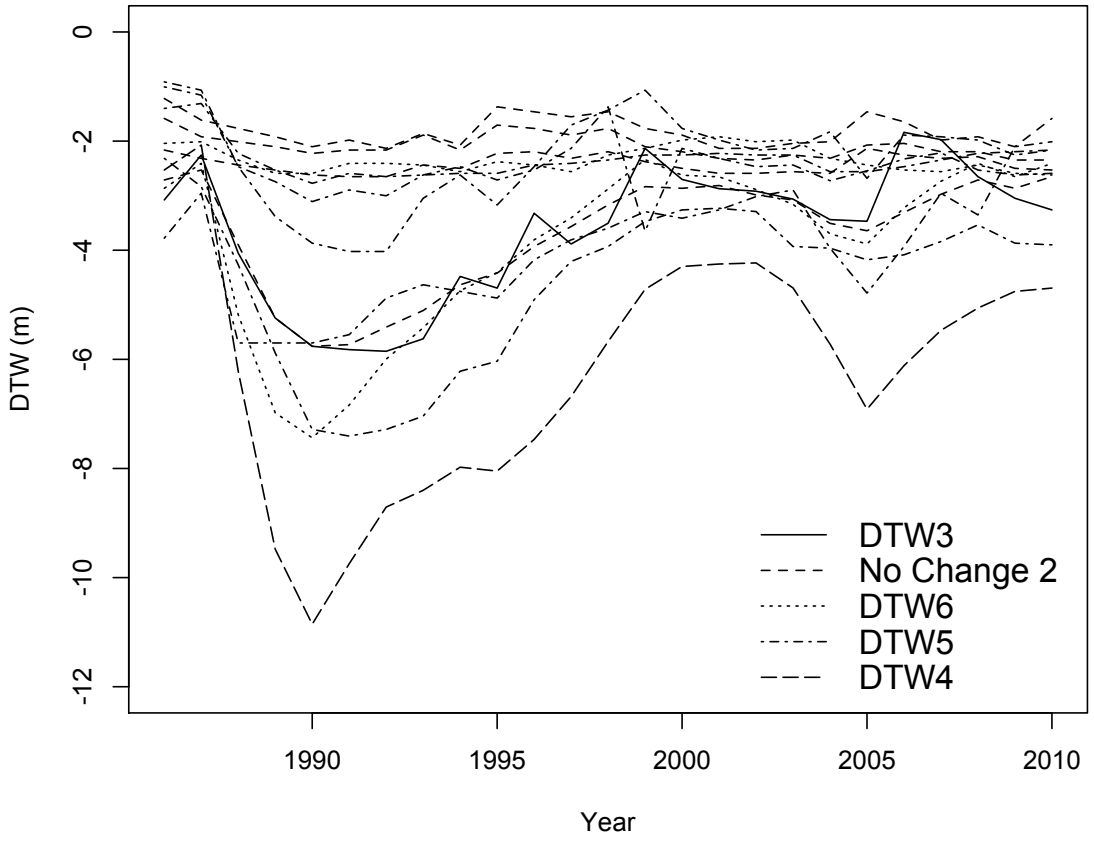

Figure 4.2. The comparison of the DTW trend in our plots classified into No change 2, DTW3, DTW4, DTW5, and DTW6 cover class from 1986 to 2010.

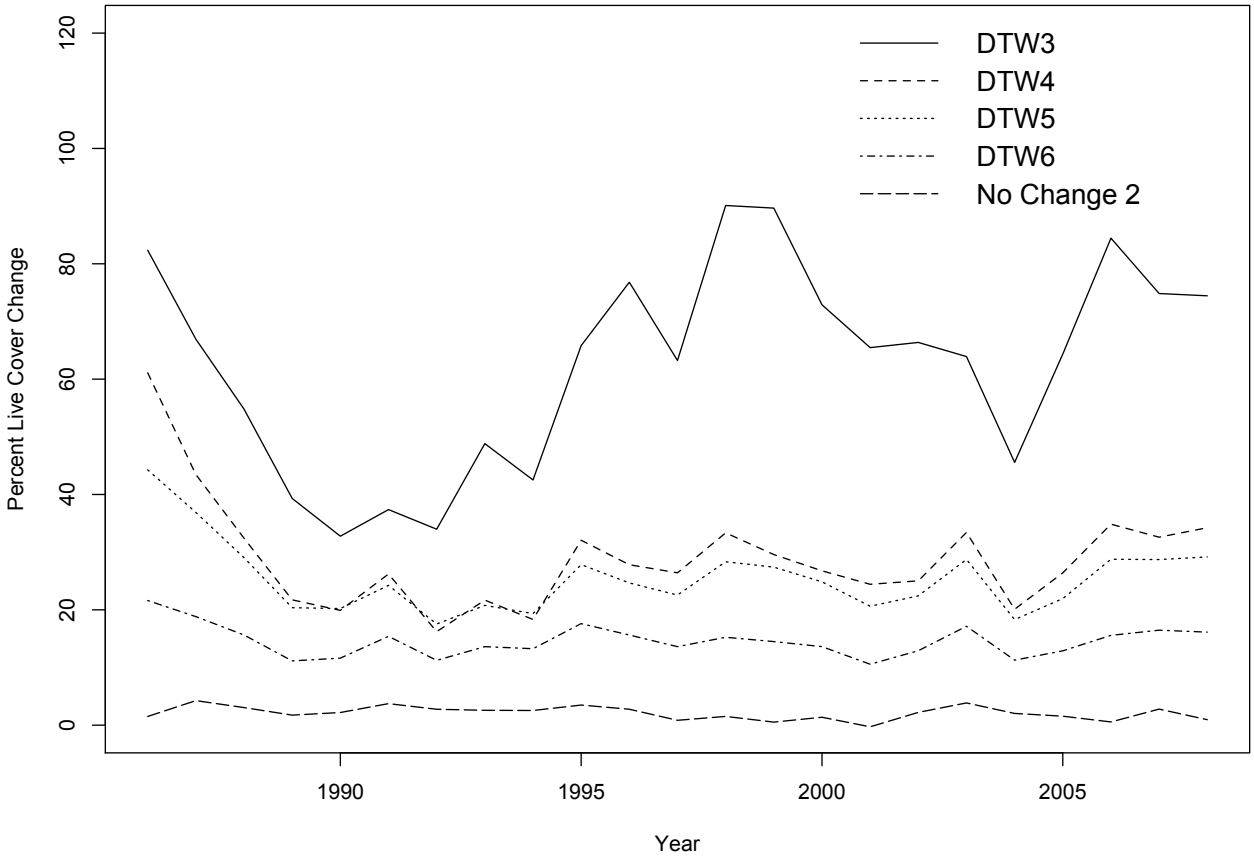

Figure 4.3 The change in percent live cover in Owens Valley from 1986 to 2008 in the five change cover classes comprising our plots based on information from Elmore et al. (2003).

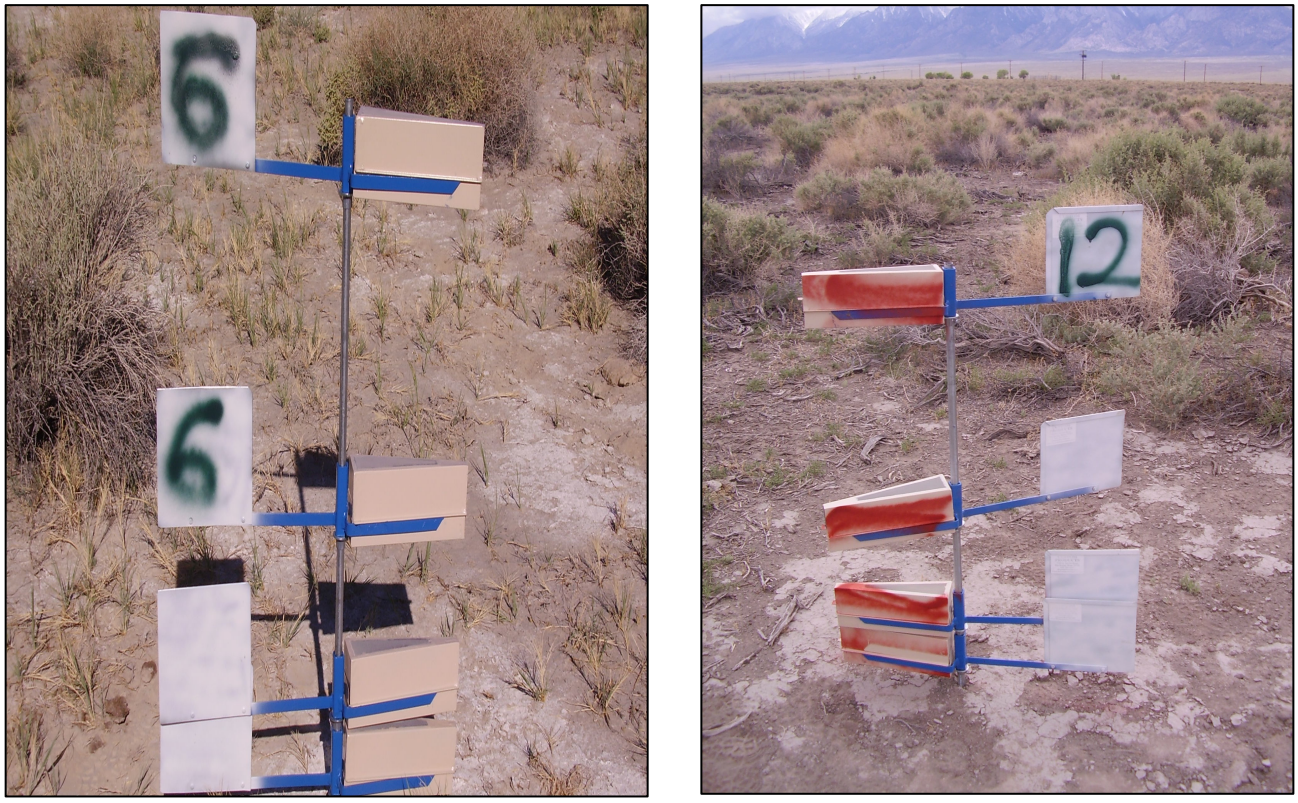

Figure 4.4. The picture on the left is of a plot in the NoChg2 cover class (plot 6), and the picture on the right is of a plot in the DTW4 cover class (plot 12).

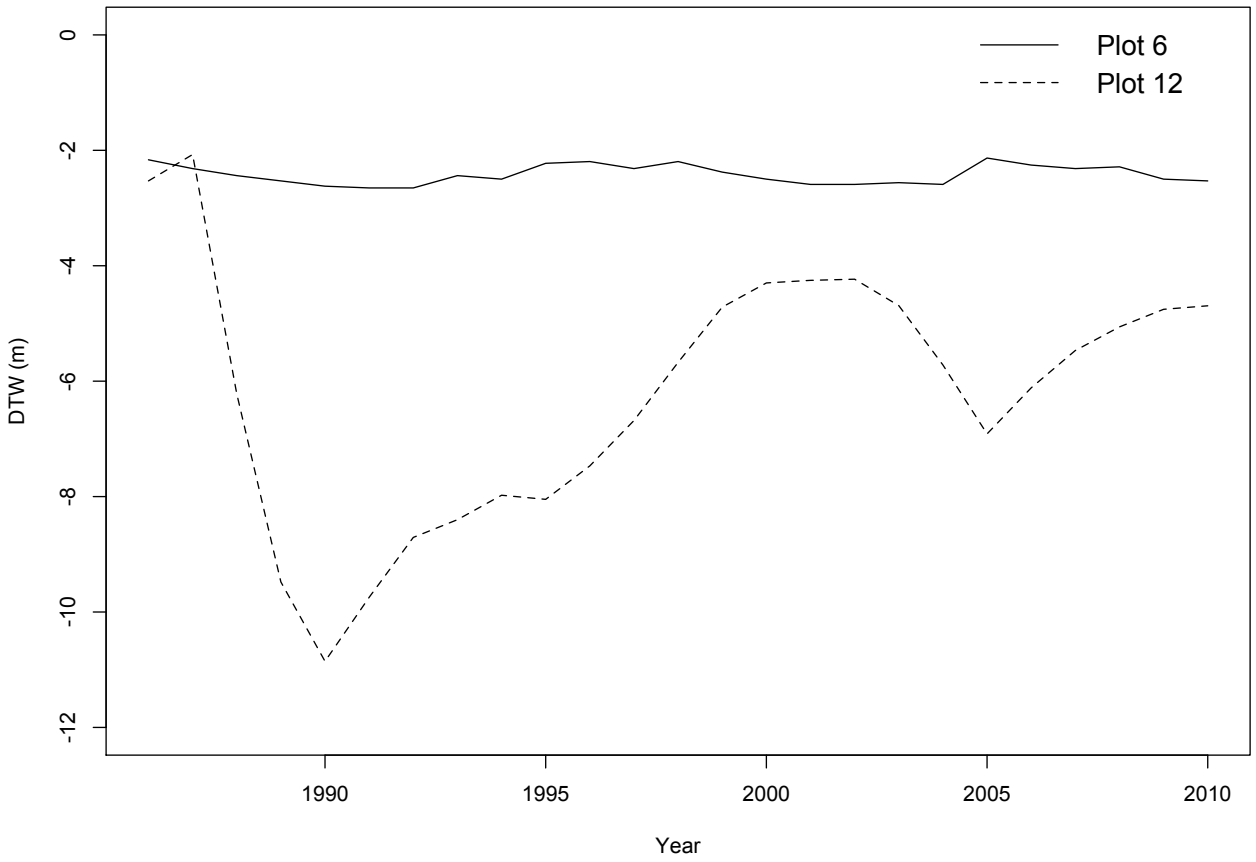

Figure 4.5. The comparison of the DTW trend between plot 6 (NoChg2 cover class) and plot 12 (DTW4 cover class) from 1986 to 2010

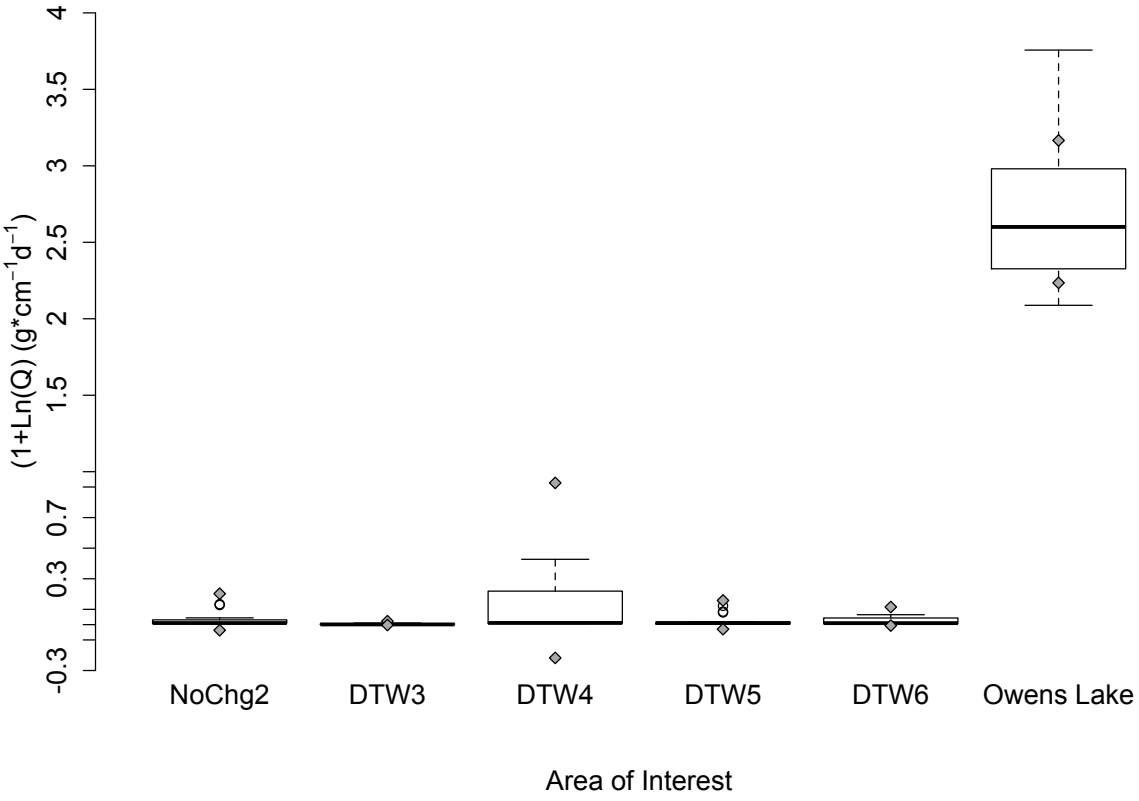

Figure 4.6. The differences between the Q from the five cover change classes as compared to the Q from Owens Dry Lake. Gray diamonds on the boxplot represent standard deviation from the mean. Owens Lake data is estimated from Gillette et al. (2001) figure 7.

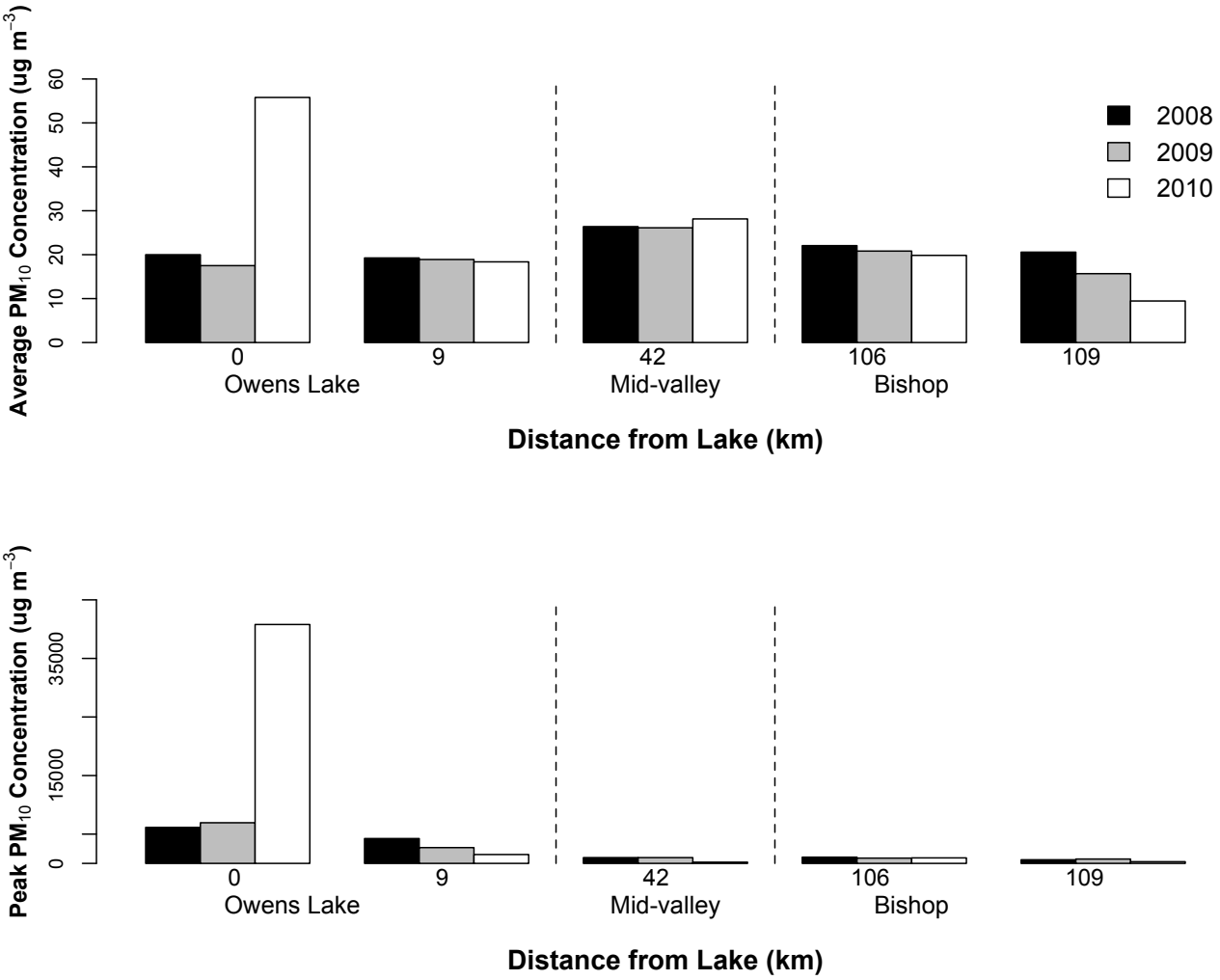

Figure 4.7 (Top) The effect of distance from Owens Lake on the average PM10 concentration, and (Bottom) the peak PM10 concentration by distance from Owens Lake.

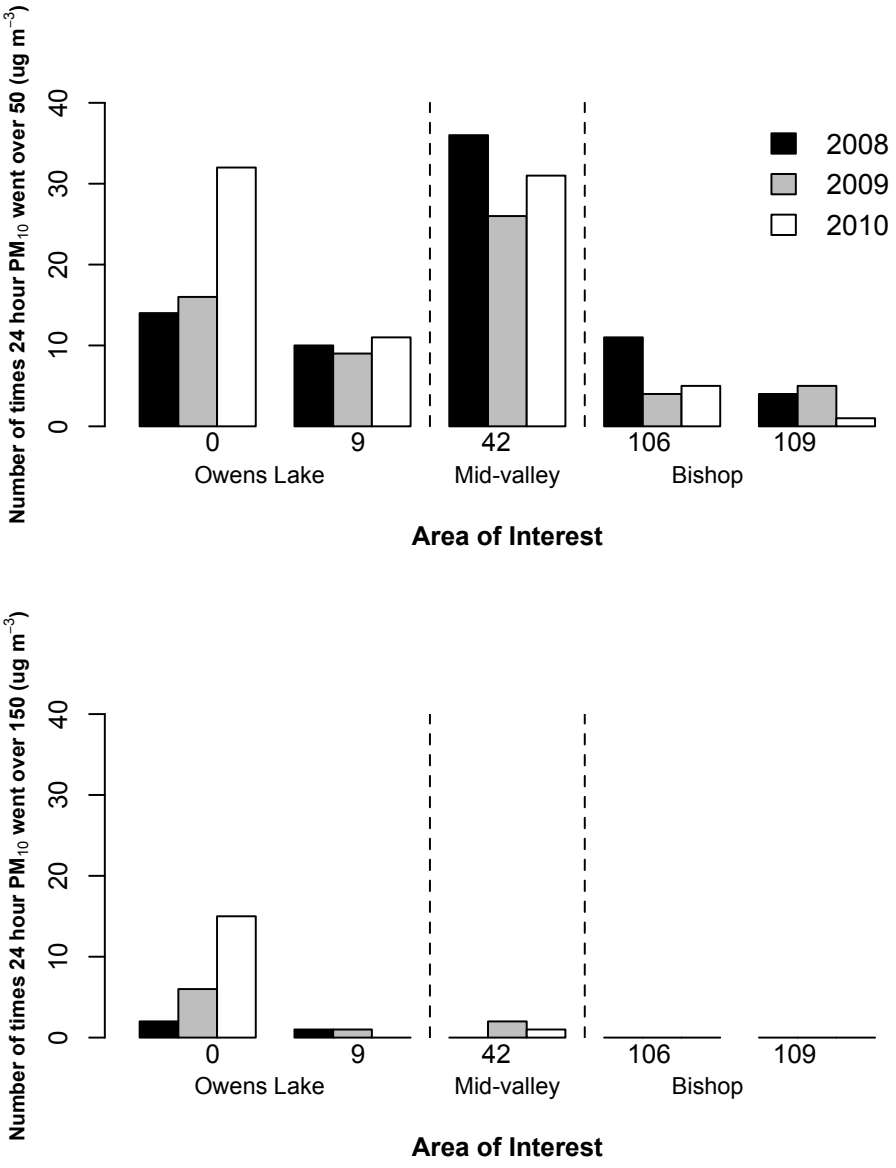

Figure 4.8. The effect of distance from Owens Lake on the number of times PM_{10} concentration exceeded the California Ambient Air Quality standards (50 μg m^{-3}) (Top) and the National Ambient Air Quality standards (150 μg m^{-3}) for 24 hour PM_{10} concentration.

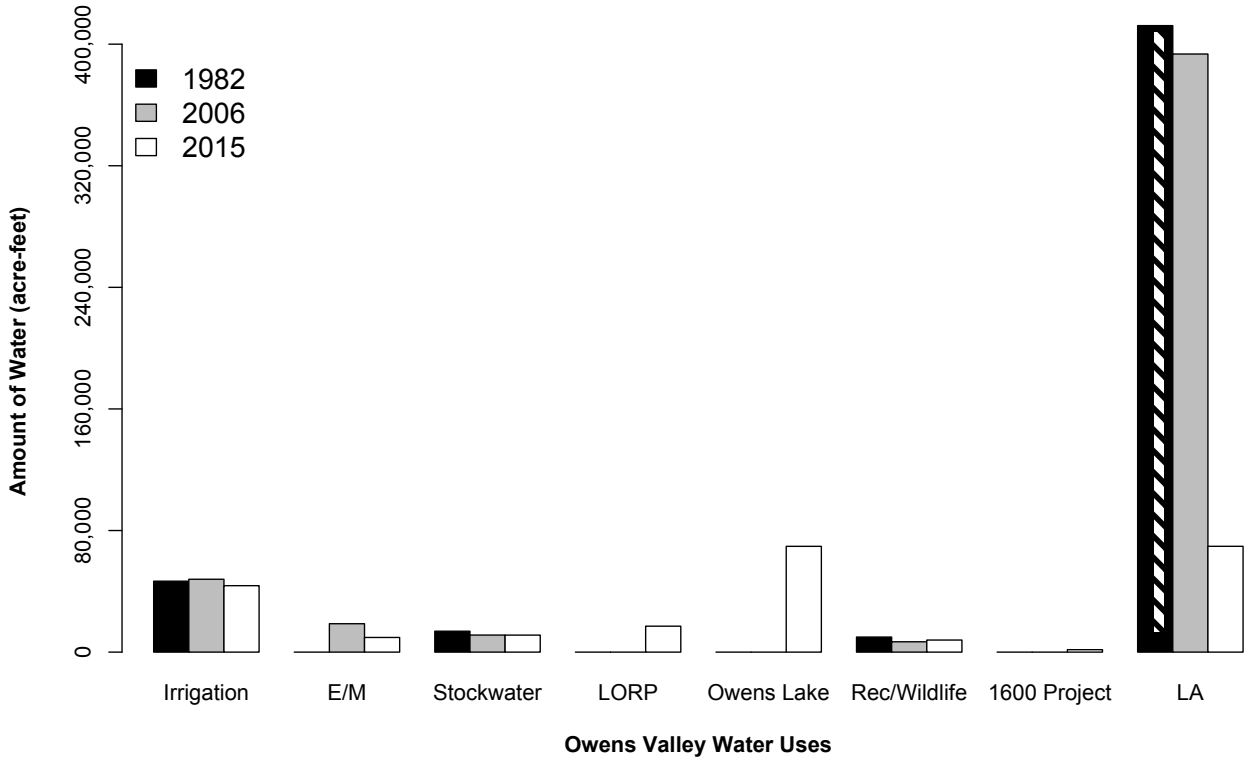

Figure 4.9. The uses of Owens Valley water compared between water years 1981-1982, 2005-2006, and 2014-2015. 1982 exports to LA (diagonal within black) were estimated based on 2006 data and the inclusion of water in the E/M category that was not present in 1981-82 (E/M – Enhancement/Mitigation; LORP – Lower Owens River Project; Rec/Wildlife – Recreation and Wildlife; 1600 Project – 1600 Acre Foot Project Mitigation of Hines Spring (Based on data from (LADWP 2005; LADWP 2014b).

Table 4.1: Mean and Range of Q and Vertical Flux Measurements from alkali meadow plots

Table 4.1: Mean and Range of Q and Vertical Flux Measurements from alkali meadow plots

Cover Change Class	Mean Q (g cm^{-1} d^{-1})	Range of Q (g m^{-1} d^{-1})	Mean Vertical Flux (g m^{-2} d^{-1})	Range of Vertical Flux (g m^{-2} d^{-1})
DTW3*	0.0098	0.0022 – 0.025	$5.4x10^{-4}$	$1.2x10^{-4}$ – $1.3x10^{-3}$
DTW4*	0.57	0.016 – 1.67	$3.1x10^{-2}$	$8.9x10^{-4}$ – $9.0x10^{-2}$
DTW5*	0.066	0.0042 – 0.33	$3.6x10^{-3}$	$2.3x10^{-4}$ – $1.8x10^{-2}$
DTW6*	0.056	0.0081 – 0.16	$3.0x10^{-3}$	$4.4x10^{-4}$ – $8.7x10^{-3}$
NoChg2*	0.086	0.016 – 0.33	$4.6x10^{-3}$	$8.7x10^{-4}$ – $2.0x10^{-2}$
Owens Dry Lake	943’	121 – 5712’	50.9	6.53 – 308

*2008, 2009, and 2010 measurements combined; ‘ Q estimated from Gillette et al. (2001) Figure 7

Table 4.2: Description of Parameters used in Paper

Table 4.2: Comparison between Plot 6 and Plot 12

Characteristics	**Plot 6**			**Plot 12**		
	2008	**2009**	**2010**	**2008**	**2009**	**2010**
Q ($g\ cm^{-1}\ d^{-1}$)	0.02	0.02	0.04	0.03	0.02	1.67
Vertical Flux ($g\ m^{-2}\ d^{-1}$)	$1.3x10^{-3}$	$1.12x10^{-3}$	$2.3x10^{-3}$	$1.4x10^{-3}$	$8.9x10^{-4}$	$9.0x10^{-2}$
Scaled Gap Size	3.6	3.6	4.7	5	4.1	4.5
Average Gap Size (cm)	58	59	32	49	35	25
Resistance Distance~		4.1			2.4	
Cover Change Class		NoChg2			DTW4	
Lowest DTW*,'		2.2m			2.07m	
Highest DTW*		2.7m			10.9m	

* During drought 1987-1996; ' First year of drought; ~ Calculated in Chapter III

Chapter 5: Conclusion

Aquifers in semi-arid grasslands provide water to groundwater-dependent vegetation, which prevents the removal of soil from the surface by wind erosion (i.e., soil stability as an ecosystem service). As groundwater is continuously allocated for other uses (e.g., urban population growth (Ragab and Prudhomme 2002)), the groundwater table may drop below the vegetation root zone affecting its ecosystem service leading to desertification. Therefore, management of these groundwater resources is important to avoid desertification. Natural resource managers need scientific techniques such as modeling and fieldwork to identify, prevent, and mitigate these areas. Modeling and fieldwork should focus on the processes that create positive feedback mechanisms for desertification such as: 1) loose soil removal by wind erosion; 2) affects of vegetation structure change; and 3) increasing connected pathways in the landscape. If groundwater withdrawals are continuously managed incorrectly (i.e., groundwater decline below vegetation root zone), the semi-arid grasslands could undergo desertification leading to a loss of ecosystem services (i.e., aeolian flux suppression), creating higher PM_{10} concentrations causing public health problems such as aggravated asthma, chronic bronchitis, and respiratory illness (Prospero 1999; Fubini and Fenogolio 2007; Zhang et al. 2013). The results of this study will be used to inform the management of these groundwater resources with the goal of avoiding desertification. This dissertation 1) developed and compared empirical, process-based, and mechanistic models that predict mass transport from field measurements of vegetation and soil structure within groundwater-dependent plant communities (Chapter II), 2) explored the role of landscape connectivity of bare

soil in enhancing aeolian transport and quantifying the magnitude of desertification across the landscape (Chapter III), and 3) measured the magnitude of wind erosion between groundwater-dependent alkali meadow with depth to water dependent vegetation changes and groundwater-dependent alkali meadow with static vegetation conditions and compared these values with wind erosion rates in other parts of the world and with projected consequences for air quality (Chapter IV),

5.1 Combined Results from PM10, Wind Erosion, and Connectivity Modeling

As degradation of semi-arid grasslands continues, wind erosion destabilizes soil leading to conditions that are unfavorable to alkali meadow reestablishment (Belnap and Gillette 1998; Li et al. 2007; Elmore et al. 2008). I found that field-measured aeolian sediment transportation can be estimated through a simple empirical model using two vegetation parameters, scaled gap size and gap size, with scaled gap size explaining the majority (56%) of model variance. As scaled gap size and gap size increase, higher amounts of aeolian sediments are mobilized. These sediments can bury neighboring plants and increase gap size by destabilizing soils and inhibiting the reestablishment of vegetation (Okin et al. 2001; McGlynn and Okin 2006). These sediments can also be emitted in the form of PM_{10} pollution creating health problems and adding to NAAQS noncompliance for PM_{10}.

To analyze the role of connected pathways as a driver of desertification, I developed a resistance grid based on the knowledge of sheer stress recovery (Okin 2008). I found that as alkali meadow areas produce more Q, they become more connected supporting the evidence that as bare soil increases, it creates "streets" of bare soil where wind can remove sediment (i.e., produce more Q) and degrade

vegetation on the edges of the gap. I also found that a majority of my plots were more connected than if there was no wind, or vegetation cover was sufficient enough to increase the threshold shear velocity at the soil surface. Further, higher groundwater decline makes the landscape more connected with increased aeolian flux. Areas that were degraded by groundwater decline previously but recovered are still more connected than the neutral model indicates by total grass cover. Many of these highly connected areas are in central Owens Valley resulting in higher observed amounts of PM_{10} concentration than previously shown.

Through these results, I provide information for natural resource managers, and tools to identify areas that are degraded by wind erosion, producing horizontal flux and PM_{10}, and prone to desertification. Managers can use the simple empirical model to target management actions in alkali meadow vegetation or heterogeneous vegetation (e.g., coastal dunes). By measuring scaled gap size and gap size in desired plots, which are easily measured in the field and do not require a wind tunnel or an estimate of multiple parameters such as required in the Okin and Raupach models, I can predict the amount of Q produced from an area. If plots are producing Q, they are also producing $PM_{10,}$ calculated using a simple relationship (Gillette et al. 1997). This occurs mainly in mid-valley degraded plots, which contribute to PM_{10} concentrations in Owens Valley. Using relationships between resistance distance, Q and scaled gap size, I can target areas that are forming connected pathways. Further, managers can use the understanding behind the behavior of a neutral model to compare that behavior to an actual managed landscape. Managers in Owens Valley can use these tools to help identify areas that are becoming more connected and try to mitigate

these effects. These tools also encompass more of an understanding of the interactions between physical and biological processes, which provides a better gauge of a well field's health rather than vegetation transects and soil moisture.

5.2 Field Identification of Vegetation Degradation and Wind Erosion

Scaled gap size is an important vegetation parameter in measuring wind erosion. Scaled gap size can easily be measured through line intercept vegetation transects at each plot, and it explains Q better than other vegetation parameters (56% of the variability in Q) including lateral cover (i.e., the most commonly used vegetation parameter in wind erosion modeling). Scaled gap size is easily measured in the field and offers natural resource managers a useful tool when assessing the wind erosion potential at a site with heterogeneous vegetation.

Alkali meadow vegetation provides 95-100% PM_{10} suppression performing a significant ecosystem service (GBUAPCD 2008). Wind erosion through degraded alkali meadows (i.e., DTW induced vegetation change cover during the drought (1987-1996)) produced larger amounts of Q and PM_{10} than intact meadows. Although Q and PM_{10} values produced from wind erosion on Owens Dry Lake are higher than alkali meadow areas, the alkali meadow areas susceptible to degradation is larger than the area of Owens Dry Lake and may eventually serve as a high source of PM_{10} in the future if groundwater levels are not managed correctly.

5.3 Integrating Field and Modeling Results

Wind erosion models that use scaled gap size (e.g., Okin model) predict Q better in heterogeneous areas than the commonly used Raupach model that uses lateral

cover. This is due to its ability to describe the heterogeneous distribution of vegetation and the amount of sheltered bare soil behind the vegetation (Okin 2008). Another important wind erosion parameter in the predictive capability of the Okin model is threshold shear velocity. When a single average threshold shear velocity was used for all plots, (0.56 m s^{-1}), Q was overestimated demonstrating the importance of knowing threshold shear velocity at each plot. Natural resource managers can use the Okin model to target management actions in alkali meadows.

The results from using a simple ratio of Q values to predict PM_{10} concentrations from our alkali meadow plots (Gillette et al. 1997) supports the idea that degradation of alkali meadow to the north of Owens Dry Lake has changed the regional pattern of PM_{10} concentrations. These degraded alkali meadow areas include portions of Native American Piute Tribal lands, and the towns of Bishop, Big Pine, Independence, and Lone Pine, which are not part of the current dust mitigation area (GBUAPCD 2008). However, Los Angeles is pumping groundwater from these alkali meadow areas supported by shallow groundwater in the northern valley to provide water to the dust mitigation projects on Owens Dry Lake (e.g., planting alkali meadow). This sole focus of dust mitigation in Owens Valley on Owens Dry Lake has resulted in a tradeoff between ecosystem services (i.e., dust suppression by alkali meadow vegetation) from the northern valley that is unlikely to reduce the overall threat of dust throughout the region.

Finally, I determined that areas of high groundwater decline during the California drought (1986-1992) were more connected than if there was no wind, or vegetation cover was sufficient enough to increase the threshold shear velocity at the soil

surface. This agrees with previous investigations that link groundwater decline below the vegetation root zone to vegetation structure change (Muñoz-Reinoso 2001; Elmore et al. 2006a; Barron et al. 2014) that increases wind erosion in degraded vegetation causing the formation of "streets" (Okin et al. 2001; McGlynn and Okin 2006), increasing threshold shear velocity, which allows for a longer fetch for saltation and dust emission (Okin et al. 2009). At the edge of these pathways, nearby vegetation is buried (Okin et al. 2009) creating longer connected pathways possibly leading to a positive feedback mechanism initiating desertification.

Field-based investigations allowed for the identification of vegetation structure and the determination of horizontal flux. Through the integration of field investigations with models, I was able to link landscape connectivity caused by vegetation structure change to groundwater decline during the California drought leading to a better understanding of the processes causing desertification in semi-arid groundwater-dependent vegetation.

5.4 Determining Thresholds for State Changes from Grassland to Shrubland

Okin et al (2009) and Turnbull et al (2008) both hypothesized that increased functional connectivity of a landscape leads to desertification. This occurs when a semi-arid landscape becomes more heterogeneous (i.e., grass to shrub dominated) with increased bare soil area between shrubs forming connected pathways for wind removal of sediment (Okin et al. 2009). A catalyst in Owens Valley for this change (i.e., alkali meadow to shrub domination) was groundwater decline during the California drought between (1987-1996). Past work shows that vegetation structure is impacted by groundwater decline due to pumping (Elmore et al. 2003; Elmore et al.

2006b), but this analysis does not address changes in vegetation configuration resulting in functional connectivity. From my results, areas that were pumped heavily during this period have higher functional connectivity, which was indicative of larger aeolian sediment movement. As functional connectivity increased with longer connected pathways of bare soil compared to vegetation height, wind erosion through these connected pathways produced larger amounts of aeolian flux removing soil nutrients required for plant growth and burying vegetation on the edge of the connected pathways producing longer connected pathways through the landscape (Okin et al. 2009). These connected pathways created a more functionally connected landscape than our neutral landscape model would suggest based on total cover (i.e., % grass; % shrub; %bare soil) possibly indicating a permanent state change from grassland to shrubland. Also, plots where vegetation structure recovered after pumping ceased were more connected than % grass cover would predict possibly indicating a hysteresis effect in the landscape and making it more susceptible to future desertification if pumping is resumed. Overall, Circuitscape was a good method to test the hypothesis of connectivity as a driver of state change in a landscape leading to desertification. It can also easily be used by managers to identify areas that have high functional connectivity and aid in the information gathering of whether to pump a well field or not.

5.5 Implications for Continued Pumping of Groundwater and Drought

In Owens Valley, Inyo County Water Department and Los Angeles Department of Water and Power (LADWP) on August 1, 1989 developed a joint long-term management plan with an overall goal of managing the water resources

within Inyo County to avoid decreases and changes in vegetation (James et al. 1990). The green book regulates the amount and location of groundwater to pump through vegetation monitoring and available soil water (James et al. 1990). However, the vegetation monitoring does not account for the subtle changes occurring that could be of concern such as larger connected pathways and changing soil chemistry. Also, the vegetation transects are roped off, and from field observations, these areas seem to have a more intact structure than the surrounding vegetation. The primary source of water for LADWP is from the Los Angeles Aqueduct (37%), local groundwater (11%), recycled water (1%), and supplemental purchase from the Metropolitan Water District of Southern California (MWD) (51%) (LADWP 2014c). LADWP this year is pumping less water than usual due to the persistent drought in California (LADWP 2014a). If the current drought continues and California is able to purchase less water from MWD, they will have no choice but to petition for more water from Inyo County. Currently, LA is already petitioning for more groundwater pumping to cover the mitigation projects in Owens Valley. A higher amount of groundwater pumping could cause increased vegetation structure change. If groundwater were pumped below the root-zone, alkali meadow degradation would elongate connected pathways leading to more aeolian flux in the valley. This would cause an increase in PM_{10} emission leading to non-compliance in national air quality standards.

5.6 Implications of Climate Change on Vegetation and Groundwater

Global climate models predict that aridity will increase in dryland systems (Seager et al. 2007). The year 2012 was one of the 10 warmest years on record, and the United States was 1.4°C above average (Blunden and Arndt 2013). Future

projections for California have a 4.1°C warming by the end of the 21st century (Goulden and Bales 2014) with a profound influence on California snow accumulations with losses increasing with warming (Cayan et al. 2008). Snowmelt from the Sierra Nevada results in $5.8x10^8m^3 – 6.3x10^8m^3$ annual runoff that recharges groundwater and surface water in the Owens River drainage basin (Hollett et al. 1991; Danskin 1998). Precipitation in the Sierra Nevada is projected to decrease with increasing evapotranspiration over the next century that could possibly reduce surface water and groundwater availability in the Owens Valley (Seager et al. 2013; Goulden and Bales 2014). For the 2014 water year in Owens Valley, the Eastern Sierra snowpack is at 30% of normal (LADWP 2014a) and snowpack nationally is decreasing too (Marshall et al. 2008). Aeolian flux from wind erosion on Owens Dry Lake and degraded vegetation structure has the possibility of reaching snowpacks high in the Eastern Sierra. When atmospheric dust falls on snowpacks, it darkens the surface leading to rapid melting and more water in streams (Marshall et al. 2008). Warming combined with the darkening of surface snow, could cause the acceleration of snowpack melting. Groundwater is replenished each year by snowpack melt; therefore, climate change combined with increased dust-on-snow might lower water availability during the dry season and increase the rate of desertification.

In Owens Valley, groundwater-dependent vegetation increases the threshold shear velocity required to mobilize sediments and initiate wind erosion and aeolian sediment emission (e.g., PM_{10} emission). These emitted aerosols can act as cloud condensation nuclei (CCN) increasing aerosols resulting in a larger cloud surface area that scatters solar radiation (Ravi et al. 2011). However, this high CCN in clouds can

suppress rainfall and cause persistent droughts regionally (Ravi et al. 2011). Precipitation is 50% of average precipitation in Owens Valley for 2014 (LADWP 2014a). Precipitation decreases coupled with aeolian flux could possibly cause vegetation structure to change rapidly accelerating desertification. As more dust is being released due to vegetation structure change, bare soil patches are increasing. As these bare soil patches increase, albedo increases (Charney 1975) inducing surface cooling and reducing convection resulting in decreased rainfall and promotion and expansion of desert areas (Taylor et al. 2002; Zeng and Yoon 2009).

5.7 Future directions and recommendations

Although this study examines comprehensively the physical, biological and chemical process that cause desertification in groundwater-dependent grasslands, there is still more research that can be done to expand and fill in gaps.

- To further refine the models using a more detailed representation of spatial and temporal variability in model parameters (e.g., threshold shear velocity, vegetation structure, and roughness height). The strongest empirical model developed only explained 58% of the variation in Q, which leaves considerable variability for measurements and approaches for estimating Q. This work will allow natural resource managers a more complete model for estimating Q at their field site.
- To continue using the Circuitscape model coupled with Qrule for the entirety of Owens Valley and apply it to other areas with groundwater-dependent vegetation (e.g., Minquin, China). Circuitscape and Okin models explain similar variability in Q and are processed-based models. However, the Okin

model uses a full probability distribution of scaled gap size to calculate Q (Okin 2008), while Circuitscape uses current theory and a user-determined landscape resistance grid mimicking wind to develop a current map and a resistance distance. This would include an improvement of the resistance values for the resistance grids through fieldwork to measure an average roughness value for bare soil at specific locations and determine the differing sheer stresses of bare soil, shrubs, and grass at certain distances downwind. This would help managers to better utilize the model for evaluating degradedness of an area.

- To develop groundwater management models that are coupled with aeolian flux and PM_{10} emission to represent new links that this work has drawn between groundwater depth, vegetation, and dust.
- To improve upon the simple empirical model to predict threshold shear velocity which can also be used to predict PM_{10} emissions in the area: I would need to investigate some uncertainties such as quantifying the impacts of grazing and other disturbances and understanding the source and consequences of spatial and temporal variability in model parameters influencing Q. Although it would be hard to measure these uncertainties, it is possible that they lead to temporal or spatial variability in the success of the empirical model.
- To develop a study evaluating the "memory" of vegetation structure change in groundwater-dependent meadows. I would need to identify if these areas have

"memory" through analyzing functional connectivity and other parameters. This research could inform pumping and mitigation decisions for managers.

To maintain a balance between LA's and vegetation's water demands, management and policy decisions will become increasingly important especially with the affects of drought and climate change. Management of groundwater pumping focuses on vegetation transects and soil moisture not accounting for their links to aeolian sediment flux. However, a better management strategy might be to identify areas that have connected pathways to manage groundwater decline because wind erosion in connected pathways increase saltation and dust emission creating a positive feedback that promotes desertification leading to increased aeolian sediment flux, reducing air quality and causing human health problems. As the demand for groundwater in these areas increases (i.e., due to climate change, continued drought, and population growth), natural resource managers in groundwater-dependent semi-arid grasslands will need to develop management plans that are coupled with aeolian flux and PM_{10} emissions that represent new links to prevent withdrawals that might lead to desertification.

Appendices

A.1 Soil chemistry data

The purpose of this appendix is to present data that was collected but ultimately not used in the dissertation chapters. By including this data, I am preserving the data for future scientific investigations. The purpose of this data was to determine the compositional and spatial distribution of soil crust properties that influence surface strength. The main question was ***how does soil chemistry and soil stability change in concert with vegetation structural changes associated with groundwater decline?*** I intended the results of this work to lend insight into interactions between vegetation structure, groundwater hydrology, and surface composition that influences soil stability. However, the results posed some problems in interpretation of these relationships; therefore, I present a write-up of the methods and tables of variables and data.

A.1.1 Plot and sampling design

Sampling was designed to study relationships both between and within plot vegetation, groundwater, and soil characteristics. Within each plot, we further characterized the variability in soil surface types and made detailed measurements of soil chemistry and physical structure in each type. We also averaged these values for each plot to assess between-plot variability.

Our analysis focused on thirteen plots (10,000 m^2 each) that were monitored for three years: 2008, 2009, and 2010. Plot selection focused on covering a range in vegetation structure, from shrubs separated by bare soil, through shrubs separated by meadow, to continuous meadow. Based on research linking vegetation structure and groundwater (Elmore et al. 2003; Elmore et al. 2006b), we found it possible to use spatial and recent temporal variation in groundwater depth to capture the needed variability in vegetation structure. However, we also required that groundwater be sufficiently close to the surface to justify a characterization of "groundwater-dependent" and the soil characteristics associated with shallow groundwater dominated systems (generally thought of as requiring groundwater within 5 m of the surface (Reynolds et al. 2007b)). To enable the establishment of plots along the required gradient in vegetation structure, plots were identified that were (1) within 100 m of a long-term monitoring well with recorded groundwater depths since 1986 (measured in April of each year); (2) located within alkali meadow, as identified by a 1986 vegetation survey (City of Los Angeles and County of Inyo 1990); and (3) within soil identified as mollisol or aridisol in Soil Survey Geographic Database (SSURGO) (Soil Survey Staff). Sixteen plots were initially selected in these areas. However, in 2008, destruction of three plots by cattle that had not been removed at the time of sediment trap installation reduced the number of study plots to thirteen (Fig. 3.1). We did not re-deploy at these three sites in 2009 or 2010. At eight of the thirteen plots, (Aubault 2009) performed soil texture analyses.

A.1.2 Total horizontal flux measurements

Total horizontal flux (Q) was measured using four Big Spring Number Eight (BSNE) aeolian sediment traps mounted on a 1m pole; henceforth, referred to as a BSNE stem. We placed a BSNE stem in each plot in 2008, 2009, and 2010 and an additional BSNE stem in two of the plots in 2009 and 2010. The mass of the sample collected in each trap was divided by sampler inlet area and the duration of the collection interval. The results from each trap were fit to an exponential equation then integrated to 1m to estimate Q (Gillette et al. 1997). The Q was adjusted based upon the efficiency of the BSNE stem, 90% ± 5% (Shao et al. 1993).

A.1.2 Vegetation Distribution

Vegetation cover, gap distribution, and vegetation height for each plot was determined using four 50 m line intercept transects run in cardinal directions from the BSNE stem (USDA and NRCS 2004). For each transect, along-transect width (greater than 0.03 m), species, height of vegetation (greater than 0.08 m), and along-transect width of bare soil patches (greater than 0.03 m) were measured. Despite the imposed detection limit in vegetation height, we found that even the shortest vegetation elements were taller than 0.08 m. The vegetation height was measured using a regulation Frisbee® with a hole carved into the center through which a wooden meter stick could be threaded. The meter stick was placed in each individual plant along the transect, and the Frisbee® was dropped vertically with the meter stick penetrating the hole in the disk. The top of the plastic disk at its stopping location was recorded as the vegetation height. Vegetation transects were conducted in May of 2008, 2009, and 2010 during BSNE stem deployment. Vest et al (2013) determined that scaled gap size (mean gap size between vegetation elements scaled by vegetation

height) explained a high level of variation in the total horizontal flux in meadows by wind erosion. Therefore, we calculated scaled gap size for each of our plots. Next, we divided our thirteen sites into degraded and intact alkali meadow by using a 15% grass cutoff (i.e., <15% grass cover = degraded and >15% grass cover = intact) based on the results of Elmore et al (2006, 2008), who show that grass cover generally declines to less than 15% when subjected to groundwater decline below the root zone.

A.1.3 Soil Chemistry

Site soil characteristics were derived from two 2-cm profiles one near vegetation and one in bare soil collected at each cm depth in February 2008 and three 2-cm profiles (i.e., one near vegetation and two in bare soil) collected at each cm depth in May 2008, September 2008, May 2009, and September 2009 at the sixteen sites described above. From these 1-cm profiles collected, organic carbon concentration and anion concentration in the soil was measured. Anion concentration was measured using an inductively coupled plasma elemental analyzer to measure Cl^{-1}, NO_3^{-1}, NO_2^{-1}, SO_4^{2-}, and PO_4^{3-}. Soil organic carbon concentration was analyzed in the laboratory using loss on ignition protocols. From loss of ignition we calculated soil organic carbon concentration to be 40% of loss on ignition concentration (Berglund 2003).

Salt crusts are an important component of soil stability in arid and semi-arid areas (Mees and Stoops 1991). Salt crusted soils occur in over 100 countries in arid and semi-arid environments; the sources of these salts are groundwater and surface water (Dehaan and Taylor 2002; Guler and Thyne 2004; Kampf et al. 2005; Rengasamy 2006). Salt crusts usually form when the groundwater level is less than

3m below the surface (Saint-Amand et al. 1987). The yearly salt flux is controlled by evaporation and underlying groundwater salinity (Tyler et al. 1997). Crusting is a key factor in the reduction of particle entrainment by wind (Langston and McKenna Neuman 2005). Small amounts of soluble salts increase TSV because they cement bonds between grains (Nickling and Ecclestone 1981). Hard crusts (i.e., containing Cl^- and usually formed in summer) and rough crusts (i.e., containing Cl^-) provide protection against wind erosion (i.e., increasing threshold shear velocity) (Nickling and Ecclestone 1981; Gillette et al. 2001) whereas soft, friable crusts (i.e., containing carbonate and sulfate and usually formed in winter) are easily destroyed by saltation (Tyler et al. 1997; Gillette et al. 2001). These friable/soft crusts are quickly replaced by a shallow groundwater table; however, if DTW increases below 3m, these friable/soft crusts will not be annually-replaced, increasing the susceptibility of soil to erosion (Reynolds et al. 2007b). Further, the destruction of surface crusts can cause aeolian transport that decreases vegetation and increases the nutrient loss eventually initiating the destruction of remaining islands of fertility (Okin et al. 2001).

Electrical conductivity might be an important factor in accessing the resistance to erosion of an area. Soils with salt crust formations are more stable and have higher electrical conductivity than soils devoid of salt crusts. Further, groundwater-dependent halophytic grass species that provide stability to the soil that also transport salts from groundwater to the surface, resulting in higher electrical conductivity in areas with a higher cover of grass (Wiebe and Walter 1972). When groundwater pumping occurs below the rootzone of GDV, grasslands die (Elmore et al. 2003; Elmore et al. 2006b) exposing salt crusts to wind erosion. This exposure

allows salt crusts to be broken up by saltation without reformation due to the groundwater table being disconnected from the soil surface (Reynolds et al. 2007b). This process leads to bare soil areas devoid of grasses and salt crusts resulting in lower soil electrical conductivity and stability (Dehaan and Taylor 2002; Rajan et al. 2010). High electric conductivity in bare soil areas might indicate an area protected by vegetation that has a low potential of erosion, while a bare soil area with low electrical conductivity might indicate an area where loose soil particles have been recently removed by erosion. We ran correlation analysis between a set of electrical conductivity measurements and anion measurements in our plots and found the Cl^{-1} was highly correlated to electrical conductivity; therefore, we will use Cl^{-1} as a proxy for electrical conductivity.

A.1.4 Depth to Water Measurements

We used depth to water (DTW) measurements taken in April from 1987 – 1996 from monitoring wells within 100m of our plots. These were the years that groundwater pumping increased below the root zone due to drought. We believe that this groundwater decline might still have a legacy effect on the vegetation structure in the valley. April DTW measurements are used because piezometers are read at this time, and April contains the highest water levels. The water levels decrease after April due to evapotranspiration or extraction, so the April readings provide maximum groundwater readings.

A.1.5 Remote Sensing of Vegetation Cover

We acquired Landsat ETM+ images in September 2008, 2009, and 2010 to estimate the fraction of photosynthetic vegetation at each site using linear spectral

mixture analysis (Elmore et al. 2000). These data were previously validated against field measurements of leaf area along 33 permanent transects and found to be accurate to within ±4.0% photosynthetic vegetation and are therefore useful for a variety of land use and land cover change investigations (Elmore et al. 2003; Elmore et al. 2006b). We sampled % photosynthetic vegetation cover at each plot from these raster data sets and calculated two different % photosynthetic vegetation statistics: single pixel and nine pixel mean at and around each plot.

A.1.6 Threshold Shear Velocity

The threshold shear velocity (TSV) is the wind shear velocity required to mobilize surface sediments. Although it is a direct measure of surface stability (Belnap and Gillette 1998), and required for any type of calculation of erosion potential, the TSV can be very spatially variable. Knowledge of spatial variability in TSV might provide insight into the process of desertification. Each time a soil profile was sampled, a photograph of the profile and location were recorded. The photos from these previous field sampling seasons (February 2008, May 2008, May 2009, and September 2009) were divided into six different classifications (cracked loose soil, loose soil, grass, shrub, litter near shrub, and light loose soil). In 2010, we matched the photo at each location with a similar location at each plot. Next, we measured TSV at each location. To measure TSV we used the simple method to estimate threshold friction velocity of wind erosion in the field developed by Li et al. (2010). A 760 pumpmaster airgun using 4.5mm spherical copper pellets (Li et al. 2010) was positioned at 15cm and pointed at a 45° angle above the soil surface (Li et al. 2010). The airgun was pumped three times to obtain a pellet velocity of about 156

cm/s (i.e., taking into account that over time the velocity will diminish due to wear and tear on the air gun) (Li et al. 2010). The pellet hole area was calculated by using the maximum diameter and a line perpendicular to the maximum diameter (Li et al. 2010). FT011 and FT444 penetrometers were used at 45° near each pellet hole to measure the resistance of the soil surface to compressional force (kg) (Li et al. 2010). This method was repeated five times for each profile area at each site. Threshold shear velocity (TSV_{field}) was calculated using linear regression for two different measurements (i.e., pellet hole area (BB_{area}) and penetrometer pressure (*Penetrometer*)) (Li et al. 2010).

$$TSV_{ln-10} = 4.095 - (0.078 * BB_{area}) + (0.191 * Penetrometer) \quad (1)$$

$$TSV = e^{TSV} + 10 \quad (2)$$

To measure the spatial variability of TSV in a bare soil area, we randomly selected a compass orientation (0º-360 º) and distance (0-50m) ten times per site. Next, we ran a transect in the nearest bare soil area to this point. TSV was measured starting at 0cm and sampled every 10 cm until termination of the bare soil area using the method described above.

A.1.7 Soil Aggregate Stability

There are many factors contributing to soil stability such as soil aggregate stability, crustal composition, and threshold shear velocity. Soil aggregate stability might be an important factor in accessing the soils surface's resistance to erosion. Soil

aggregates are soil particles that are bound more closely to each other than other soil particles (USDA 1996). These aggregates can be formed through the breakdown of roots and litter and through fungal strands that bind soil particles (USDA 1996). Soil aggregates are important to erosion resistance, water availability, and root growth (USDA 1996). Large, stable aggregates can resist degradation and removal by wind (USDA 1996). Soil aggregate stability is usually measured to assess relative differences in soil quality and is an accepted indicator of soil health (Herrick et al. 2001; Seybold and Herrick 2001; Bestelmeyer et al. 2006). It is also related to ecosystem processes, properties, and functions including the quantity and composition of soil organic matter, soil biotic activity, and infiltration capacity (Herrick et al. 2001; Bestelmeyer et al. 2006). When other factors (vegetation cover and wind velocity) are held constant, low soil aggregate stability indicates an easily erodible area (Herrick et al. 2001; Seybold and Herrick 2001)We measured soil aggregate stability near each TSV measurement in the similar profile areas following the methods in Chapter 14: Soil Stability Test from the 2004 NRI Handbook of Instructions for Rangeland Field Study Data Collection. Soil aggregate stability measurements were taken in the profile areas every time a TSV measurement was obtained. Also, soil aggregate stability was measured at each TSV measurement in the bare soil transects.

Table A.1: Results of anion chemical analysis for Chloride, Nitrite, Phosphate, and Sulfate

Table A.1: Results of anion chemical analysis for Chloride, Nitrite, Phosphate, and Sulfate

Plot	Profile	Month	Year	CL (mg kg^{-1})	Nitrite (mg kg^{-1})	Nitrate (mg kg^{-1})	Phosphate (mg kg^{-1})	Sulfate (mg kg^{-1})
1	3	Sep	2008	4,326.48	0.00	7.58	107.54	16,2078.2
10	1	May	2009	2,299.16	0.00	2.06	62.04	18,0467.0
10	1	Sep	2008	799.74	0.00	20.29	52.08	11,3739.2
10	2	Feb	2008	3.77	0.28	1.68	4.94	127.18
10	2	May	2009	1,588.83	0.19	7.10	0.00	14,0095.2
10	2	Sep	2008	MD	MD	MD	MD	MD
10	3	Sep	2008	741.59	0.22	7.35	56.84	10,2431.9
11	1	May	2008	2.11	0.12	11.19	4.03	14.41
11	1	May	2009	16.08	0.93	9.86	5.99	57.85
11	1	Sep	2008	20.89	1.65	6.77	4.57	80.15
11	2	May	2008	4.27	0.68	16.08	7.36	91.54
11	2	May	2009	45.48	0.32	8.58	11.60	108.99
11	2	Sep	2008	537.05	2.57	25.68	6.56	3,671.05
11	3	May	2008	6.58	14.71	13.25	4.71	18.65
11	3	May	2009	14.43	2.71	7.63	12.69	115.56
11	3	Sep	2008	5.27	1.42	7.37	8.76	20.60
12	1	May	2008	107.36	0.21	25.96	14.58	109.94
12	1	Sep	2008	30.06	5.77	19.19	17.66	66.26
12	2	May	2008	10.92	0.18	23.55	11.22	56.15
12	2	Sep	2008	244.02	2.19	3.98	35.63	143.51

Table A.1: Results of anion chemical analysis for Chloride, Nitrite, Phosphate, and Sulfate

Plot	Profile	Month	Year	CL (mg kg^{-1})	Nitrite (mg kg^{-1})	Nitrate (mg kg^{-1})	Phosphate (mg kg^{-1})	Sulfate (mg kg^{-1})
12	3	May	2008	1,190.46	0.75	5.16	38.82	891.99
12	3	Sep	2008	36.26	1.67	5.69	23.25	90.89
17	1	Feb	2008	34.48	0.00	14.38	6.96	137.23
17	1	May	2009	15.57	1.22	2.39	4.02	95.16
17	1	Sep	2008	383.03	0.41	14.42	0.00	5,0831.10
17	2	Feb	2008	150.75	0.00	59.30	9.59	2,035.68
17	2	May	2009	226.32	4.43	22.79	26.66	336.13
17	2	Sep	2008	MD	MD	MD	MD	MD
17	3	Sep	2008	817.88	0.00	15.25	0.00	60,908.70
20	1	Feb	2008	69.11	1.79	23.92	16.10	163.43
20	1	May	2009	269.82	2.75	5.59	17.12	1,220.88
20	1	Sep	2008	216.22	3.07	40.84	22.21	1,803.11
20	2	Feb	2008	8.29	0.34	41.04	53.60	8,115.02
20	2	May	2009	535.44	0.00	41.93	1.31	7,138.95
20	2	Sep	2008	59.37	1.01	12.16	16.89	413.12
20	3	Sep	2008	7,349.09	0.00	47.37	317.00	21,765.32
21	1	Feb	2008	39.85	0.52	1.96	19.20	140.73
21	1	May	2009	69.38	3.29	7.83	15.45	98.17
21	1	Sep	2008	44.97	2.34	27.70	15.73	147.82
21	2	May	2009	244.55	5.99	8.78	32.65	198.21
21	3	Feb	2008	55.00	0.00	30.20	33.07	165.73

Table A.1: Results of anion chemical analysis for Chloride, Nitrite, Phosphate, and Sulfate

Plot	Profile	Month	Year	CL (mg kg^{-1})	Nitrite (mg kg^{-1})	Nitrate (mg kg^{-1})	Phosphate (mg kg^{-1})	Sulfate (mg kg^{-1})
22	1	May	2008	1,875.07	0.00	72.22	23.22	9,494.87
22	1	May	2009	541.81	0.00	3.87	55.75	3,8769.92
22	1	Sep	2008	431.31	0.00	194.98	66.76	3,406.87
22	2	May	2008	2,443.57	1.22	116.85	0.00	0.00
22	2	May	2009	30.37	0.26	8.13	8.92	282.20
22	3	May	2008	1,720.60	2.07	53.18	0.00	0.00
22	3	May	2009	1,291.05	1.96	5.52	20.88	9,378.93
25	1	May	2009	30.05	2.74	5.24	12.72	48.18
25	1	Sep	2008	24.75	1.13	4.49	9.45	49.72
25	2	May	2009	60.55	2.91	6.97	5.85	143.69
25	2	Sep	2008	35.27	2.43	9.04	8.50	85.14
25	3	Sep	2008	26.90	0.20	9.45	10.31	57.63
4	1	May	2008	993.11	1.32	0.65	46.12	7,239.83
4	1	Sep	2008	480.41	2.41	20.95	12.90	8,469.90
4	2	May	2008	17.10	0.00	34.89	0.00	44,048.93
4	2	May	2009	279.52	2.92	17.72	0.00	41,834.68
4	2	Sep	2008	524.65	1.83	13.71	0.00	46,578.04
4	3	May	2008	4.73	0.96	14.87	0.00	41,922.92
4	3	May	2009	304.14	2.72	10.73	2.72	10,771.83
4	3	Sep	2008	150.02	3.92	13.67	0.00	44,602.08
6	1	Feb	2008	128.66	0.00	6.83	5.25	294.64

Table A.1: Results of anion chemical analysis for Chloride, Nitrite, Phosphate, and Sulfate

Plot	Profile	Month	Year	CL (mg kg^{-1})	Nitrite (mg kg^{-1})	Nitrate (mg kg^{-1})	Phosphate (mg kg^{-1})	Sulfate (mg kg^{-1})
6	1	May	2009	686.10	0.00	7.03	5.28	1,239.26
6	1	Sep	2008	19,247.1	2,736.71	3.34	2.97	12,237.49
6	2	Feb	2008	MD	MD	MD	MD	MD
6	2	May	2009	2,452.23	0.00	17.89	32.03	29,763.99
6	2	Sep	2008	1,279.58	0.00	6.50	0.00	25,872.61
6	3	May	2009	48.28	0.00	2.50	1.21	59.33
6	3	Sep	2008	365.81	0.00	9.02	0.00	0.00
7	1	Feb	2008	31.38	3.00	11.20	7.06	98.80
7	1	May	2009	208.24	0.00	8.84	7.55	1,954.87
7	1	Sep	2008	32.59	1.73	2.61	4.83	54.68
7	2	Feb	2008	167.24	0.00	2.52	2.99	548.27
7	2	May	2009	43.52	1.51	3.16	7.62	138.89
7	2	Sep	2008	2.65	0.16	0.50	3.57	32.33
7	3	Sep	2008	74.41	1.91	6.55	5.78	88.70
9	1	Feb	2008	29.32	0.00	7.93	5.91	93.30
9	1	May	2009	9.40	0.64	12.59	7.60	143.08
9	1	Sep	2008	92.58	0.29	9.98	11.39	86.68
9	2	May	2009	20.36	0.84	10.05	13.98	304.49
9	2	Sep	2008	5.67	0.23	2.08	6.25	17.56
9	3	Sep	2008	6.73	0.35	1.49	3.64	27.63
Average				744.52	35.98	17.77	19.21	15,701.68

Table A.1: Results of anion chemical analysis for Chloride, Nitrite, Phosphate, and Sulfate

Plot	Profile	Month	Year	CL (mg kg^{-1})	Nitrite (mg kg^{-1})	Nitrate (mg kg^{-1})	Phosphate (mg kg^{-1})	Sulfate (mg kg^{-1})
Standard Deviation				2,364.81	307.76	27.15	38.98	36,263.86
Medium				74.41	0.68	9.04	8.50	165.73
Coefficient of Variation				3.18	8.55	1.53	2.03	2.31

Missing Data (MD) means that those samples were not analyzed.

Table A.2: Results from soil organic carbon analysis and TSV measurements in the field, vegetation characteristics of each profile, and groundwater depth for each plot.

Table A.2: Results from soil organic carbon analysis and TSV measurements in the field, vegetation characteristics of each profile, and groundwater depth for each plot

Plot	Profile	Month	Year	Soil Organic Carbon 40% (g kg^{-1})	Soil Organic Carbon 60% (g kg^{-1})	Veg	TSV (cm $s^{-1)}$	DTW (m)
1	3	Sep	2008	0.10	0.15	Veg	83.00	2.65
10	1	May	2009	0.02	0.03	Veg	91.47	2.87
10	1	Sep	2008	0.01	0.02	No Veg	91.47	2.71
10	2	Feb	2008	0.01	0.01	Veg	91.47	2.71
10	2	May	2009	0.01	0.02	No Veg	91.47	2.87
10	2	Sep	2008	0.01	0.02	No Veg	91.47	2.71
10	3	Sep	2008	0.01	0.02	Veg	91.47	2.71
11	1	May	2008	0.02	0.02	No Veg	40.33	3.54
11	1	May	2009	0.02	0.02	No Veg	40.33	3.87
11	1	Sep	2008	0.02	0.03	No Veg	40.33	3.54
11	2	May	2008	0.02	0.03	Veg	40.33	3.54
11	2	May	2009	0.01	0.02	No Veg	40.33	3.87
11	2	Sep	2008	0.02	0.03	No Veg	40.33	3.54
11	3	May	2008	0.02	0.02	Veg	40.33	3.54
11	3	May	2009	0.02	0.03	Veg	40.33	3.87
11	3	Sep	2008	0.01	0.02	Veg	40.33	3.54
12	1	May	2008	0.02	0.04	No Veg	50.65	5.06

Table A.2: Results from soil organic carbon analysis and TSV measurements in the field, vegetation characteristics of each profile, and groundwater depth for each plot

Plot	Profile	Month	Year	Soil Organic Carbon 40% (g kg^{-1})	Soil Organic Carbon 60% (g kg^{-1})	Veg	TSV (cm $s^{-1)}$	DTW (m)
12	1	Sep	2008	0.02	0.03	No Veg	50.65	5.06
12	2	May	2008	0.03	0.04	Veg	50.65	5.06
12	2	Sep	2008	0.04	0.06	Veg	50.65	5.06
12	3	May	2008	0.05	0.08	Veg	50.65	5.06
12	3	Sep	2008	0.03	0.04	No Veg	50.65	5.06
17	1	Feb	2008	0.02	0.03	No Veg	50.65	2.23
17	1	May	2009	0.02	0.02	No Veg	50.65	2.19
17	1	Sep	2008	0.02	0.03	No Veg	50.65	2.23
17	2	Feb	2008	0.02	0.03	Veg	50.65	2.23
17	2	May	2009	0.02	0.03	Veg	50.65	2.19
17	2	Sep	2008	0.02	0.03	Veg	50.65	2.23
17	3	Sep	2008	0.02	0.04	Veg	50.65	2.23
20	1	Feb	2008	0.02	0.04	Veg	58.20	1.98
20	1	May	2009	0.02	0.03	Veg	58.20	2.26
20	1	Sep	2008	0.03	0.04	Veg	58.20	1.98
20	2	Feb	2008	0.02	0.03	No Veg	58.20	1.98
20	2	May	2009	0.01	0.02	No Veg	58.20	2.26
20	2	Sep	2008	0.02	0.03	No Veg	58.20	1.98
20	3	Sep	2008	0.03	0.04	No Veg	58.20	1.98

Table A.2: Results from soil organic carbon analysis and TSV measurements in the field, vegetation characteristics of each profile, and groundwater depth for each plot

Plot	Profile	Month	Year	Soil Organic Carbon 40% (g kg^{-1})	Soil Organic Carbon 60% (g kg^{-1})	Veg	TSV (cm $s^{-1)}$	DTW (m)
21	1	Feb	2008	0.03	0.05	Veg	50.65	2.44
21	1	May	2009	0.02	0.04	No Veg	50.65	2.59
21	1	Sep	2008	0.02	0.03	No Veg	50.65	2.44
21	2	May	2009	0.03	0.05	Veg	50.65	2.59
21	3	Feb	2008	0.02	0.04	No Veg	50.65	2.43
22	1	May	2008	0.03	0.04	No Veg	43.44	2.53
22	1	May	2009	0.03	0.04	No Veg	43.44	2.62
22	1	Sep	2008	0.02	0.03	No Veg	43.44	2.53
22	2	May	2008	0.02	0.04	No Veg	43.44	2.53
22	2	May	2009	0.02	0.03	No Veg	43.44	2.62
22	3	May	2008	0.03	0.05	Veg	43.44	2.53
22	3	May	2009	0.03	0.05	Veg	43.44	2.62
25	1	May	2009	0.02	0.03	No Veg	55.50	2.07
25	1	Sep	2008	0.02	0.04	No Veg	55.50	2.10
25	2	May	2009	0.03	0.05	Veg	55.50	2.07
25	2	Sep	2008	0.03	0.04	No Veg	55.50	2.10
25	3	Sep	2008	0.03	0.04	Veg	55.50	2.10
4	1	May	2008	0.03	0.05	Veg	68.36	1.92
4	1	Sep	2008	0.02	0.02	Veg	68.36	1.92

Table A.2: Results from soil organic carbon analysis and TSV measurements in the field, vegetation characteristics of each profile, and groundwater depth for each plot

Plot	Profile	Month	Year	Soil Organic Carbon 40% (g kg^{-1})	Soil Organic Carbon 60% (g kg^{-1})	Veg	TSV (cm $s^{-1)}$	DTW (m)
4	2	May	2008	0.01	0.02	No Veg	68.36	1.92
4	2	May	2009	0.02	0.02	No Veg	68.36	2.10
4	2	Sep	2008	0.01	0.02	No Veg	68.36	1.92
4	3	May	2008	0.02	0.03	No Veg	68.36	1.92
4	3	May	2009	0.02	0.02	No Veg	68.36	2.10
4	3	Sep	2008	0.01	0.02	No Veg	68.36	1.92
6	1	Feb	2008	0.01	0.02	No Veg	57.94	2.29
6	1	May	2009	0.01	0.01	Veg	57.94	2.50
6	1	Sep	2008	0.02	0.02	No Veg	57.94	2.29
6	2	Feb	2008	0.01	0.02	Veg	57.94	2.29
6	2	May	2009	0.01	0.02	Veg	57.94	2.50
6	2	Sep	2008	0.01	0.02	Veg	57.94	2.29
6	3	May	2009	0.01	0.01	No Veg	57.94	2.50
6	3	Sep	2008	0.01	0.02	No Veg	57.94	2.29
7	1	Feb	2008	0.01	0.01	Veg	36.45	2.19
7	1	May	2009	0.01	0.01	Veg	36.45	2.35
7	1	Sep	2008	0.01	0.01	No Veg	36.45	2.19
7	2	Feb	2008	0.01	0.01	No Veg	36.45	2.19
7	2	May	2009	0.01	0.01	No Veg	36.45	2.35

Table A.2: Results from soil organic carbon analysis and TSV measurements in the field, vegetation characteristics of each profile, and groundwater depth for each plot

Plot	Profile	Month	Year	Soil Organic Carbon 40% (g kg^{-1})	Soil Organic Carbon 60% (g kg^{-1})	Veg	TSV (cm $s^{-1)}$	DTW (m)
7	2	Sep	2008	0.01	0.01	No Veg	36.45	2.19
7	3	Sep	2008	0.01	0.01	Veg	36.45	2.19
9	1	Feb	2008	0.01	0.02	No Veg	39.74	2.70
9	1	May	2009	0.01	0.02	No Veg	39.74	2.97
9	1	Sep	2008	0.01	0.02	No Veg	39.74	2.70
9	2	May	2009	0.01	0.02	Veg	39.74	2.97
9	2	Sep	2008	0.01	0.02	Veg	39.74	2.70
9	3	Sep	2008	0.01	0.02	No Veg	39.74	2.70
Average				0.02	0.03	NA	53.65	2.69
Standard Deviation				0.01	0.02	NA	14.57	0.83
Medium				0.02	0.03	NA	50.65	2.44
Coefficient of Variation				0.63	0.63	NA	0.27	0.31

Not Applicable (NA) means the analysis was not applicable for the parameter.

Table A.3: Results from field measured Q, Average TSV of the profiles at each plot, stability, TSV at each profile and soil type at profiles within the plots.

Table A.3: Results from field measured Q, Average TSV of the profiles at each plot, stability, TSV at each profile, and soil type at profiles within the plots.

Plot	Profile	Month	Year	Q ($g\ cm^{-1}d^{-1}$)	TSVbbavg ($cm\ s^{-1}$)	Soil Type	Stability	TSVbb ($cm\ s^{-1}$)
1	3	Sep	2008	0.00	1,487.10	grass	4.67	367.57
10	1	May	2009	0.02	32.12	grass	3.00	86.37
10	1	Sep	2008	0.02	32.12	light loose salt	1.40	1,903.77
10	2	Feb	2008	0.02	32.12	litter near shrub	6.00	24.55
10	2	May	2009	0.02	32.12	light loose salt	1.40	1,903.77
10	2	Sep	2008	0.02	32.12	cracked loose	4.00	96.50
10	3	Sep	2008	0.02	32.12	cracked loose	4.00	96.50
11	1	May	2008	0.02	22.16	hard cracked pan	3.00	56.71
11	1	May	2009	0.03	22.16	cracked loose	3.60	64.15
11	1	Sep	2008	0.02	22.16	hard cracked pan	3.00	56.71
11	2	May	2008	0.02	22.16	shrub	3.20	58.00
11	2	May	2009	0.03	22.16	hard cracked pan	3.00	56.71
11	2	Sep	2008	0.02	22.16	hard cracked pan	3.00	56.71
11	3	May	2008	0.02	22.16	hard cracked pan	3.00	56.71

Table A.3: Results from field measured Q, Average TSV of the profiles at each plot, stability, TSV at each profile, and soil type at profiles within the plots.

Plot	Profile	Month	Year	Q ($g\ cm^{-1}d^{-1}$)	TSVbbavg ($cm\ s^{-1}$)	Soil Type	Stability	TSVbb ($cm\ s^{-1}$)
11	3	May	2009	0.03	22.16	shrub	3.20	58.00
11	3	Sep	2008	0.02	22.16	shrub	3.20	58.00
12	1	May	2008	0.03	10.76	shrub	2.60	53.11
12	1	Sep	2008	0.02	10.76	cracked loose	2.60	63.01
12	2	May	2008	0.03	10.76	cracked loose	2.60	63.01
12	2	Sep	2008	0.02	10.76	litter near shrub	2.60	56.70
12	3	May	2008	0.03	10.76	litter near shrub	2.60	56.70
12	3	Sep	2008	0.03	10.76	cracked loose	2.60	63.01
17	1	Feb	2008	0.01	361.72	hard cracked pan	2.20	291.73
17	1	May	2009	0.01	361.72	hard cracked pan	2.20	291.73
17	1	Sep	2008	0.01	361.72	cracked loose	2.78	91.38
17	2	Feb	2008	0.01	361.72	shrub	2.25	61.86
17	2	May	2009	0.01	361.72	litter near shrub	3.00	24.55
17	2	Sep	2008	0.01	361.72	cracked loose	2.78	12,826.6
17	3	Sep	2008	0.01	361.72	litter near shrub	3.00	24.55
20	1	Feb	2008	0.01	62.90	shrub	2.40	78.17
20	1	May	2009	0.00	62.90	grass	2.20	103.95

Table A.3: Results from field measured Q, Average TSV of the profiles at each plot, stability, TSV at each profile, and soil type at profiles within the plots.

Plot	Profile	Month	Year	Q ($g\ cm^{-1}d^{-1}$)	TSVbbavg ($cm\ s^{-1}$)	Soil Type	Stability	TSVbb ($cm\ s^{-1}$)
20	1	Sep	2008	0.01	62.90	cracked loose	2.40	801.80
20	2	Feb	2008	0.01	62.90	cracked loose	2.40	801.80
20	2	May	2009	0.00	62.90	cracked loose	2.40	801.80
20	2	Sep	2008	0.01	62.90	cracked loose	2.40	801.80
20	3	Sep	2008	0.01	62.90	cracked loose	2.40	801.80
21	1	Feb	2008	0.02	77.55	shrub	3.00	78.17
21	1	May	2009	0.01	77.55	cracked loose	2.78	91.38
21	1	Sep	2008	0.02	77.55	cracked loose	2.78	91.38
21	2	May	2009	0.01	77.55	shrub	2.78	78.17
21	3	Feb	2008	0.02	77.55	cracked loose	2.78	91.38
22	1	May	2008	0.01	62.90	grass	2.00	318.04
22	1	May	2009	0.01	62.90	shrub	2.60	62.66
22	1	Sep	2008	0.01	62.90	loose crust	2.60	465.03
22	2	May	2008	0.01	62.90	loose crust	2.60	465.03
22	2	May	2009	0.01	62.90	loose crust	2.60	465.03
22	3	May	2008	0.01	62.90	grass	2.00	318.04
22	3	May	2009	0.01	62.90	grass	2.00	318.04
25	1	May	2009	0.03	6.12	hard cracked pan	1.60	64.58
25	1	Sep	2008	0.02	6.12	loose crust	1.00	57.52
25	2	May	2009	0.03	6.12	shrub	2.25	42.33

Table A.3: Results from field measured Q, Average TSV of the profiles at each plot, stability, TSV at each profile, and soil type at profiles within the plots.

Plot	Profile	Month	Year	Q ($g\ cm^{-1}d^{-1}$)	TSVbbavg ($cm\ s^{-1}$)	Soil Type	Stability	TSVbb ($cm\ s^{-1}$)
25	2	Sep	2008	0.02	6.12	shrub	2.25	42.33
25	3	Sep	2008	0.02	6.12	shrub	2.25	42.33
4	1	May	2008	0.03	1,047.28	litter near shrub	3.17	78.12
4	1	Sep	2008	0.03	1,047.28	litter near shrub	3.17	78.12
4	2	May	2008	0.03	1,047.28	hard cracked pan	2.14	130.96
4	2	May	2009	0.02	1,047.28	hard cracked pan	2.14	130.96
4	2	Sep	2008	0.03	1,047.28	cracked loose	1.80	74.73
4	3	May	2008	0.03	1,047.28	hard cracked pan	2.14	130.96
4	3	May	2009	0.02	1,047.28	cracked loose	1.80	74.73
4	3	Sep	2008	0.03	1,047.28	cracked loose	1.80	74.73
6	1	Feb	2008	0.02	174.52	light loose salt	1.70	66.75
6	1	May	2009	0.02	174.52	litter near shrub	2.00	50.75
6	1	Sep	2008	0.02	174.52	loose crust	1.00	32.06
6	2	Feb	2008	0.02	174.52	light loose salt	2.00	66.75
6	2	May	2009	0.02	174.52	loose crust	1.00	32.06
6	2	Sep	2008	0.02	174.52	light loose salt	2.00	66.75
6	3	May	2009	0.02	174.52	loose	1.00	32.06

Table A.3: Results from field measured Q, Average TSV of the profiles at each plot, stability, TSV at each profile, and soil type at profiles within the plots.

Plot	Profile	Month	Year	Q ($g\ cm^{-1}d^{-1}$)	TSVbbavg ($cm\ s^{-1}$)	Soil Type	Stability	TSVbb ($cm\ s^{-1}$)
6	3	Sep	2008	0.02	174.52	crust light loose salt	2.00	66.75
7	1	Feb	2008	0.02	317.39	grass	1.67	47.26
7	1	May	2009	0.02	317.39	grass	2.80	47.26
7	1	Sep	2008	0.02	317.39	loose crust	1.00	31.32
7	2	Feb	2008	0.02	317.39	loose crust	1.93	31.32
7	2	May	2009	0.02	317.39	loose crust	1.00	31.32
7	2	Sep	2008	0.02	317.39	hard cracked pan	2.60	130.96
7	3	Sep	2008	0.02	317.39	loose crust	1.00	31.32
9	1	Feb	2008	0.02	317.39	cracked loose	1.20	64.35
9	1	May	2009	0.02	317.39	loose crust	1.00	32.07
9	1	Sep	2008	0.02	317.39	loose crust	1.00	32.07
9	2	May	2009	0.02	317.39	shrub	1.00	78.12
9	2	Sep	2008	0.02	317.39	shrub	1.00	78.12
9	3	Sep	2008	0.02	317.39	loose crust	1.00	32.07
Average				0.02	239.94	NA	2.34	342.76
Standard Deviation				0.01	330.19	NA	0.89	1,435.5
Medium				0.02	77.55	NA	2.4	66.75
Coefficient of Variation				0.43	1.38	NA	0.38	4.19

Not Applicable (NA) means the analysis was not applicable for the parameter.

Table A.4: Results from field measured Penetrometer readings and elliptical area of BB impression, average DTW, number of times DTW was higher than 2.5, and intact vs. degraded alkali meadow at each plot.

Table A.4: Results from field measured Penetrometer readings and elliptical area of BB impression, average DTW, number of times DTW was higher than 2.5, and intact vs. degraded alkali meadow at each plot.

Plot	Profile	Month	Year	45Pen	BBEllipse	Average DTW (1987-1996)	# of times higher than 2.5m	Alkali Meadow
1	3	Sep	2008	9.07	1.81	4.64	0.9	Intact
10	1	May	2009	1.96	0.93	4.57	1	Intact
10	1	Sep	2008	0.00	13.84	4.57	1	Intact
10	2	Feb	2008	0.00	20.12	4.57	1	Intact
10	2	May	2009	0.00	13.84	4.57	1	Intact
10	2	Sep	2008	4.37	3.81	4.57	1	Intact
10	3	Sep	2008	8.42	2.57	4.57	1	Intact
11	1	May	2008	0.52	4.62	5.76	1	Degraded
11	1	May	2009	3.38	3.38	5.76	1	Degraded
11	1	Sep	2008	0.52	4.62	5.76	1	Degraded
11	2	May	2008	0.00	2.92	5.76	1	Degraded
11	2	May	2009	0.52	4.62	5.76	1	Degraded
11	2	Sep	2008	0.52	4.62	5.76	1	Degraded
11	3	May	2008	0.52	4.62	5.76	1	Degraded
11	3	May	2009	0.00	2.92	5.76	1	Degraded
11	3	Sep	2008	0.00	2.92	5.76	1	Degraded

Table A.4: Results from field measured Penetrometer readings and elliptical area of BB impression, average DTW, number of times DTW was higher than 2.5, and intact vs. degraded alkali meadow at each plot.

Plot	Profile	Month	Year	45Pen	BBEllipse	Average DTW (1987-1996)	# of times higher than 2.5m	Alkali Meadow
12	1	May	2008	0.10	4.63	7.79	0.9	Degraded
12	1	Sep	2008	0.34	2.48	7.79	0.9	Degraded
12	2	May	2008	0.34	2.48	7.79	0.9	Degraded
12	2	Sep	2008	0.10	3.33	7.79	0.9	Degraded
12	3	May	2008	0.10	3.33	7.79	0.9	Degraded
12	3	Sep	2008	0.34	2.48	7.79	0.9	Degraded
17	1	Feb	2008	7.84	1.79	2.43	0.7	Degraded
17	1	May	2009	7.84	1.79	2.43	0.7	Intact
17	1	Sep	2008	2.74	4.03	2.43	0.7	Degraded
17	2	Feb	2008	0.10	2.20	2.43	0.7	Degraded
17	2	May	2009	0.10	2.20	2.43	0.7	Intact
17	2	Sep	2008	2.74	4.03	2.43	0.7	Degraded
17	3	Sep	2008	0.10	2.20	2.43	0.7	Degraded
20	1	Feb	2008	1.63	2.13	2.90	0.7	Intact
20	1	May	2009	2.97	1.86	2.90	0.7	Intact
20	1	Sep	2008	13.72	2.91	2.90	0.7	Intact
20	2	Feb	2008	13.72	2.91	2.90	0.7	Intact
20	2	May	2009	13.72	2.91	2.90	0.7	Intact
20	2	Sep	2008	13.72	2.91	2.90	0.7	Intact

Table A.4: Results from field measured Penetrometer readings and elliptical area of BB impression, average DTW, number of times DTW was higher than 2.5, and intact vs. degraded alkali meadow at each plot.

Plot	Profile	Month	Year	45Pen	BBEllipse	Average DTW (1987-1996)	# of times higher than 2.5m	Alkali Meadow
20	3	Sep	2008	13.72	2.91	2.90	0.7	Intact
21	1	Feb	2008	0.10	2.20	2.43	0.3	Intact
21	1	May	2009	2.74	4.03	2.43	0.3	Intact
21	1	Sep	2008	2.74	4.03	2.43	0.3	Intact
21	2	May	2009	0.10	2.20	2.43	0.3	Intact
21	3	Feb	2008	2.74	4.03	2.43	0.3	Intact
22	1	May	2008	9.96	2.08	2.53	0.7	Intact
22	1	May	2009	0.65	3.39	2.53	0.7	Intact
22	1	Sep	2008	9.70	1.16	2.53	0.7	Intact
22	2	May	2008	9.70	1.16	2.53	0.7	Intact
22	2	May	2009	9.70	1.16	2.53	0.7	Intact
22	3	May	2008	9.96	2.08	2.53	0.7	Intact
22	3	May	2009	9.96	2.08	2.53	0.7	Intact
25	1	May	2009	0.72	5.21	3.94	1	Degraded
25	1	Sep	2008	0.14	1.63	3.94	1	Degraded
25	2	May	2009	0.00	7.98	3.94	1	Degraded
25	2	Sep	2008	0.00	7.98	3.94	1	Degraded
25	3	Sep	2008	0.00	7.98	3.94	1	Degraded
4	1	May	2008	1.52	1.73	1.80	0	Degraded

Table A.4: Results from field measured Penetrometer readings and elliptical area of BB impression, average DTW, number of times DTW was higher than 2.5, and intact vs. degraded alkali meadow at each plot.

Plot	Profile	Month	Year	45Pen	BBEllipse	Average DTW (1987-1996)	# of times higher than 2.5m	Alkali Meadow
4	1	Sep	2008	1.78	1.73	1.80	0	Degraded
4	2	May	2008	4.66	1.17	1.80	0	Degraded
4	2	May	2009	4.66	1.17	1.80	0	Intact
4	2	Sep	2008	1.14	1.59	1.80	0	Degraded
4	3	May	2008	4.66	1.17	1.80	0	Degraded
4	3	May	2009	1.14	1.59	1.80	0	Intact
4	3	Sep	2008	1.14	1.59	1.80	0	Degraded
6	1	Feb	2008	0.56	1.68	2.44	0.4	Intact
6	1	May	2009	0.13	5.35	2.44	0.4	Intact
6	1	Sep	2008	0.00	13.51	2.44	0.4	Intact
6	2	Feb	2008	0.56	1.68	2.44	0.4	Intact
6	2	May	2009	0.00	13.51	2.44	0.4	Intact
6	2	Sep	2008	0.56	1.68	2.44	0.4	Intact
6	3	May	2009	0.00	13.51	2.44	0.4	Intact
6	3	Sep	2008	0.56	1.68	2.44	0.4	Intact
7	1	Feb	2008	0.00	6.39	2.00	0	Intact
7	1	May	2009	0.00	6.39	2.00	0	Intact
7	1	Sep	2008	0.10	13.96	2.00	0	Intact
7	2	Feb	2008	0.10	13.96	2.00	0	Intact

Table A.4: Results from field measured Penetrometer readings and elliptical area of BB impression, average DTW, number of times DTW was higher than 2.5, and intact vs. degraded alkali meadow at each plot.

Plot	Profile	Month	Year	45Pen	BBEllipse	Average DTW (1987-1996)	# of times higher than 2.5m	Alkali Meadow
7	2	May	2009	0.10	13.96	2.00	0	Intact
7	2	Sep	2008	4.66	1.17	2.00	0	Intact
7	3	Sep	2008	0.10	13.96	2.00	0	Intact
9	1	Feb	2008	0.87	3.25	5.84	0.95	Intact
9	1	May	2009	0.00	13.73	5.84	0.95	Intact
9	1	Sep	2008	0.00	13.73	5.84	0.95	Intact
9	2	May	2009	0.00	13.84	5.84	0.95	Intact
9	2	Sep	2008	0.00	13.84	5.84	0.95	Intact
9	3	Sep	2008	0.00	13.73	5.84	0.95	Intact
Average				2.73	5.05	3.66	0.63	NA
Standard Deviation				4.11	4.67	1.81	0.37	NA
Medium				0.54	2.92	2.53	0.70	NA
Coefficient of Variation				1.51	0.92	0.50	0.58	NA

Not Applicable (NA) means the analysis was not applicable for the parameter.

Table A.5: Results from Remote Sensing of Vegetation Cover

Table A.5: Results from Remote Sensing of Vegetation Cover

Plot	Profile	Month	Year	Single Pixel	Pixel_AVG
1	3	Sep	2008	166	165.78
10	1	May	2009	86	83.33
10	1	Sep	2008	84	80.56
10	2	Feb	2008	84	80.56
10	2	May	2009	86	83.33
10	2	Sep	2008	84	80.56
10	3	Sep	2008	84	80.56
11	1	May	2008	79	75.67
11	1	May	2009	77	73.89
11	1	Sep	2008	79	75.67
11	2	May	2008	79	75.67
11	2	May	2009	77	73.89
11	2	Sep	2008	79	75.67
11	3	May	2008	79	75.67
11	3	May	2009	77	73.89
11	3	Sep	2008	79	75.67
12	1	May	2008	85	85.56
12	1	Sep	2008	85	85.56
12	2	May	2008	85	85.56

Table A.5: Results from Remote Sensing of Vegetation Cover

Plot	Profile	Month	Year	Single Pixel	Pixel_AVG
12	2	Sep	2008	85	85.56
12	3	May	2008	85	85.56
12	3	Sep	2008	85	85.56
17	1	Feb	2008	88	84.22
17	1	May	2009	90	86.78
17	1	Sep	2008	88	84.22
17	2	Feb	2008	88	84.22
17	2	May	2009	90	86.78
17	2	Sep	2008	88	84.22
17	3	Sep	2008	88	84.22
20	1	Feb	2008	105	109.11
20	1	May	2009	108	112.89
20	1	Sep	2008	105	109.11
20	2	Feb	2008	105	109.11
20	2	May	2009	108	112.89
20	2	Sep	2008	105	109.11
20	3	Sep	2008	105	109.11
21	1	Feb	2008	88	90.44
21	1	May	2009	91	94.33
21	1	Sep	2008	88	90.44
21	2	May	2009	91	94.33

Table A.5: Results from Remote Sensing of Vegetation Cover

Plot	Profile	Month	Year	Single Pixel	Pixel_AVG
21	3	Feb	2008	88	90.44
22	1	May	2008	108	112.78
22	1	May	2009	101	106.67
22	1	Sep	2008	108	112.78
22	2	May	2008	108	112.78
22	2	May	2009	101	106.67
22	3	May	2008	108	112.78
22	3	May	2009	101	106.67
25	1	May	2009	101	100.11
25	1	Sep	2008	110	106.56
25	2	May	2009	101	100.11
25	2	Sep	2008	110	106.56
25	3	Sep	2008	110	106.56
4	1	May	2008	86	89.78
4	1	Sep	2008	86	89.78
4	2	May	2008	86	89.78
4	2	May	2009	80	82
4	2	Sep	2008	86	89.78
4	3	May	2008	86	89.78
4	3	May	2009	80	82
4	3	Sep	2008	86	89.78

Table A.5: Results from Remote Sensing of Vegetation Cover

Plot	Profile	Month	Year	Single Pixel	Pixel_AVG
6	1	Feb	2008	83	83.89
6	1	May	2009	85	84.6
6	1	Sep	2008	83	83.89
6	2	Feb	2008	83	83.89
6	2	May	2009	85	84.6
6	2	Sep	2008	83	83.89
6	3	May	2009	85	84.6
6	3	Sep	2008	83	83.89
7	1	Feb	2008	83	82.67
7	1	May	2009	83	81.56
7	1	Sep	2008	82	82.67
7	2	Feb	2008	82	82.67
7	2	May	2009	83	81.56
7	2	Sep	2008	82	82.67
7	3	Sep	2008	82	82.67
9	1	Feb	2008	85	87.56
9	1	May	2009	86	87.11
9	1	Sep	2008	85	87.56
9	2	May	2009	86	87.11
9	2	Sep	2008	85	87.56

Table A.5: Results from Remote Sensing of Vegetation Cover

Plot	Profile	Month	Year	Single Pixel	Pixel_AVG
9	3	Sep	2008	85	87.56
Average				90.22	90.70
Standard Deviation				12.86	14.13
Medium				86.00	85.56
Coefficient of Variation				0.14	0.16

Table A.6: Description of Parameters

Table A.6: Description of Parameters

Description	Parameters
Chloride Concentration	CL (mg kg^{-1})
Nitrite Concentration	Nitrite (mg kg^{-1})
Nitrate Concentration	Nitrate (mg kg^{-1})
Phosphate Concentration	Phosphate (mg kg^{-1})
Sulfate Concentration	Sulfate (mg kg^{-1})
Soil Organic Carbon 40%	Soil Organic Carbon 40% (g kg^{-1})
Soil Organic Carbon 60%	Soil Organic Carbon 60% (g kg^{-1})
Vegetation or No Vegetation	Veg
Threshold Sheer Velocity	TSV (cm s^{-1})
Depth to Water	DTW (m)
Total Horizontal Flux	Qtot (g $cm^{-1}d^{-1}$)
Threshold Sheer Velocity BB Method Average Threshold Shear Velocity determined by the BB method	TSVbbavg (cm s^{-1})
Soil Type	Soil Type
Stability	Stability
Threshold Sheer Velocity BB Method	TSVbb (cm s^{-1})
Intact or Degraded Alkali Meadow	Alkali Meadow
Penetrometer at 45 degrees	45Pen
BB impact area as an ellipse	BBEllipse
Average DTW 1987 to 1996	AverageDTW (m)

Table A.6: Description of Parameters

Description	Parameters
Number of times DTW is higher than 2.5m	# of times lower than 2.5m
Single Pixel Value	Single Pixel
Average Pixel Value from Nine Pixels	Pixel_AVG

Table A.7: Dates and number of times field and other data was collected

Table A.7: Dates and number of times field and other data was collected

Variables measured	Feb 2008	May 2008	Sep 2008	Apr 2009	May 2009	Sep 2009	Apr 2010	May 2010	Sep 2010	Apr 2010	Number of times measured per plot per year
CL (mg kg^{-1})	x	x	x		x	x					Feb 2008: 2 times; May and Sep 2008: 3 times; 2009: 3 times
Nitrite (mg kg^{-1})	x	x	x		x	x					Feb 2008: 2 times; May and Sep 2008: 3 times; 2009: 3 times
Nitrate (mg kg^{-1})	x	x	x		x	x					Feb 2008: 2 times; May and Sep 2008: 3 times; 2009: 3 times
Phosphate (mg kg^{-1})	x	x	x		x	x					Feb 2008: 2 times; May and Sep 2008: 3 times; May and Sep 2009: 3 times
Sulfate (mg kg^{-1})	x	x	x		x	x					Feb 2008: 2 times; May and Sep 2008: 3 times; May and Sep 2009: 3 times
Soil Organic Carbon 40% (g kg^{-1})	x	x	x		x	x					Feb 2008: 2 times; May and Sep 2008: 3 times; May and Sep 2009: 3 times
Soil Organic Carbon 60% (g kg^{-1})	x	x	x		x	x					Feb 2008: 2 times; May and Sep 2008: 3 times; May and Sep 2009: 3 times
Veg		x			x			x			2008: 1 time; 2009: 1 time
DTW				x			x			x	[1]2008: 1 time; 2009: 1 time
Q (g $cm^{-1}d^{-1}$)			x			x			x		2008: 1 time; 2009: 1 time
TSVbbavg (cm s^{-1})									x		[2] 2010: Average of 5 times
Stability									x		[2] 2010: 1 time
TSVbb (cm s^{-1})									x		[3] 2010: 10 times
45Pen									x		[3] 2010: 10 times
BBEllipse									x		[3] 2010: 10 times
Average DTW (m)											[1,4] 1987 - 1996: 1 time
# of times higher than 2.5m											[1,4] 1987 - 1996: 1 time
Single Pixel			x			x					2008: 1 time; 2009: 1 time
Pixel_AVG			x			x					2008: 1 time; 2009: 1 time

[1] Measured by ICWD and LADWP

Table A.7: Dates and number of times field and other data was collected

Variables measured	Feb 2008	May	Sep	Apr	May 2009	Sep	Apr	May 2010	Sep	Apr	Number of times measured per plot per year

[2] Measured in 2010 and matched to 2008 and 2009 data
[3] Measured in bare soil from BSNE stem
[4] Used data from 1987 to 1996 to coincide with the drought

Bibliography

Alcantara-Carrio J, Alonso I (2002) Measurement and Prediction of Aeolian Sediment Transport at Jandia Isthmus (Fuerteventura, Canary Islands). Journal of Coastal Research 18:300–315.

Archer S, Schimel D, Holland E (1995) Mechanisms of shrubland expansion: land use, climate or CO2? Climatic Change 29:91–99. doi: 10.1007/BF01091640

Aubault H (2009) Impacts modeling of change textures due to groundwater decline on the dust emission rates, Owens Valley (Californie). Université Paris 7 - Diderot

Barone JB, Ashbaugh LL, Kusko BH, Cahill TA (1981) The effect of Owens Dry Lake on air quality in the Owens Valley with implications for the Mono Lake area. Chem Soc Symp Ser 167:327–346.

Barron O, Froend R, Hodgson G, et al (2014) Projected risks to groundwater-dependent terrestrial vegetation caused by changing climate and groundwater abstraction in the Central Perth Basin, Western Australia. Hydrol Process 28:5513–5529. doi: 10.1002/hyp.10014

Belnap J (1995) Surface disturbances: Their role in accelerating desertification. Environmental Monitoring and Assessment 37:39–57–57.

Belnap J, Gillette DA (1998) ScienceDirect - Journal of Arid Environments : Vulnerability of desert biological soil crusts to wind erosion: the influences of crust development, soil texture, and disturbance. Journal of Arid Environments 39:133–142.

Bergametti G, Gillette DA (2010) Aeolian sediment fluxes measured over various plant/soil complexes in the Chihuahuan desert. J Geophys Res 115:F03044.

Berglund BE (2003) Handbook of Holocene Palaeoecology and Palaeohydrology. The Blackburn Press

Bestelmeyer BT (2005) Does desertificaiton diminish biodiversity? Enhancement to ant diversity by shrub invation in soutwestern USA. Diversity and Distributions 11:45–55.

Bestelmeyer BT, Ward JP, Herrick JE, Tugel AJ (2006) Fragmentation Effects on Soil Aggregate Stability in a Patchy Arid Grassland. Rangeland Ecology & Management 59:406–415.

Blunden J, Arndt DS (2013) State of the Climate in 2012. Bull Amer Meteor Soc 94:S1–S258. doi: 10.1175/2013BAMSStateoftheClimate.1

Breshears DD, Whicker JJ, Zou CB, et al (2009) A conceptual framework for dryland aeolian sediment transport along the grassland-forest continuum: Effects of woody plant canopy cover and disturbance. Geomorphology 105:28–38. doi: doi: DOI: 10.1016/j.geomorph.2007.12.018

Brewer M (2014) US Drought Monitor. In: U.S. Drought Portal. http://www.drought.gov/drought/content/products-current-drought-and-monitoring-drought-indicators/us-drought-monitor. Accessed 27 Oct 2014

Brown S, Nickling WG, Gillies JA (2008) A wind tunnel examination of shear stress partitioning for an assortment of surface roughness distributions. Journal of Geophysical Research 113:F02S06. doi: 10.1029/2007JF000790

Buckley R (1987) The effect of sparse vegetation on the transport of dune sand by wind. Nature 325:426–428. doi: 10.1038/325426a0

Bunn AG, Urban DL, Keitt TH (2000) Landscape connectivity: A conservation application of graph theory. Journal of Environmental Management 59:265–278. doi: doi: DOI: 10.1006/jema.2000.0373

Cahill TA, Gill TE, Reid JS, et al (1996) Saltating particles, playa crusts and dust aerosols at Owens (dry) Lake, California. Earth Surface Processes and Landforms 21:621–639.

Caswell H (1976) Community structure: a neutral model analysis. Ecological Monographs 46:327–354.

Cayan D, Maurer E, Dettinger M, et al (2008) Climate change scenarios for the California region. Climatic Change 87:21–42. doi: 10.1007/s10584-007-9377-6

Ceballos G, Davidson A, List R, et al (2010) Rapid Decline of a Grassland System and Its Ecological and Conservation Implications. PLOS One 5:e8562.

Charney JG (1975) Dynamics of Deserts and Drought in Sahel. Quarterly Journal of the Royal Meteorological Society 101:193–202. doi: 10.1002/qj.49710142802

City of Los Angeles and County of Inyo (1990) Technical Appendix F Green book for the long-term groundwater management plan for the Owens Valley and Inyo County. In Draft EIR: water from the Owens Valley to supply the second Los Angeles Aqueduct; 1970 to 1990, and 1990 onward, pursuant to a long term groundwater management plan. State Clearing House no. 89080705, Department of Water and Power, City of Los Angeles, California, USA.

D'Odorico P, Okin GS, Bestelmeyer BT (2012) A synthetic review of feedbacks and drivers of shrub encroachment in arid grasslands. Ecohydrology 5:520–530.

Danskin WR (1998) Evaluation of the Hydrologic System and Selected Water-Management Alternatives in the Owens Valley, California. USGS, Owens Valley, CA

Day SJ, Norton JB, Kelleners TJ, Strom CF (2015) Drastic Disturbance of Salt-Affected Soils in a Semi-Arid Cool Desert Shrubland. Arid Land Res Manag 29:306–320. doi: 10.1080/15324982.2014.962666

Dehaan RL, Taylor GR (2002) Field-derived spectra of salinized soils and vegetation as indicators of irrigation-induced soil salinization. Remote Sensing of Environment 80:406–417. doi: doi: DOI: 10.1016/S0034-4257(01)00321-2

Dong ZB, Gao SY, Fryrear DW (2001) Drag coefficients, roughness length and zero-plane displacement height as disturbed by artificial standing vegetation. Journal of Arid Environments 49:485–505. doi: 10.1006/jarc.2001.0807

Dong ZB, Man D, Luo W, et al (2010) Horizontal aeolian sediment flux in the Minqin area, a major source of Chinese dust storms. Geomorphology 116:58–66. doi: doi: DOI: 10.1016/j.geomorph.2009.10.008

Dorsaz J-M, Gironás J, Escauriaza C, Rinaldo A (2013) The geomorphometry of endorheic drainage basins: implications for interpreting and modelling their evolution. Earth Surf Process Landforms 38:1881–1896. doi: 10.1002/esp.3475

Elmore AJ, Kaste JM, Okin GS, Fantle MS (2008) Groundwater influences on atmospheric dust generation in deserts. Journal of Arid Environments 72:1753–1765.

Elmore AJ, Manning SJ, Mustard JF, Craine JM (2006a) Decline in alkali meadow vegetation cover in California: the effects of groundwater extraction and drought. Journal of Applied Ecology 770–779.

Elmore AJ, Manning SL, Mustard JF, Craine JM (2006b) Decline in alkali meadow vegetation cover in California: the effects of groundwater extraction and drought. Journal of Applied Ecology 43:770–779. doi: 10.1111/j.1365-2664.2006.01197

Elmore AJ, Mustard JF, Manning SJ, Lobell DB (2000) Quantifying Vegetation Change in Semiarid Environments: Precision and Accuracy of Spectral Mixture Analysis and the Normalized Difference Vegetation Index. Remote Sensing of Environment 73:87–102. doi: doi: DOI: 10.1016/S0034-4257(00)00100-0

Elmore AJ, Mustard JF, Manning SL (2003) Regional patterns of plant community response to changes in water: Owens Valley, California. Ecological Applications 13:443–460.

Ferrari J, Lookingbill T, Neel M (2007) Two measures of landscape-graph connectivity: assessment across gradients in area and configuration. Landscape Ecology 22:1315–1323.

Fryrear DW (1985) Soil cover and wind erosion. Trans ASAE 28:781–784.

Fubini B, Fenogolio I (2007) Toxic Potential of Mineral Dusts. Elements 3:407–414.

Fulbright TE, Ortega-Santos JA, Lozano-Cavazos A, Ramírez-Yanez LE (2006) Establishing Vegetation on Migrating Inland Sand Dunes in Texas. Rangeland Ecology & Management 59:549–556. doi: 10.2111/06-025R1.1

Fuller T, Munguia M, Mayfield M, et al (2006) Incorporating connectivity into conservation planning: A multi-criteria case study from central Mexico. Biological Conservation 133:131–142. doi: 10.1016/j.biocon.2006.04.040

Gardner RH (1986) A computer program for landscape hypothesis testing.

Gardner RH, Milne BT, Turner MG, O'Neill RV (1987) Neutral models for the analysis of broad-scale landscape pattern. Landscape Ecology 1:19–28.

Gardner RH, Urban DL (2007) Neutral models for testing landscape hypotheses. Landscape Ecology 15–29. doi: 10.1007/s10980-006-9011-4

GBUAPCD (2008) 2008 Owens Valley Planning Area Demonstration of Attainment State Implementation Plan.

GBUAPCD (2012) Owens Lake Dust Control Final 2012 Supplemental Control Requirements Determination.

GBUAPCD (2013) SIP Revision 2013 Amendment to Owens Valley PM10 SIP (Board Order #130916-01). GBUAPCD

GBUAPCD (2011) Consideration of a request from Inyo County for use of the District's Owens Lake water wells for hydrological testing associated with the Los Angeles Department of Water and power's Owens Lake Groundwater Evaluation Program. Bishop, CA

GBUAPCD (2015) Owens Lake Dust ID Network Map.

Gill TE (1996) Eolian sediments generated by anthropogenic disturbance of playas: Human impacts on the geomorphic system and geomorphic impacts on the human system. Geomorphology 17:207–228.

Gill TE, Cahill TA (1992) Playa-generated Dust Storms from Owens Lake. The History of Water: Eastern Sierra Nevada, Owens Valley, White-Inyo Mountains. Regents of the University of California, pp 63 – 73

Gillette DA (1997) Soil derived dust as a source of silica: Aerosol properties, emissions, deposition, and transport. Journal of Exposure Analysis and Environmental Epidemiology 7:303–311.

Gillette DA, Adams J, Endo A, et al (1980) Threshold Velocities for Input of Soil Particles into the Air by Desert Soils. Journal of Geophysical Research 85:5621–5630. doi: 10.1029/JC085iC10p05621

Gillette DA, Adams J, Muhs D, Kihl R (1982) Threshold Friction Velocities and Rupture Moduli for Crusted Desert Soils for the Input of Soil Particles into the Air. J Geophys Res 87:9003–9015.

Gillette DA, Fryrear DW, Gill TE, et al (1997) Relation of vertical flux of particles smaller than 10 μm to total aeolian horizontal mass flux at Owens Lake. J Geophys Res 102:26009–26015.

Gillette DA, Herrick JE, Herbert GA (2006) Wind characteristics of mesquite streets in the northern Chihuahuan Desert, New Mexico, USA. Environmental Fluid Mechanics 6:241–275.

Gillette DA, Niemeyer TC, Helm PJ (2001) Supply-limited horizontal sand drift at an ephemerally crusted, unvegetated saline playa. J Geophys Res 106:18085–18098.

Gillette DA, Passi R (1988) Modeling Dust Emission Caused by Wind Erosion. J Geophys Res 93:14233–14242.

Goudie AS, Middleton NJ (1992) The changing frequency of dust storms through time. Climatic Change 20:197–225–225.

Goulden ML, Bales RC (2014) Mountain runoff vulnerability to increased evapotranspiration with vegetation expansion. Proceedings of the National Academy of Sciences 111:14071–14075. doi: 10.1073/pnas.1319316111

Guler C, Thyne GD (2004) Hydrologic and geologic factors controlling surface and groundwater chemistry in Indian Wells-Owens Valley area, southeastern California, USA. Journal of Hydrology 285:177–198. doi: doi: DOI: 10.1016/j.jhydrol.2003.08.019

Helldén U (1991) Desertification: Time for an Assessment? Ambio 20:372–383.

Herrick JE, Whitford WG, de Soyza AG, et al (2001) Field soil aggregate stability kit for soil quality and rangeland health evaluations. CATENA 44:27–35.

Hervàs A, Camarero L, Reche I, Casamayor EO (2009) Viability and potential for immigration of airborne bacteria from Africa that reach high mountain lakes in Europe. Environmental Microbiology 11:1612–1623. doi: 10.1111/j.1462-2920.2009.01926.x

Hollett KJ, Danskin WR, McCaffrey WF, Walti CL (1991) Geology and Water Resources of Owens Valley, California.

Huenneke LF, Anderson JP, Remmenga M, Schlesinger WH (2002) Desertification alters patterns of aboveground net primary production in Chihuahuan ecosystems. Global Change Biology 8:247–264. doi: 10.1046/j.1365-2486.2002.00473.x

Hulme M, Kelly M (1993) Exploring the links between Desertification and Climate Change. Enviornment: Science and Policy for Sustainable Development 35:4–45.

James G, Groenveld D, Hutchison B, et al (1990) Greenbook for The Long-Term Groundwater Management Plan for the Owens Valley and Inyo County.

Kampf SK, Tyler SW, Ortiz CA, et al (2005) Evaporation and land surface energy budget at the Salar de Atacama, Northern Chile. Journal of Hydrology 310:236–252. doi: doi: DOI: 10.1016/j.jhydrol.2005.01.005

Kepner WG, Watts CJ, Edmonds CM, et al (2000) A Landscape Approach for Detecting and Evaluating Change in a Semi-Arid Environment. Environmental Monitoring and Assessment 64:179–195.

Kieft TL, White CS, Loftin SR, et al (1998) Temporal Dynamics in Soil Carbon and Nitrogen Resources at a Grassland-Shrubland Ecotone. Ecology 79:671–683.

King J, Nickling WG, Gillies JA (2005) Respresentation of Vegetation and other nonerodible elements in aeolian shear stress partitioning models for predicting transport threshold. Journal of Geophysical Research 110:F04015. doi: 10.1029/2004JF000281

King J, Nickling WG, Gillies JA (2006) Aeolian shear stress ratio measurements within mesquite-dominated landscapes of the Chihuahuan Desert, New Mexico, USA. Geomorphology 82:229 – 244. doi: DOI: 10.1016/j.geomorph.2006.05.004

LACWD (2015) Los Angeles County Waterworks Districts. In: What are the Statewide Water Restrictions adopted in 2014 and the NEW restrictions adopted in March 2015? http://dpw.lacounty.gov/wwd/web/Conservation/Drought.aspx.

LADWP (2014a) Draft 2014 Annual Owens Valley Report. Los Angeles Department of Water and Power

LADWP (2014b) 2014 Annual Operations Plan for the Second Six Months Final.

LADWP (2011) LADWP: Owens Valley Water Uses and Pumping. In: LADWP: Owens Valley Water Uses and Pumping. In: Los Angeles Department of

Water and Power Owens Valley Water Uses and Pumping. Accessed 26 Oct 2011

LADWP (2005) Annual Owens Valley Operations Plan for Runoff Year 2005-06.

LADWP (2014c) LADWP: Owens Valley Water Uses and Pumping. In: Los Angeles Department of Water and Power Owens Valley Water Uses and Pumping. http://www.ladwp.com/ladwp/cms/ladwp007333.jsp. Accessed 17 Nov 2014

Lal R (2003) Soil erosion and the global carbon budget. Environment International 29:437–450. doi: doi: DOI: 10.1016/S0160-4120(02)00192-7

Lancaster N, Baas A (1998) Influence of vegetation cover on sand transport by wind: Field studies at Owens Lake, California. Earth Surface Processes and Landforms 23:69–82.

Langston G, McKenna Neuman C (2005) An experimental study on the susceptibility of crusted surfaces to wind erosion: A comparison of the strength properties of biotic and salt crusts. Geomorphology 72:40–53. doi: doi: DOI: 10.1016/j.geomorph.2005.05.003

Le Houffrou HN (1996) Climate change, drought and desertification. Journal of Arid Environments 34:133–185. doi: doi: DOI: 10.1006/jare.1996.0099

Levin N, Kidron GJ, Ben-Dor E (2006) The spatial and temporal variability of sand erosion across a stabilizing coastal dune field. Sedimentology 53:697–715. doi: Article

Li J, Okin GS, Alvarez L, Epstein H (2007) Quantitative effects of vegetation cover on wind erosion and soil nutrient loss in a desert grassland of southern New Mexico, USA. Biogeochemistry 85:317–332.

Li J, Okin GS, Herrick JE, et al (2010) A Simple Method to Estimate Threshold Friction Velocity of Wind Erosion in the Field.

Li L, Shaomin L, Zeiwei X, et al (2009) The Characteristics and Parameterization of Aerodynamic Roughness Length over Heterogeneous Surfaces. Advances in Atmospheric Sciences 26:180–190.

Mannetje LT, Jones RM (2000) Field and Laboratory Methods for Grassland and Animal Production Research. CABI Publishing, New York, NY

Marshall JD, Blair JM, Peters DPC, et al (2008) Predicting and Understanding Ecosystem Responses to Climate Change at Continental Scales. Frontiers in Ecology and the Environment 6:273–280. doi: 10.2307/20440888

Marshall JK (1971) Drag Measurements in Roughness Arrays of Varying Density and Distribution. Agricultural Meteorology 8:269–292.

Marticorena B, Bergametti G (1995) Modeling the atmospheric dust cycle: 1. Design of a soil-derived dust emission scheme. J Geophys Res 100:16415–16430.

Marticorena B, Bergametti G, Aumont B, et al (1997) Modeling the atmospheric dust cycle .2. Simulation of Saharan dust sources. Journal of Geophysical Research-Atmospheres 102:4387 – 4404.

McGlynn IO, Okin GS (2006) Characterization of shrub distribution using high spatial resolution remote sensing: Ecosystem implications for a former Chihuahuan Desert grassland. Remote Sensing of Environment 101:554–566. doi: doi: DOI: 10.1016/j.rse.2006.01.016

McRae BH (2006) Isolation by Resistance. Evolution 60:1551–1561.

McRae BH, Dickson BG, Keitt TH, Shah VB (2008) Using Circuit Theory To Model Connectivity in ecology, evolution, and Conservation. Ecology 89:2712–2724. doi: doi: 10.1890/07-1861.1

McRae BH, Shah VB (2009) Circuitscape User Guide. ONLINE.The University of California, Santa Barbara. Available at: http://www.circuitscape.org.

Mees F, Stoops G (1991) Minerological Study of Salt Efflorenscences on Soil of the Jequetepeque Valley, Northern Peru. Geoderma 49:255–272.

Megerian C, Stevens M, Boxall B (2015) Brown orders California's first mandatory water restrictions: "It"s a different world'. Los Angeles Times

Mini C, Hogue TS, Pincetl S (2015) The effectiveness of water conservation measures on summer residential water use in Los Angeles, California. Resources, Conservation and Recycling 94:136–145. doi: 10.1016/j.resconrec.2014.10.005

Minor ES, Urban DL (2007) Graph Theory as a Proxy for Spatially Explicit Population Models in Conservation Planning. Ecological Applications 17:1771–1782.

Minor ES, Urban DL (2008) A Graph-Theory Framework for Evaluating Landscape Connectivity and Conservation Planning. Conservation Biology 22:297–307. doi: 10.1111/j.1523-1739.2007.00871.x

Muñoz-Reinoso JC (2001) Vegetation changes and groundwater abstraction in SW Doñana, Spain. Journal of Hydrology 242:197–209. doi: 10.1016/S0022-1694(00)00397-8

Musick HB, Gillette DA (1990) Land degradation & rehabilitation.: Field evaluation of relationships between a vegetation structural parameter and sheltering against wind erosion. Land Degredation and Rehabilitation 2:87–94.

Musick HB, Trujillo SM, Truman CR (1996) Wind-tunnel modelling of the influence of vegetation structure on saltation threshold. Earth Surface Processes and Landforms 21:589–605.

Nash MS, Jackson E, Whitford WG (2004) Effects of intense, short-duration grazing on microtopography in a Chihuahuan Desert grassland. Journal of Arid Environments 56:383–393. doi: 10.1016/S0140-1963(03)00062-4

Nichols RO (2011) Owens Lake Dust Control Final 2011 Supplemental Control Requirements Determination.

Nicholson SE, Tucker CJ, Ba MB (1998) Desertification, drought, and surface vegetation: An example from the West African Sahel. Bulletin of the American Meteorological Society 79:815. doi: Article

Nickling WG (1984) The stabilizing role of bonding agents on the entrainment of sediment by wind. Sedimentology 31:111 – 117.

Nickling WG, Ecclestone M (1981) The effects of soluble salts on the threshold shear velocity of fine sand. Sedimentology 28:505 – 510.

Nickling WG, Neuman CM (1997) Wind tunnel evaluation of a wedge-shaped aeolian sediment trap. Geomorphology 18:333–345. doi: doi: DOI: 10.1016/S0169-555X(96)00040-2

O'Grady AP, Eamus D, Cook PG, Lamontagne S (2006) Groundwater use by riparian vegetation in the wet–dry tropics of northern Australia. Australian Journal of Botany 54:145–154.

Okin GS (2008) A new model of wind erosion in the presence of vegetation. Journal of Geophysical Research-Earth Surface. doi: 10.1029/2007JF000758

Okin GS (2005) Dependence of wind erosion and dust emission on surface heterogeneity: Stochastic modeling. Journal of Geophysical Research-Atmospheres. doi: 10.1029/2004JD005288

Okin GS (2010) Conference Call with Greg Okin discussing wind erosion.

Okin GS, Gillette DA (2001) Distribution of vegetation in wind-dominated landscapes: Implications for wind erosion modeling and landscape processes. Journal of Geophysical Research-Atmospheres 106:9673–9683.

Okin GS, Gillette DA, Herrick JE (2006) Multi-scale controls on and consequences of aeolian processes in landscape change in arid and semi-arid environments. Journal of Arid Environments 65:253–275. doi: doi: DOI: 10.1016/j.jaridenv.2005.06.029

Okin GS, Murry B, Schlesinger WH (2001) Degradation of sandy arid shrubland environments: observations, process modelling, and management implications. Journal of Arid Environments 47:123–144.

Okin GS, Parsons AJ, Wainwright J, et al (2009) Do Changes in Connectivity Explain Desertification? BioScience 59:237–244.

Orme AR, Orme AJ (2008) Late Pleistocene shorelines of Owens Lake, California, and their hydroclimatic and tectonic implications. Geological Society of America Special Paper 439:207–225.

Overton IC, Jolly ID, Slavich PG, et al (2006) Modelling vegetation health from the interaction of saline groundwater and flooding on the Chowilla floodplain, South Australia. Australian Journal of Botany 54:207–220.

Park S-U, In H-J (2003) Parameterization of dust emission for the simulation of the yellow sand (Asian dust) event observed in March 2002 in Korea. J Geophys Res 108:4618. doi: 10.1029/2003JD003484

Peters DPC, Bestelmeyer BT, Herrick JE, et al (2006) Disentangling complex landscapes: New insights into arid and semiarid system dynamics. BioScience 56:491–501.

Prigent C, Tegen I, Aires F, et al (2005) Estimation of the aerodynamic roughness length in arid and semi-arid regions over the globe with the ERS scatterometter. Journal of Geophysical Research 110:D09205. doi: 10.1029/2004JD005370

Prince SD, Becker-Reshef I, Rishmawi K (2009) Detection and mapping of long-term land degradation using local net production scaling: Application to Zimbabwe. Remote Sensing of Environment 113:1046–1057. doi: doi: DOI: 10.1016/j.rse.2009.01.016

Prince SD, Brown, Kravitz, de Colstoun (1998) Evidence from rain-use efficiencies does not indicate extensive Sahelian desertification. Global Change Biology 4:359–374. doi: Article

Prospero JM (1999) Long-Range Transport of Mineral Dust in the Global Atmosphere: Impact of African Dust on the Environment of the Southeastern United States. Proceedings of the National Academy of Sciences of the United States of America 96:3396–3403.

Ragab R, Prudhomme C (2002) Climate Change and Water Resources Management in Arid and Semi-arid Regions: Prospective and Challenges for the 21st Century. Biosystems Engineering 81:3–34.

Rajan K, Natarajan A, Kumar KS, et al (2010) Soil Organic Carbon - the most reliable indicator for monitoring land degradation by soil erosion. Current Science 99:823–827.

Raupach MR, Gillette DA, Leys JF (1993) The Effect of Roughness Elements on Wind Erosion Threshold. Journal of Geophysical Research-Atmospheres 98:3023–3029.

Ravi S, D'Odorico P, Breshears DD, et al (2011) AEOLIAN PROCESSES AND THE BIOSPHERE. Rev Geophys 49:RG3001. doi: 10.1029/2010RG000328

Reheis MC (1997) Dust deposition downwind of Owens (dry) Lake, 1991–1994: Preliminary findings. J Geophys Res 102:25999–26008.

Reheis MC (2006) A 16-year record of eolian dust in Southern Nevada and California, USA: Controls on dust generation and accumulation. Journal of Arid Environments 67:487 – 520. doi: DOI: 10.1016/j.jaridenv.2006.03.006

Reheis MC, Budahn JR, Lamothe PJ, Reynolds RL (2009) Compositions of modern dust and surface sediments in the Desert Southwest, United States.

Reid JS, Flocchini RG, Cahill TA, et al (1994) Local meteorological, transport, and source aerosol characteristics of late autumn Owens Lake (dry) dust storms. Atmospheric Environment 28:1699–1706. doi: 10.1016/1352-2310(94)90315-8

Rengasamy P (2006) World Salinization with Emphasis on Australia. Journal of Experimental Biology 57:1017–1023.

Reynolds JF, Smith D, Lambin EF, et al (2007a) Global Desertification: Building a Science for Dryland Development. Science 316:847–851.

Reynolds RL, Yount JC, Reheis MC, et al (2007b) Dust emission from wet and dry playas in the Mojave desert, USA. Earth Surface Processes and Landforms 32:1811–1827. doi: 10.1002/esp.1515

Rubio JL, Bochet E (1998) Desertification indicators as diagnosis criteria for desertification risk assessment in Europe. Journal of Arid Environments 39:113–120. doi: doi: DOI: 10.1006/jare.1998.0402

Saint-Amand P, Gaines C, Saint-Amand D (1987) Owens Lake, an Ionic Soap Opera staged on a Natric Playa. Geological Society of America Special Field Guide - Cordileran Section 113–118.

Schlesinger WH, Pilmanis AM (1998) Plant-Soil Interactions in Deserts. Biogeochemistry 42:169–187.

Schlesinger WH, Raikes JA, Hartley AE, Cross AF (1996a) On the Spatial Pattern of Soil Nutrients in Desert Ecosystems. Ecology 77:364–374.

Schlesinger WH, Raikes JA, Hartley AE, Cross AF (1996b) On the Spatial Pattern of Soil Nutrients in Desert Ecosystems. Ecology 77:364–374.

Schlesinger WH, Reynolds JF, Cunningham GL, et al (1990) Biological Feedbacks in Global Desertification. Science 247:1043–1048.

Seager R (2007) Model projections of an imminent transition to a more arid climate in southwestern North America. Science 16:1181–1184.

Seager R, Ting M, Held I, et al (2007) Model Projections of an Imminent Transition to a More Arid Climate in Southwestern North America. Science 316:1181 – 1184. doi: 10.1126/science.1139601

Seager R, Ting M, Li C, et al (2013) Projections of declining surface-water availability for the southwestern United States. Nature Clim Change 3:482–486.

Seeboonruang U (2014) Physico-chemical characterization of saline subsurface system near small endorheic ponds in Thailand. Environ Earth Sci 71:3273–3286. doi: 10.1007/s12665-014-3052-9

Seybold CA, Herrick JE (2001) Aggregate stability kit for soil quality assessments. CATENA 44:37–45. doi: doi: DOI: 10.1016/S0341-8162(00)00175-2

Shafroth P, Stromberg JC, Patten D (2000) Woody riparian vegetation response to different alluvial water table regimes. Western North American Naturalist 60:66–76.

Shao Y, Ishizuka M, Mikami M, Leys JF (2011) Parameterization of size-resolved dust emission and validation with measurements. J Geophys Res 116:D08203. doi: 10.1029/2010JD014527

Shao Y, Raupach MR (1992) The Overshoot and Equilibration of Saltation. J Geophys Res 97:20559–20564.

Shao YP (2000) Physics and Modelling of Wind Erosion. Kluwer Academic Publishers, Norwell, MA

Shao YP, McTainsh GH, Leys JF, Raupach MR (1993) Efficiencies of Sediment Samplers for Wind Erosion Measurement. Australian Journal of Soil Research 31:519–532.

Sharma KD (1998) The hydrological indicators of desertification. Journal of Arid Environments 39:121–132. doi: doi: DOI: 10.1006/jare.1998.0403

Singer MJ, Shainberg I (2004) Mineral soil surface crusts and wind and water erosion. Earth Surf Process Landforms 29:1065–1075. doi: 10.1002/esp.1102

Soil Survey Staff Natural Resources Conservation Service, United States Department of Agriculture. In: Soil Survey Geographic (SSURGO) Database for [CA732, California]. http://soildatamart.nrcs.usda.gov accessed [4/15/2010].

Sorenson S, Dileanis P, Branson F (1991) Soil and Vegetation Response to Precipitation and Changes in Depth to Groundwater in Owens Valley.

Spear SF, Balkenhol N, Fortin MJ, et al (2010) Use of resistance surfaces for landscape genetic studies: considerations for parameterization and analysis. Molecular Ecology 19:3576–3591. doi: 10.1111/j.1365-294X.2010.04657.x

State of California (2015) Executive Order B-29-15.

Stromberg JC, Tiller R, Richter B (1996) Effects of Groundwater Decline on Riparian Vegetation of Semiarid Regions: The San Pedro, Arizona. Ecological Applications 6:113–131.

Su YZ, Zhao WZ, Su PX, et al (2007) Ecological effects of desertification control and desertified land reclamation in an oasis-desert ecotone in an and region: A case study in Hexi Corridor, northwest China. Ecol Eng 29:117–124. doi: 10.1016/j.ecoleng.2005.10.015

Sun D, Dawson R, Li H, et al (2007) A landscape connectivity index for assessing desertification: a case study of Minqin County, China. Landscape Ecology 22:531–543. doi: 10.1007/s10980-006-9046-6

Taylor CM, Lambin EF, Stephenne N, et al (2002) The Influence of Land Use Change on Climate in the Sahel. Journal of Climate 15:3615.

Throop H, Reichmann L, Sala O, Archer S (2012) Response of dominant grass and shrub species to water manipulation: an ecophysiological basis for shrub invasion in a Chihuahuan Desert Grassland. Oecologia 169:373–383. doi: 10.1007/s00442-011-2217-4

Turnbull L, Wainwright J, Brazier RE (2008) A conceptual framework for understanding semi-arid land degradation: ecohydrological interactions across multiple-space and time scales. Ecohydrol 1:23–34. doi: 10.1002/eco.4

Turner MG, Gardner RH, O'Neill RV (2001) Landscape Ecology In Theory and Practice Pattern and Process. Springer Science, New York

Tyler SW, Kranz S, Parlange MB, et al (1997) Estimation of groundwater evaporation and salt flux from Owens Lake, California, USA. Journal of Hydrology 200:110–135. doi: doi: DOI: 10.1016/S0022-1694(97)00007-3

Urban DL, Minor ES, Treml EA, Schick RS (2009) Graph models of habitat mosaics. Ecology Letters 12:260–273. doi: 10.1111/j.1461-0248.2008.01271.x

US EPA (2008) Particulate Matter Pollution in California's Owens Valley. In: Region 9 Air Programs. U.S. Environmental Protection Agency. http://epa.gov/region09/air/owens/pmplan.html#52507. Accessed 12 Dec 2008

USDA (1996) Soil Quality Indicators: Aggregate Stability. USDA

USDA, NRCS (2004) Chapter 16 - Line Point Transects for Basal and Canopy Gaps. 2004 National Resources Inventory (NRI) Handbook of Instructions for Rangeland Field Study Data Collection. USDA, Washington DC,

USEPA (2007) United States Environmental Protection Agency, Owens Valley Nonattainment Area; Particulate Matter of 10 Microns or Less. Federal Register; Volume 72

USGS (2013) Frequently Asked Questions about the Landsat Missions. In: Landsat Missions. http://landsat.usgs.gov/best_spectral_bands_to_use.php. Accessed 8 Oct 2014

Vest KR, Elmore AJ, Kaste JM, et al (2013) Estimating total horizontal aeolian flux within shrub-invaded groundwater-dependent meadows using empirical and mechanistic models. Journal of Geophysical Research-Earth Surface 118:1132–1146. doi: 10.1002/jgrf.20048

Wiebe HH, Walter H (1972) Mineral Ion Composition of Halophytic Species from Northern Utah. American Midland Naturalist 87:241–245.

Wiggs GF, O'Hara SL, Wegerdt J, et al (2003) The dynamics and characteristics of aeolian dust in dryland Central Asia: possible impact on human exposure and respiratory health in the Aral Sea basin. Geographical Journal 169:142. doi: Article

Wolfe SA, Nickling WG (1996) Shear stress partitioning in sparsely vegetated desert canopies. Earth Surface Processes and Landforms 21:607–619.

Zeng N, Yoon J (2009) Expansion of the world's deserts due to vegetation-albedo feedback under global warming. Geophys Res Lett 36:L17401. doi: 10.1029/2009GL039699

Zhang X, Wu L, Zhang R, et al (2013) Evaluating the relationships among economic growth, energy consumption, air emissions and air environmental protection investment in China. Renewable and Sustainable Energy Reviews 18:259–270. doi: 10.1016/j.rser.2012.10.029

Zhong S, Li J, Whiteman CD, et al (2008) Climatology of High Wind Events in the Owens Valley, California. Mon Wea Rev 136:3536–3552. doi: 10.1175/2008MWR2348.1